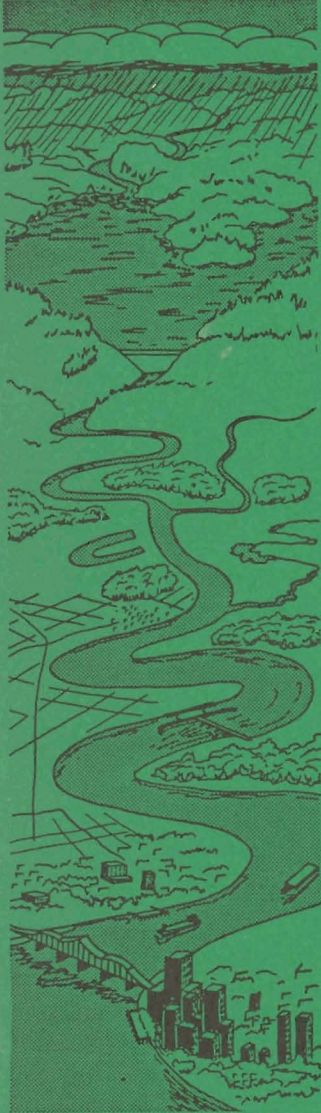




US Army Corps  
of Engineers



## ENVIRONMENTAL AND WATER QUALITY OPERATIONAL STUDIES

TECHNICAL REPORT E-86-7

# AN ASSESSMENT OF RESERVOIR MIXING PROCESSES

by

Dennis E. Ford, Linda S. Johnson

Ford, Thornton, Norton and Associates, Ltd.  
3 Inwood Circle  
Little Rock, Arkansas 72211



July 1986  
Final Report

Approved For Public Release; Distribution Unlimited

Prepared for DEPARTMENT OF THE ARMY  
US Army Corps of Engineers  
Washington, DC 20314-1000

Under Purchase Order No. DACW39-82-M-2042  
(EWQOS Work Unit IA.2)

Monitored by Environmental Laboratory  
US Army Engineer Waterways Experiment Station  
PO Box 631, Vicksburg, Mississippi 39180-0631



Unclassified

SECURITY CLASSIFICATION OF THIS PAGE (When Data Entered)

REPORT DOCUMENTATION PAGE		READ INSTRUCTIONS BEFORE COMPLETING FORM	
1. REPORT NUMBER Technical Report E-86-7	2. GOVT ACCESSION NO.	3. RECIPIENT'S CATALOG NUMBER	
4. TITLE (and Subtitle) AN ASSESSMENT OF RESERVOIR MIXING PROCESSES		5. TYPE OF REPORT & PERIOD COVERED Final report	
		6. PERFORMING ORG. REPORT NUMBER	
7. AUTHOR(s) Dennis E. Ford, Linda S. Johnson		8. CONTRACT OR GRANT NUMBER(s) Purchase Order No. DACW39-82-M-2042	
9. PERFORMING ORGANIZATION NAME AND ADDRESS Ford, Thornton, Norton and Associates, Ltd. 3 Innwood Circle Little Rock, Arkansas 72211		10. PROGRAM ELEMENT, PROJECT, TASK AREA & WORK UNIT NUMBERS EWQOS Work Unit IA.2	
11. CONTROLLING OFFICE NAME AND ADDRESS DEPARTMENT OF THE ARMY US Army Corps of Engineers Washington, DC 20314-1000		12. REPORT DATE July 1986	
		13. NUMBER OF PAGES 162	
14. MONITORING AGENCY NAME & ADDRESS (if different from Controlling Office) US Army Engineer Waterways Experiment Station Environmental Laboratory PO Box 631, Vicksburg, Mississippi 39180-0631		15. SECURITY CLASS. (of this report) Unclassified	
		15a. DECLASSIFICATION/DOWNGRADING SCHEDULE	
16. DISTRIBUTION STATEMENT (of this Report) Approved for public release; distribution unlimited.			
17. DISTRIBUTION STATEMENT (of the abstract entered in Block 20, if different from Report)			
18. SUPPLEMENTARY NOTES Available from National Technical Information Service, 5285 Port Royal Road, Springfield, Virginia 22161.			
19. KEY WORDS (Continue on reverse side if necessary and identify by block number) Environmental impact analysis Reservoirs Water quality			
20. ABSTRACT (Continue on reverse side if necessary and identify by block number) Since mixing and the resultant hydrothermal regime are dominant factors in determining what takes place chemically and biologically in a reservoir, techniques for predicting the characteristics of the major mixing mechanisms that occur in reservoirs can help the US Army Corps of Engineers (CE) regulate the quality of reservoir and release waters. This report provides a literature review of reservoir internal mixing processes, in which general transport processes, reservoir mixing processes and			

(Continued)

Unclassified

Unclassified

SECURITY CLASSIFICATION OF THIS PAGE(When Data Entered)

20. ABSTRACT (Continued).

their effect on water quality, and one-dimensional predictive techniques and computer algorithms are presented and analyzed. The historical development of the recommended predictive techniques, including the assumptions, limitations, and advantages of the techniques used in the development, is also documented.

The recommended one-dimensional mixing algorithm is generalized with respect to CE reservoirs and is not constrained by extensive data requirements nor limited in the mixing processes considered. The algorithm includes all major mixing processes in order to predict changes in the reservoir's mixing regime resulting from changes in hydrometeorological conditions and project operation. The recommended algorithm was used to simulate the thermal structure of over 15 reservoirs and lakes of varying geographical locations, size, hydrometeorological regime, and operational configurations. The recommendations for the mixing algorithm are the opinions of the authors, and all phases of it are not necessarily incorporated in the current one-dimensional CE reservoir model (CE-QUAL-R1).

Unclassified

SECURITY CLASSIFICATION OF THIS PAGE(When Data Entered)

## PREFACE

This report was prepared as part of the Environmental and Water Quality Operational Studies (EWQOS) Program, Work Unit IA.2, Develop and Verify Techniques for Describing Internal Reservoir Mixing Processes. The EWQOS Program is sponsored by the Office, Chief of Engineers (OCE), US Army, and is assigned to the US Army Engineer Waterways Experiment Station (WES), under the purview of the Environmental Laboratory (EL). The OCE Technical Monitors were Mr. Earl Eiker, Dr. John Bushman, and Mr. James L. Gottesman. Dr. J. L. Mahloch, EL, is the Program Manager of EWQOS.

The study was conducted by Dr. Dennis E. Ford and Ms. Linda S. Johnson of the Water Quality Modeling Group (WQMG), Environmental Research and Simulation Division (ERSD), EL. The work was conducted under the direct supervision of Mr. Mark Dortch, Chief, WQMG, and under the general supervision of Mr. D. L. Robey, Chief, ERSD, and Dr. John Harrison, Chief, EL. The report was prepared for WES under Purchase Order No. DACW39-82-M-2042 by Ford, Thornton, Norton and Associates, Ltd., Little Rock, Ark.

The report was reviewed and coordinated for publication by Ms. Sandra Bird, WQMG, and was edited by Ms. Jessica S. Ruff of the WES Publications and Graphic Arts Division.

Director of WES was COL Allen F. Grum, USA. Technical Director was Dr. Robert W. Whalin.

This report should be cited as follows:

Ford, D. E., and Johnson, L. S. 1986. "An Assessment of Reservoir Mixing Processes," Technical Report E-86-7, prepared by Ford, Thornton, Norton and Associates, Ltd., for the US Army Engineer Waterways Experiment Station, Vicksburg, Miss.

## CONTENTS

	<u>Page</u>
PREFACE . . . . .	1
SECTION 1. INTRODUCTION . . . . .	4
SECTION 2. BACKGROUND AND REVIEW . . . . .	6
2.1 Introduction . . . . .	6
2.2 Density Stratification . . . . .	6
2.2.1 Definitions and Importance . . . . .	6
2.2.2 Factors Affecting Stratification . . . . .	9
2.2.3 Temporal Variations . . . . .	11
2.2.4 Horizontal Variations . . . . .	14
2.2.5 Data Interpretation and Generalizations . . . . .	18
2.3 Potential Energy . . . . .	24
2.4 General Transport Processes . . . . .	30
2.4.1 Advection . . . . .	30
2.4.2 Shear . . . . .	32
2.4.3 Molecular Diffusion . . . . .	32
2.4.4 Turbulence and Turbulent Diffusion . . . . .	34
2.4.5 Entrainment . . . . .	37
2.4.6 Convection . . . . .	38
2.4.7 Dispersion . . . . .	40
SECTION 3. RESERVOIR MIXING AND WATER QUALITY . . . . .	43
3.1 Introduction . . . . .	43
3.2 Description of Reservoir Mixing Processes . . . . .	43
3.2.1 Atmospheric Heating (Cooling) . . . . .	43
3.2.2 Wind Processes . . . . .	45
3.2.3 Circulation Currents . . . . .	49
3.2.4 Internal Waves . . . . .	54
3.2.5 Inflows . . . . .	56
3.2.6 Outflows . . . . .	59
3.2.7 Barometric Pressure and Gravity . . . . .	60
3.2.8 Summary . . . . .	61
3.3 Influence of Mixing on Reservoir Water Quality . . . . .	61
3.3.1 Inflows and Outflows . . . . .	62
3.3.2 Upwelling, Seiches, and Internal Waves . . . . .	65
3.3.3 Turbulence, Turbulent Mixing, and Entrainment . . . . .	67
3.3.4 Langmuir Circulation . . . . .	70
3.4 Synthesis . . . . .	70
SECTION 4. REVIEW OF ONE-DIMENSIONAL PREDICTIVE TECHNIQUES . . . . .	74
4.1 Introduction . . . . .	74
4.2 One-Dimensional Assumption . . . . .	75
4.3 Eddy Coefficient (Diffusion) Models . . . . .	78
4.3.1 Description . . . . .	78
4.3.2 Eddy Coefficient Formulations . . . . .	80

	<u>Page</u>
4.3.3 Assumptions and Limitations . . . . .	91
4.4 Mixed-Layer Models . . . . .	92
4.4.1 Background . . . . .	92
4.4.2 Description . . . . .	94
4.4.3 Assumptions and Limitations . . . . .	97
4.5 Summary . . . . .	97
SECTION 5. ALGORITHM DEVELOPMENT . . . . .	98
5.1 Introduction . . . . .	98
5.2 Evaluation Procedures . . . . .	99
5.3 Historical Development . . . . .	106
5.3.1 WQRRS . . . . .	106
5.3.2 Variable Layer Formulation . . . . .	110
5.3.3 Mixed-Layer Dynamics . . . . .	112
5.3.4 Diffusion Coefficient Formulation . . . . .	118
5.4 Recommended Algorithm . . . . .	119
5.4.1 Variable Layer Formulation . . . . .	120
5.4.2 Mixed-Layer Dynamics . . . . .	120
5.4.3 Diffusion Coefficient Formulation . . . . .	124
5.5 Applications and Verification . . . . .	127
SECTION 6. SUMMARY AND CONCLUSIONS . . . . .	132
6.1 Literature Review Findings . . . . .	132
6.2 Recommended Algorithm . . . . .	133
REFERENCES . . . . .	135
APPENDIX A: STRATIFICATION COMPUTATIONS . . . . .	A1
A.1 Introduction . . . . .	A1
A.2 Densimetric Froude Number . . . . .	A1
A.2.1 Description . . . . .	A1
A.2.2 Examples . . . . .	A2
A.3 Wind Mixing Depth . . . . .	A3
A.3.1 Description . . . . .	A3
A.3.2 Examples . . . . .	A5
A.4 Pond Number . . . . .	A7
A.4.1 Description . . . . .	A7
A.4.2 Examples . . . . .	A8
A.5 Summary . . . . .	A10
APPENDIX B: NOTATION . . . . .	B1

# AN ASSESSMENT OF RESERVOIR MIXING PROCESSES

## SECTION 1. INTRODUCTION

Mixing refers to all physical transport processes and mechanisms which cause a parcel of water and its associated water quality constituents to blend with or be diluted by another parcel of water. Examples of specific transport processes that are included in this definition are molecular diffusion, dispersion, and convection, among others. The relative importance of any one specific transport process (e.g., dispersion) will vary both temporally and spatially and depend on the physical characteristics of the water body, time of year, and type of forcing event (e.g., the wind).

In lakes and reservoirs, mixing results from the cumulative effects of external energy inputs such as surface heat exchange; absorption of solar radiation with depth; wind magnitude and direction; inflow magnitude, density, and location; outflow magnitude and location; and changes in project operation (i.e., withdrawal depth, pool level changes, etc.). Mixing is therefore dynamic since its effectiveness varies in response to those dynamic forcing events.

A thorough understanding of mixing is required since it and the resultant hydrothermal regime, which includes thermal stratification, is a dominant factor in determining what takes place chemically and biologically in a reservoir. Sensitivity analyses on reservoir water quality models have shown the mixing coefficient to be highly sensitive, indicating the importance of having an accurate formulation for mixing (Thornton et al. 1979).

The objective of this study is twofold:

- a. To review and document the major mixing mechanisms in Corps of Engineers (CE) reservoirs and their importance to reservoir water quality.
- b. To develop a mathematical algorithm for one-dimensional water quality models (i.e., CE-QUAL-R1, Environmental Laboratory 1982) which realistically represents all major mixing processes occurring in CE reservoirs.

The review will emphasize the transport and dispersion of substances due to a given hydrothermal regime and not the specific details of the hydrodynamic processes themselves. The mathematical algorithm must be sufficiently general to be applicable to the majority of CE reservoirs which vary in size and location and are therefore driven by different hydrometeorologic forcing events. The algorithm must also be able to accurately simulate changes in the mixing regime due to changes in project operations, such as a change in conservation pool level or withdrawal depth.

## SECTION 2. BACKGROUND AND REVIEW

### 2.1 Introduction

Although the ultimate objective of this review is knowledge of the sum or cumulative effects of all reservoir mixing processes or mechanisms and their impact on reservoir water quality, it is first necessary to review density stratification and the individual transport processes. In many instances, this is not a simple task because the individual transport mechanisms act together, reinforcing one another with unknown synergistic effects. In addition, mixing determines the observed thermal structure, but the thermal (density) stratification modifies the mixing regime. It is therefore impossible to discuss reservoir mixing without knowledge of thermal stratification and to understand thermal stratification and reservoir water quality without an understanding of the individual mixing processes.

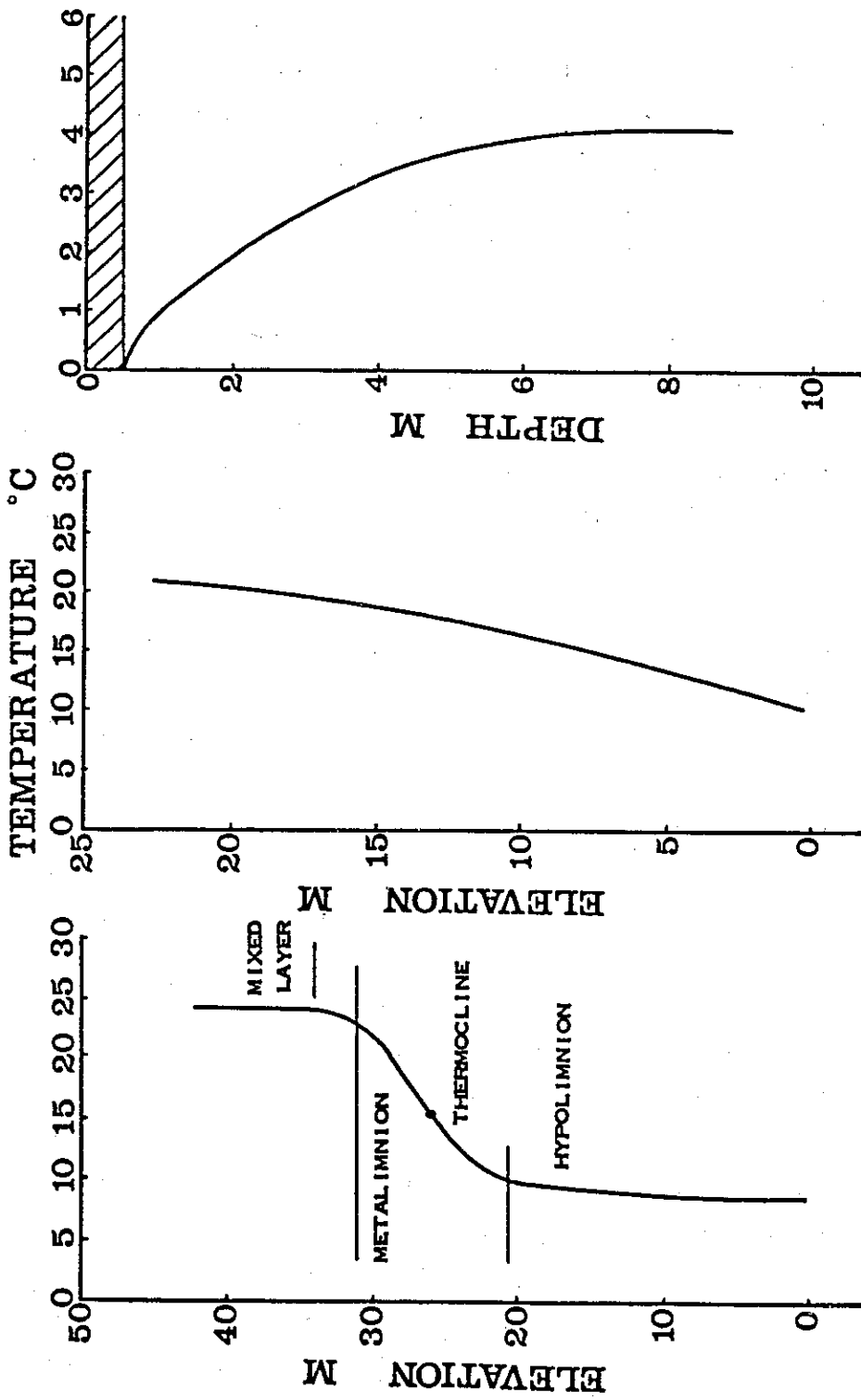
In this section, the concepts of thermal stratification and potential energy will first be reviewed. Then, definitions for several fundamental transport processes will be presented. This background information will be used in the next section to construct a complete picture of reservoir mixing based on energy sources and concepts and to determine the significance of mixing on reservoir water quality.

### 2.2 Density Stratification

#### 2.2.1 Definitions and Importance

Density stratification is the nonhomogeneous layering of a fluid due to differences in density. In reservoirs, density stratification is primarily caused by temperature (i.e., thermal stratification), but density differences resulting from variations in suspended and dissolved solids concentrations can also be important. Density and/or thermal stratification therefore implies incomplete vertical mixing.

Many deep reservoirs exhibit the classical three-layer stratification (Figure 1a). The epilimnion is the upper stratum of warm,



a. Classical three-layered system (Lake Greason, Arkansas, 6 Oct 72)

b. Linear stratification (Lake Shelbyville, Illinois, 6 Jun 73)

c. Inverse winter stratification (Lake Eau Galle, Wisconsin, 22 Feb 79)

Figure 1. Examples of stratification

turbulent water. It is usually characterized by relatively uniform temperatures. The deep, cold, relatively undisturbed region is termed the hypolimnion. Between the epilimnion and hypolimnion is a transition zone, the metalimnion, which is characterized by a strong temperature (density) gradient. The plane of inflection or of maximum temperature gradient is termed the thermocline. Other definitions have been proposed for the thermocline (e.g., the  $1^{\circ}$  C/m criterion), but they are not used herein. Another term illustrated in Figure 1a is the "mixed layer." The mixed layer is, as implied by the name, the overlying isotropic layer. Since the mixed layer refers to the instantaneous depth of the overlying isotropic layer, it differs from the epilimnion, which is an averaged mixed layer, in two respects. First, the mixed layer depth is usually less than the depth of the epilimnion. Second, it is much more dynamic than the epilimnion.

Many shallow reservoirs with short hydraulic residence times do not exhibit a classical three-layered system (e.g., Figure 1b). Instead of having a well-defined hypolimnion, the metalimnion appears to extend to the reservoir bottom. It is also possible to have systems that do not appear to have a well-defined epilimnion.

In cold regions, reservoirs may inversely stratify during the winter months (Figure 1c). At low temperatures (near  $4^{\circ}$  C), even small quantities of solids can significantly alter the water density and impact the observed thermal structure. In general, there is no well-defined epilimnion and metalimnion in inversely stratified systems. The thickness of the zone of density gradient (i.e., the epilimnion and metalimnion) under the ice varies from a metre or two in small reservoirs to tens of metres in large, deep reservoirs. In deep reservoirs, the effects of hydrostatic pressure (i.e., depth) also modify the density distribution (Farmer and Carmack 1982).

Many other terms are used to describe the thermal structure of a lake. These are defined in Hutchinson (1957), Ruttner (1963), Wetzel (1983), among others. In general, these terms are related either to the number of turnovers (i.e., periods of complete vertical mixing) occurring within a lake or to the strength of the stratification. It is,

however, important to distinguish between holomictic and meromictic lakes. In holomictic lakes, the entire water column completely circulates or turns over. Lakes that cannot circulate completely and exhibit a deep stratum that is perennially stagnant in the water column are termed meromictic lakes (Hutchinson 1957). The reason for this condition may be physical, chemical, or biological. Turbidity-induced meromixis has been observed in a CE reservoir (Larson 1979). Whatever the cause of meromixis, it can have a profound effect on the temperature and mixing structure and, consequentially, on the water quality of lake. Bottom withdrawal can be an effective management alternative to eliminate this undesirable condition.

Thermal stratification is important because all chemical and biological processes are, to some extent, temperature dependent. More important, however, is the layering of the lake which can isolate the metalimnion and hypolimnion from light and transfers across the air/water interface, resulting in vertical variations in water quality.

### 2.2.2 Factors Affecting Stratification

The principal factors influencing the formation, strength, and extent of stratification are the density of water; solar radiation and the heat transfer at the air/water interface; and the mixing resulting from advection (inflows and outflows) and wind-induced phenomena.

It is well known that the density of water varies with temperature (Figure 2). The importance of this variation in determining the distribution of heat within a lake was originally documented by Birge (1910). Two factors are important. First, the maximum density of water occurs at approximately 4° C. Second, water density decreases at an escalating rate with both increasing and decreasing temperatures from 4° C. There is over an order of magnitude difference in the energy requirements to mix or destratify a 1° C temperature difference at 25° C than at 5° C.

The energy available to warm the waters of a reservoir ultimately comes from solar radiation, which varies seasonally and with latitude (Figure 3). The seasonal variation of solar radiation follows a sinusoidal curve with a maximum in late June. In addition, diurnal cycles

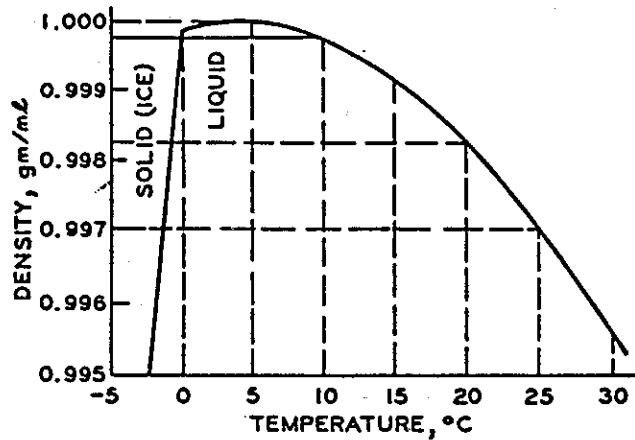


Figure 2. Variations of water density with temperature

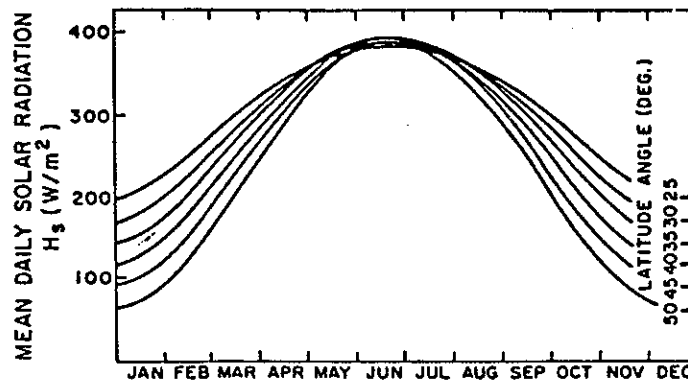


Figure 3. Seasonal variations in solar radiation (after Koberg 1962)

also occur. Water temperatures respond to both of these cycles with a slight delay. Solar radiation is absorbed at the water surface and selectively with depth depending on the wavelength of the light, properties of the water, and the matter suspended in the water. This absorption is usually assumed to be exponential with depth (i.e., Beer's Law), but surface effects result in minor discrepancies in the top metre or so of a lake (Figure 4).

In contrast to heating, cooling of a water body can occur only at the water surface. It is therefore possible for the surface water to decrease in temperature while deeper water increases in temperature. If the temperature of the surface water drops below the temperature of the

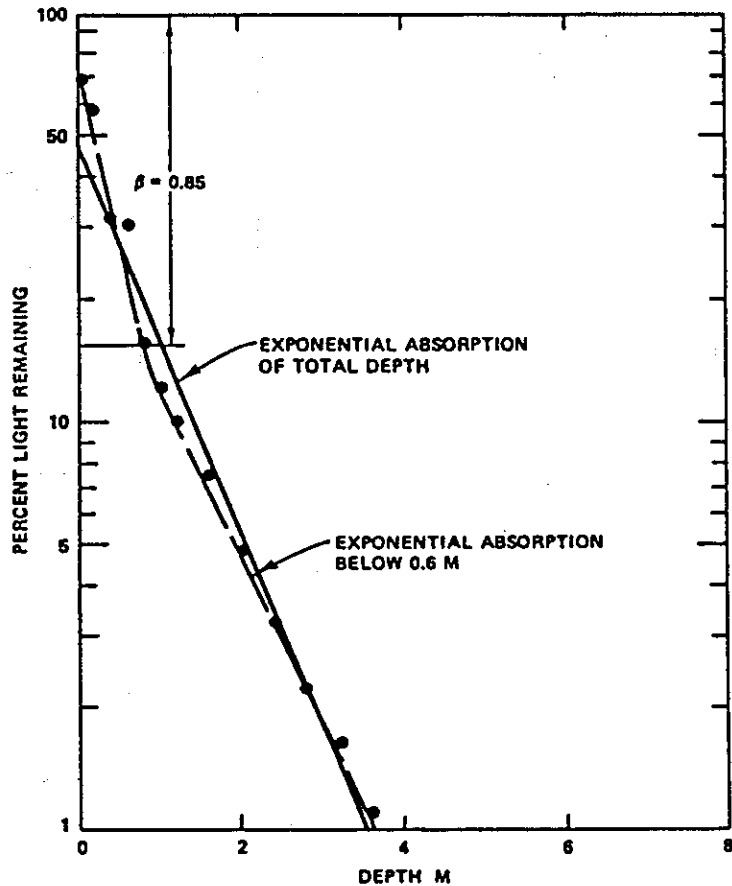


Figure 4. Extinction of light with depth

deeper water and still remains above 4° C, the water column becomes thermally unstable and natural convection and mixing commence.

Mixing causes the shape of the vertical temperature profile to change from an exponential decrease with depth (i.e., warming due to absorption of solar radiation) to the classical profile of a well-mixed layer overlying a zone of temperature gradient (Figure 5). Reservoir mixing is discussed in detail in Section 3.

### 2.2.3 Temporal Variations

Because the factors which determine the thermal stratification are always changing, the thermal structure is always undergoing change. There are, however, three distinct cycles of importance: annual, synoptic, and diel. The annual cycle has a period of 365 days and exhibits

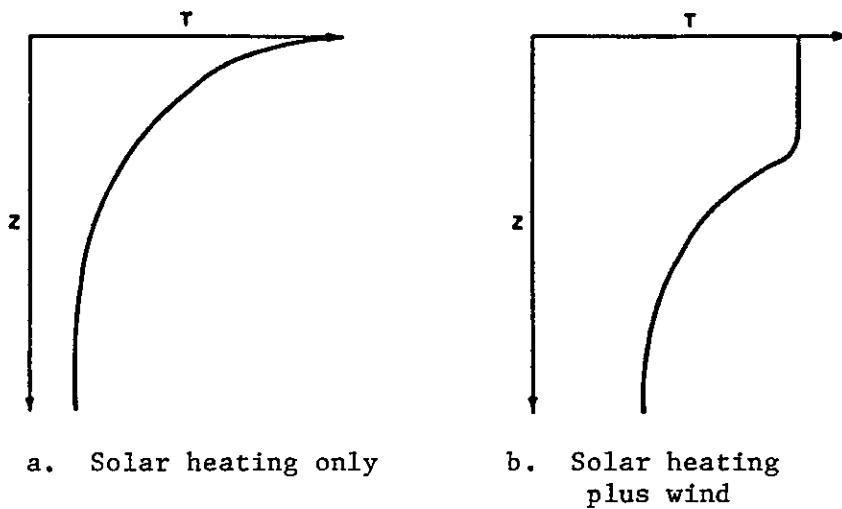


Figure 5. Effect of mixing on the thermal profile

seasonal changes in temperature resulting from seasonal changes in solar radiation, air temperature, wind, and flow. Synoptic cycles typically have periods of 5 to 7 days and correspond with the passage of major weather systems (i.e., warm or cold fronts). Diel cycles have a period of 24 hr and correspond to daytime heating and nighttime cooling.

Annual cycle. The annual temperature cycle for a large reservoir with long residence time is shown in Figure 6. During the period of spring turnover (late February to early March), the entire water column undergoes complete mixing. The density differences at the low temperatures ( $4^{\circ}$  to  $5^{\circ}$  C) are insufficient to prevent complete mixing. As the water column warmed, density differences increase and it becomes more difficult to mix the entire water column. Stratification started to form near the bottom of the lake (late March) because the density differences and resulting buoyancy forces were small compared to the kinetic energy input (i.e., wind). As the solar radiation increased, water temperatures increased, density difference increased, and the thermocline moved upward because the kinetic energy input could not overcome the ever-increasing buoyancy forces of density stratification. The minimum thermocline depth was achieved about the time of summer solstice or time of maximum heat input (late June). Once stratification formed, the hypolimnetic temperatures remained relatively constant until

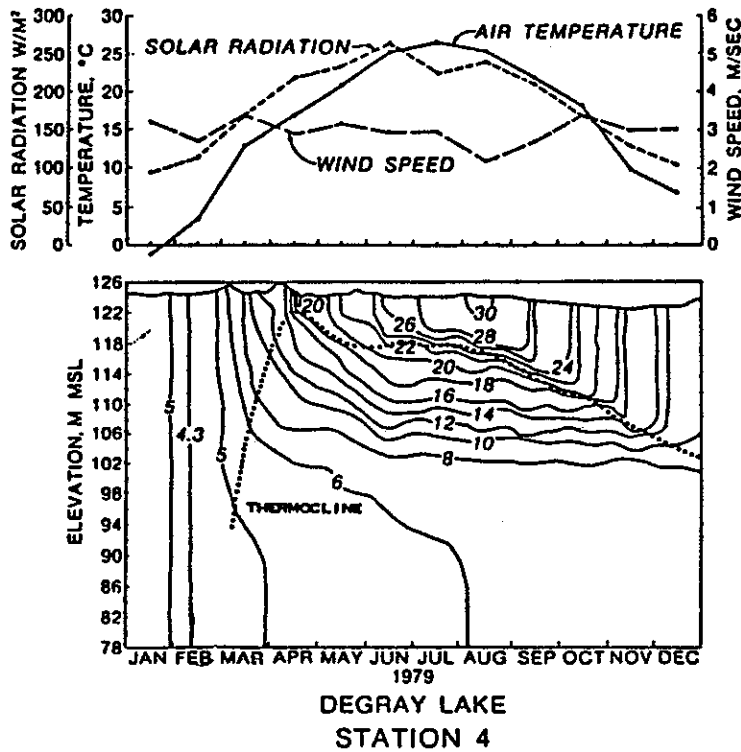


Figure 6. Annual temperature variations in a deep reservoir with a long residence time

the surface temperatures cooled to near the hypolimnetic temperatures and complete vertical mixing of the water column occurred (i.e., fall overturn).

The increased mixing resulting from inflows and outflows in reservoirs can result in deviations from the above example. For instance, periods of overturn may be extended and become more frequent, and the slope of the isotherms may be increased. If bottom withdrawal is used, hypolimnetic temperatures may increase. For example, in Figure 7, the hypolimnetic temperatures in Beltzville Lake, Pennsylvania, during 1976 remained relatively constant when only small amounts of water were released through the lower ports. In contrast, during 1972, when large quantities of water were released through the floodgates in response to Hurricane Agnes, the hypolimnetic temperatures increased. Other variations such as pumped-storage operations can also increase mixing and hypolimnion temperatures (Figure 8).

## BELTZVILLE LAKE

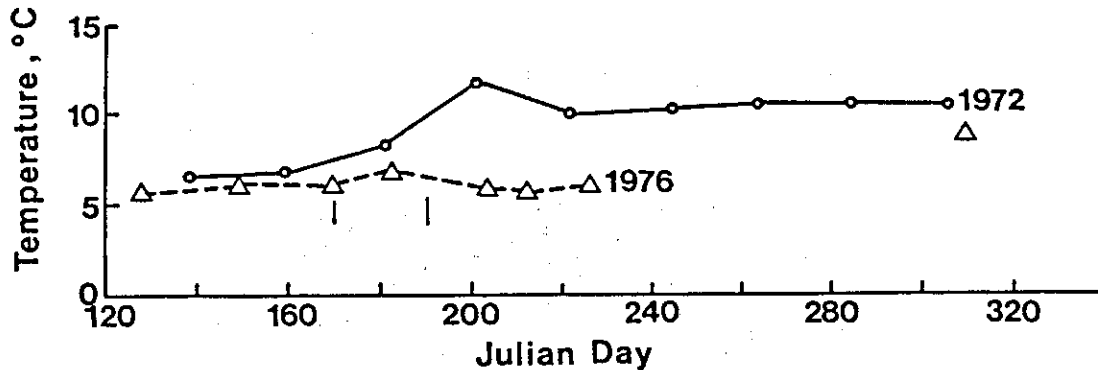


Figure 7. Seasonal variation in hypolimnetic temperature

Synoptic variations. Examples of synoptic temperature variations are shown in Figure 9. Temporary periods of stratification occur during periods of warm, calm weather and are destroyed during periods of cold, windy weather. Synoptic variations are on the order of a few degrees Celsius.

Diel variations. Diel variations are typically on the order of 1° to 2° C but can be as large as 7° C or more. The actual magnitude will depend on the depth of the upper mixed layer, the amount of surface mixing, and the quantity of solar insolation. The deeper the mixed layer and/or the larger the surface mixing, the smaller the diurnal variation. A typical diel variation is shown in Figure 10.

### 2.2.4 Horizontal Variations

Horizontal variations in temperature and stratification occur as a result of differential heating, inflow, or mixing. Differential heating occurs when the smaller volume of water in the coves, littoral zones, and headwaters of an impoundment warms or cools more rapidly than the open-water regions. In large lakes, this phenomenon is significant and results in the formation of thermal bars. Similarly, rivers flowing into a reservoir may be of different temperatures, creating longitudinal variations. Horizontal variations resulting from a river inflow are illustrated in Figure 11. Horizontal variations resulting from a river

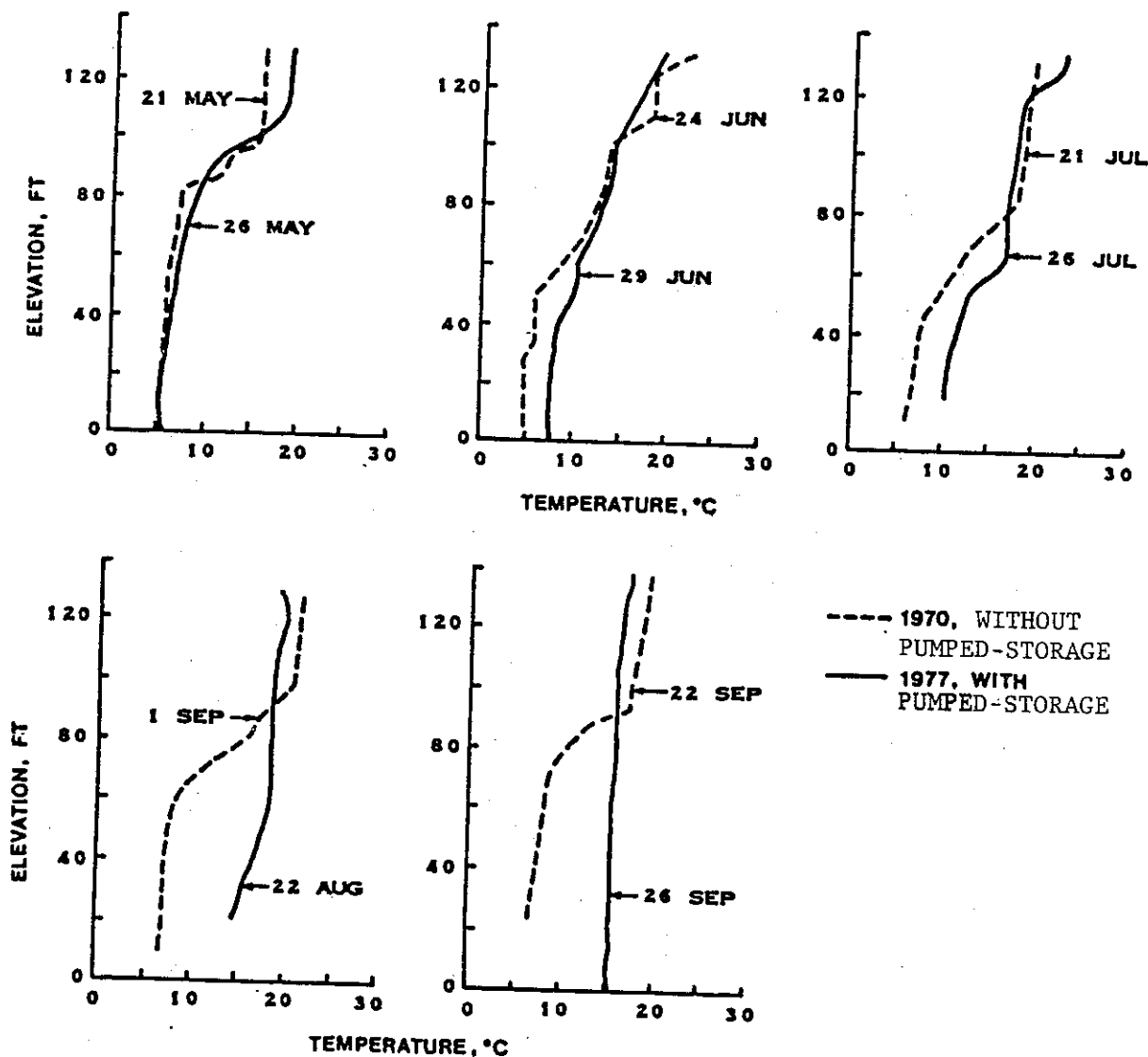


Figure 8. Effect of pumped-storage operations on the thermal structure of Kinzua Lake, Pennsylvania (after Dortch 1981) (to convert feet to metres, multiply by 0.3048)

inflow typically create temperature differences of 1° or 2° C or more. Spatial variations in both the horizontal and vertical directions can also occur as a result of seiching and upwelling (see Sections 3.2.2 and 3.3.2). These variations are highly dynamic.

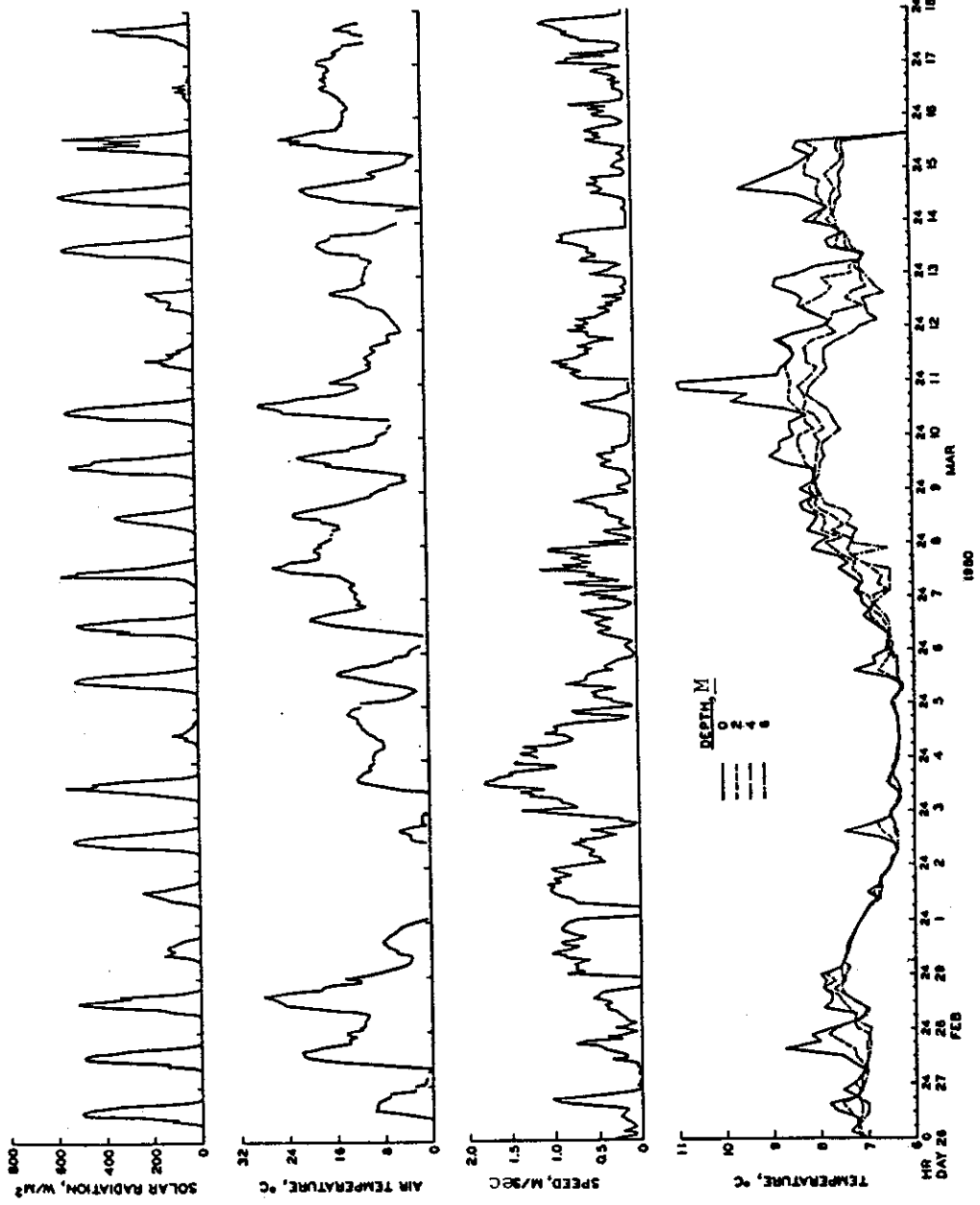


Figure 9. Example of synoptic variations in water temperature, DeGray Lake, Arkansas

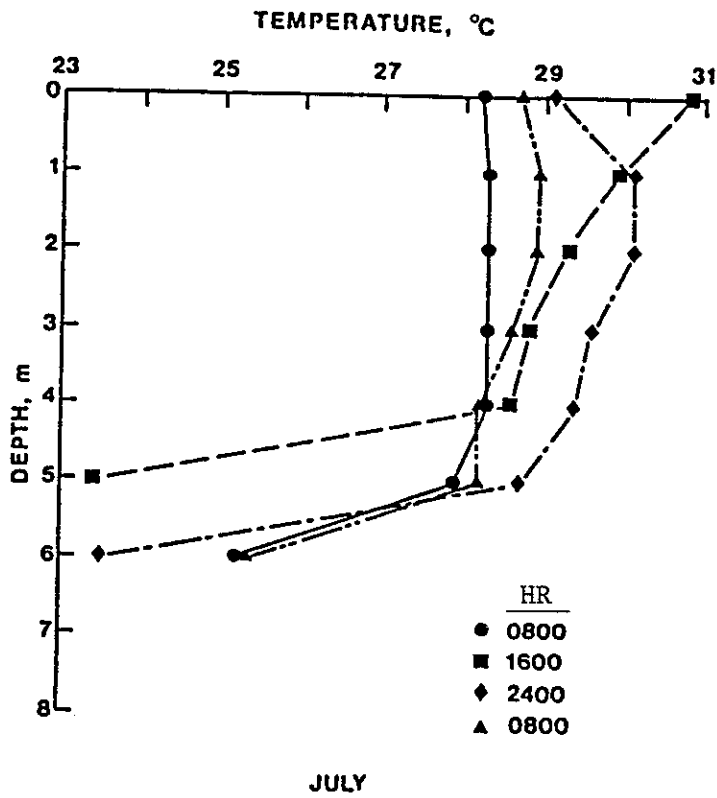


Figure 10. Example of a typical diel temperature cycle, DeGray Lake, Arkansas

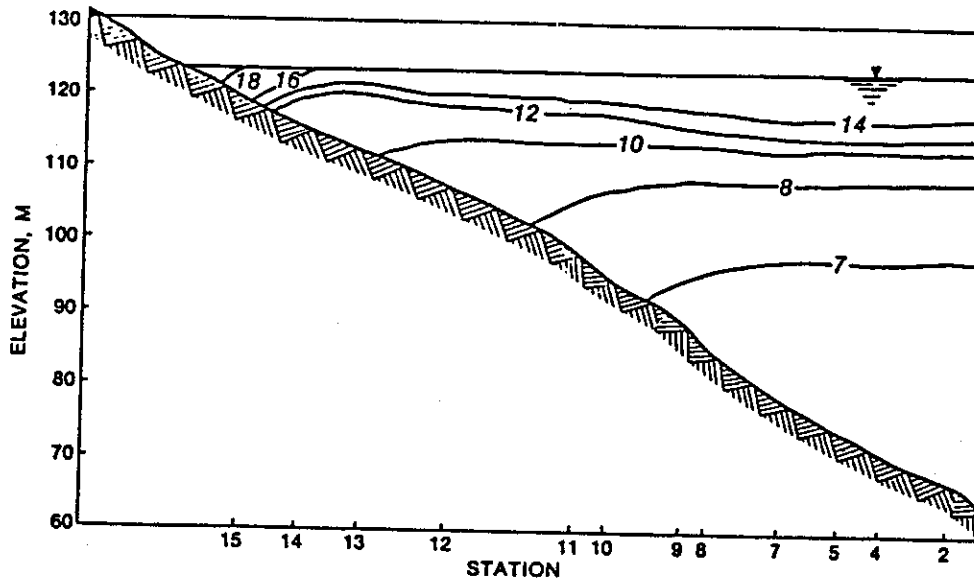


Figure 11. Horizontal variations in temperature resulting from river inflow, DeGray Lake, Arkansas, 2 Apr 74

### 2.2.5 Data Interpretation and Generalizations

Temperature data interpretation. Much of our knowledge concerning mixing in reservoirs and lakes is based on the interpretation of vertical temperature profile data (i.e., stratification data). In addition to understanding the factors which affect stratification and its temporal and spatial variations (Sections 2.2.2-2.2.4), the correct interpretation of stratification data also requires detailed knowledge of the field sampling (e.g., station location, sampling time, etc.), hydro-meteorological conditions (e.g., inflows, wind speed and direction), project operation (e.g., release rates and outlet locations), and reservoir mixing processes. There should be a logical, physically based explanation for all observations (Ford 1978).

For example, most field data are collected during daylight hours and may represent maximum daily water temperature and minimum mixed layer depths (see Figure 10). If there is wind, warm surface water may be pushed to one side of the reservoir (Figure 12) and/or the thermocline may tilt, changing the depth of the upper mixed layer.

When interpreting stratification data, it is usually beneficial to draw isotherms relative to the water surface (e.g., Figure 13). For reservoirs, it is essential that the variation in water surface elevation be considered since there is the potential for large variations in water levels and since the slope of the isotherms indicates the degree of mixing. The relatively flat isotherms in the lower metalimnion (i.e., 16° and 18° C) during midsummer indicate little mixing in this region while the steep slope of the 22° and 24° C isotherms in the upper metalimnion during the same period possibly indicates more intensive mixing. If the variation in the water surface elevation is not taken into consideration, the slope of the isotherms may be misrepresented. Short-term variations in the isotherms (i.e., order of days) indicate seiching and/or internal waves (Section 3.2.2) and should be averaged when comparing isotherm slopes. This should not be a problem if the time interval between sampling dates is greater than 2 weeks.

Once the isotherms are constructed, the importance of inflows, outflows, and light penetration can be determined by comparing periods

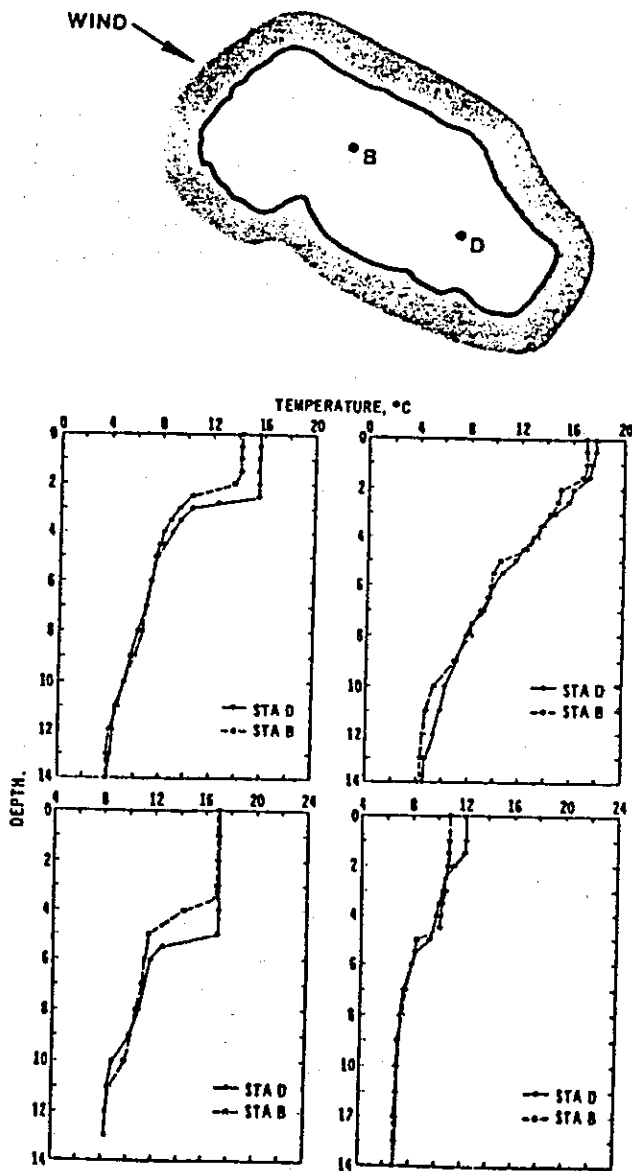


Figure 12. Effect of wind on temperature profiles, McCarrons Lake, Minnesota, 1974

and regions of mixing with the inflow quantity and placement (based on density or temperature) (Figure 14a), the outflow quantity and depth (Figure 14b), and the seasonal variation in twice the Secchi disc depth (i.e., ca. 1 percent light level) (Figure 14c). For example, the intensive mixing that occurred during April and May, as evidenced by the

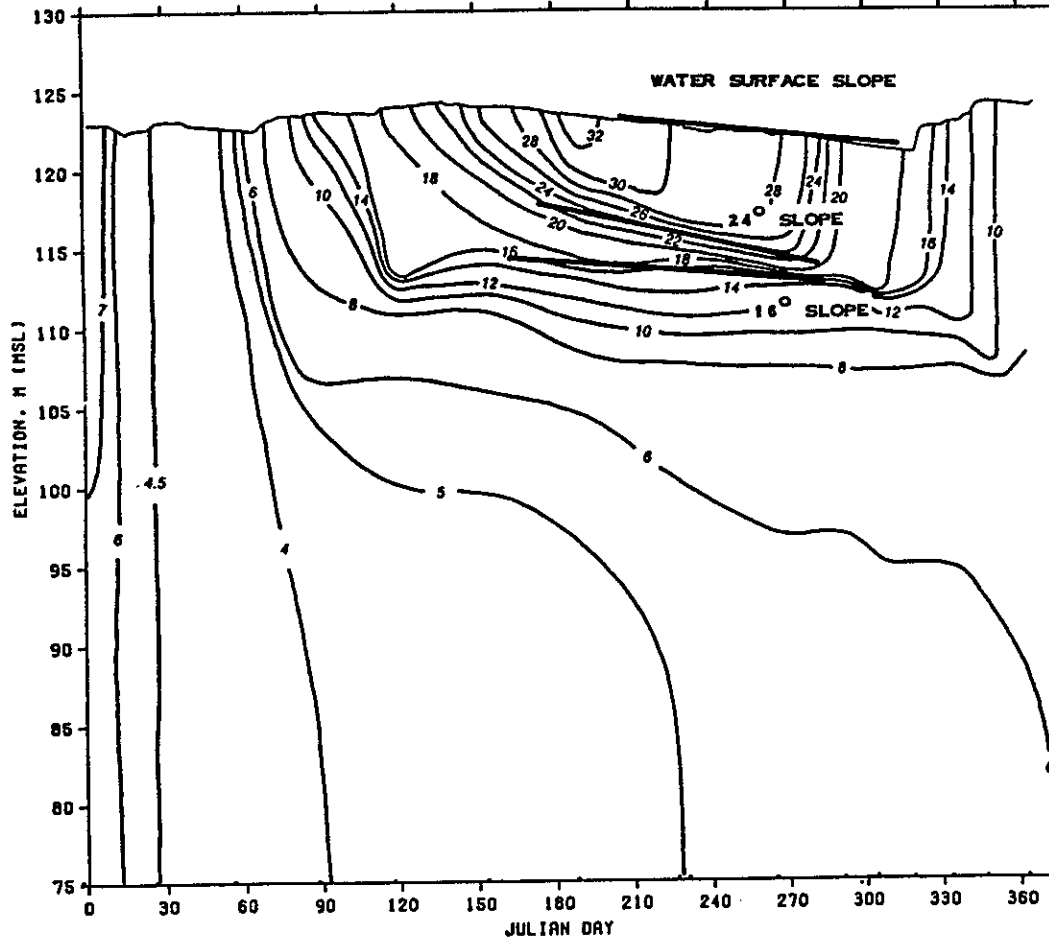
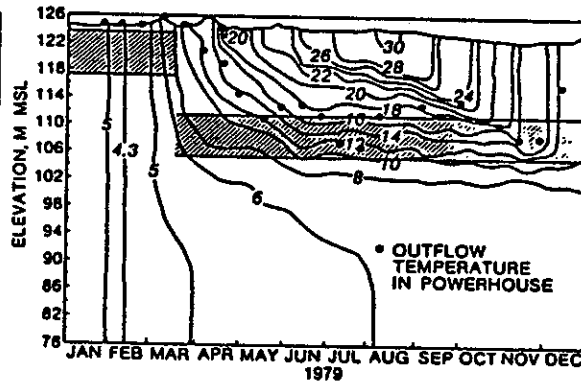
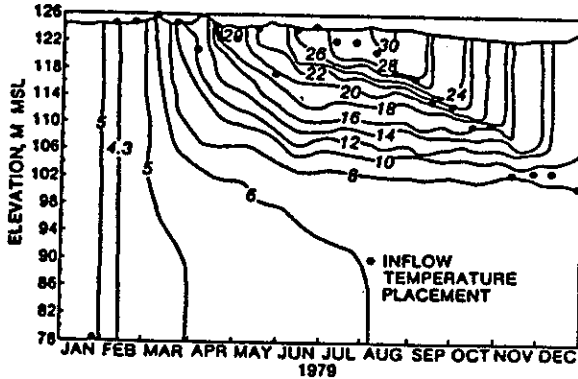
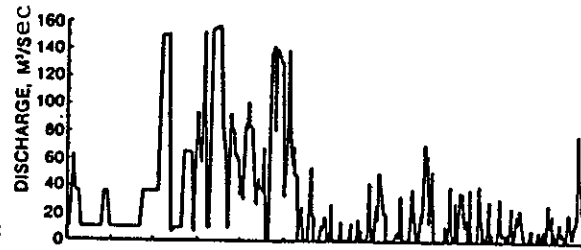
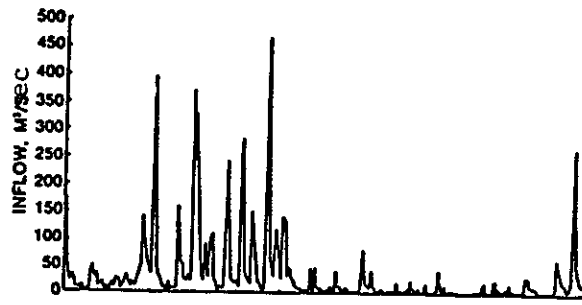


Figure 13. Construction of isotherms relative to water surface level, DeGray Lake, Arkansas, 1978

steep slope of the 10° to 18° C isotherms, is probably the result of the large outflows and change in withdrawal depth (Figure 14b) since light (thermal energy) did not penetrate to these depths (Figure 14c). In contrast, in Figure 15 the steep gradient of the 14° to 16° C isotherms during early June is the result of internal absorption of solar radiation since the light penetration increased significantly during this period and winds and flows were low.

One aspect of data interpretation that is commonly overlooked is the error associated with field measurements. Because of the intrinsic variability of temperature in reservoirs and calibration error associated with field equipment, historical temperature data should be

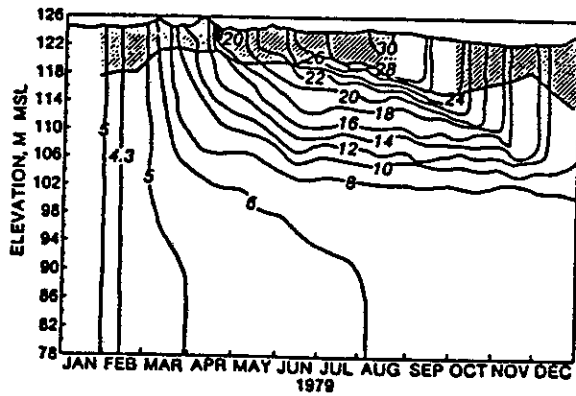


DEGRAY LAKE  
STATION 4

DEGRAY LAKE  
STATION 4

a. Inflow quantity and placement

b. Outflow quantity and  
withdrawal zone



DEGRAY LAKE  
STATION 4

c. Photic zone

Figure 14. DeGray Lake, Arkansas, 1979

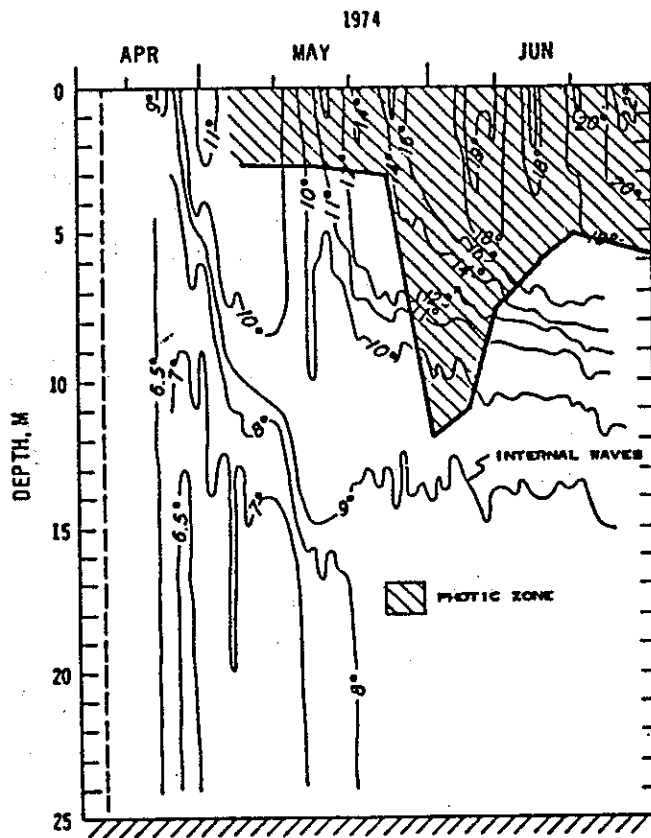


Figure 15. Comparison of isotherms and photic zone, Lake Calhoun, Minnesota, 1974

considered no better than  $\pm 1^\circ \text{C}$ . For example, pockets of cold water in the hypolimnion of a lake (Figure 16) are sometimes attributed to an influx of cold ground water rather than a data error. Such a situation is highly unlikely since ground-water movement is slow. If it should occur, it would be apparent in the daily water budget (i.e., change in pool level or outflow rate) as well as in the temperature profile.

Generalizations concerning stratification. Several generalizations concerning stratification in CE reservoirs can be made based upon a review of temperature data collected at reservoirs throughout the United States. First and foremost, all reservoirs stratify, albeit some for only a few hours and a few degrees Celsius. Second, if the mean annual theoretical hydraulic residence time (i.e., volume/mean annual flow for period of record) is greater than 6 months, the stratification

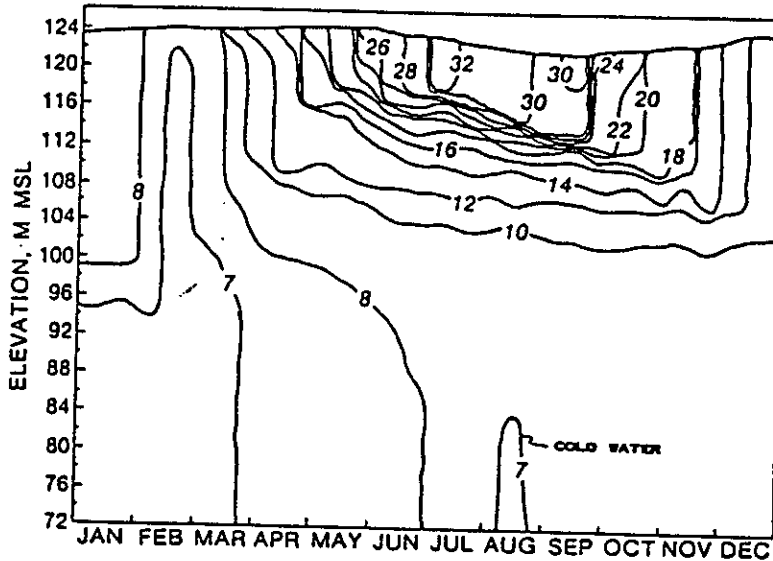


Figure 16. Isotherms for DeGray Lake, Arkansas, 1980

is dominated by meteorological forcing. Stratification in this type of lake is characterized by several features:

- a. Since the major factors responsible for stratification (e.g., wind and solar radiation) act at the air/water interface, horizontal variations are minimized.
- b. There is not much variability in stratification from year to year. Stratification forms and fall overturn occurs at approximately the same time each year. Hypolimnetic temperatures and thermocline depths are similar from year to year (e.g., Table 1).
- c. The larger the surface area, the more wind (kinetic) energy input, the longer the periods of turnover, the deeper the upper mixed layer.
- d. The deeper the lake, the less wind (kinetic) energy per unit volume available for mixing, and the stronger the stratification.
- e. Lakes in similar geographic areas will be exposed to similar hydrometeorological conditions and exhibit similar stratification patterns. For example, Lakes DeGray, Greeson, and Ouachita are located within 55 km of each other in the Ouachita Mountains of southwestern Arkansas, are deep (i.e., >30 m), have residence times greater than 12 months, and therefore exhibit similar stratification profiles (Figure 17).

Third, if the mean annual theoretical hydraulic residence time is small (less than 20 days), the system is advectively (inflows and

Table I  
Variation in August Stratification Characteristics  
DeGray Lake, Arkansas

<u>Year</u>	<u>Withdrawal Location</u>	<u>Hypolimnetic Temperature, °C</u>	<u>Thermocline Depth, m</u>
1974	Surface	7.0	8
1975	Surface	8.0	8
1976	Surface	7.0	7
1977	Surface	6.0	7
1978	Surface	6.0	7
1979	Lower	6.5	8
1980	Lower	7.5	8
1981	Lower	6.8	10
1982	Lower	6.2	8
1983	Surface	7.0	8

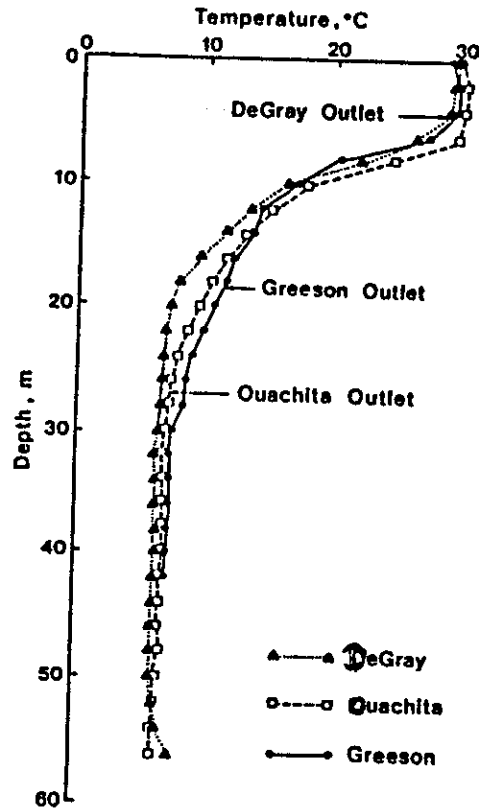
outflows) dominated, is weakly and intermittently stratified, and will exhibit characteristics similar to the inflows. During storms, the residence times of these projects may be only a few hours, indicating that detailed knowledge of the storm runoff may be required to explain and predict the density (thermal) structure of these projects. Fourth, if the mean annual theoretical hydraulic residence time is greater than 20 days but less than 6 months, the stratification will be controlled both by meteorological forcing and advection. In these projects, it is possible for the stratification pattern to vary significantly from year to year.

Specific guidance concerning criteria to evaluate the stratification potential of a reservoir is given in Appendix A.

### 2.3 Potential Energy

Closely related to density (thermal) stratification is the concept

Figure 17. Comparison of temperature profiles from Lakes DeGray, Greeson, and Ouachita, Arkansas, 1982



of potential energy (PE\*). Potential energy is a form of stored energy that a system possesses because of its configuration. The PE associated with density stratification is dependent on gravity and conservative force, and can be fully recovered and converted into kinetic energy. The PE of a reservoir is defined as:

$$(1) \quad PE = mgH = \int_0^{Z_m} g z A(z) \rho(z,t) dz$$

where

- m = the total mass of the reservoir, kg
- g = the acceleration due to gravity, m/sec<sup>2</sup>
- H = height of the center of mass of the reservoir, m
- Z<sub>m</sub> = the maximum elevation, m

\* For convenience, symbols and abbreviations are listed in the Notation (Appendix B).

$z$  = the elevation above the reservoir bottom, m  
 $A(z)$  = the horizontal area of the reservoir at elevation  $z$ ,  
 $m^2$   
 $\rho(z,t)$  = the reservoir density at elevation  $z$  and time  $t$ ,  
 $kg/m^3$

The PE of a reservoir can therefore be changed by heating or cooling to modify the water density and/or by changing the elevation of the center of mass. For a well-mixed body of water, the center of mass is the center of volume. For a stratified body of water, the surface waters are less dense and the center of mass is deeper. The potential energy concept is similar to Birge's wind work and Schmidt's stability (Hutchinson 1957). For example, Schmidt's stability is the change in PE (using Equation 1) between an initial stratified density profile and the resulting isothermal condition following complete mixing.

The significance of the potential energy concept is its relationship with work and kinetic energy (KE) as defined in classical physics. It indicates that work is required to mix a stably stratified fluid since the center of mass must be raised against the force of gravity. For example, completely mixing the two-layered fluid in Figure 18 changed the PE by  $\Delta\rho VH/8$  and raised the center of mass to  $H/2$ .

The PE, as defined in Equation 1, has limitations when applied to reservoirs because the horizontal areas,  $A(z)$ , are much larger and dominate over the small differences in water density,  $\rho(z,t)$ . Additionally, the PE as defined by Equation 1 decreases as stratification increases. A more practical formulation that increases as stratification increases is the relative potential energy (RPE):

$$RPE = \int_0^{z_m} g z A(z) (\rho_m - \rho(z,t)) dz \quad (2)$$

where  $\rho_m$  = maximum density in water column.

If  $\rho_m$  is a constant, the magnitude of the change in PE between two

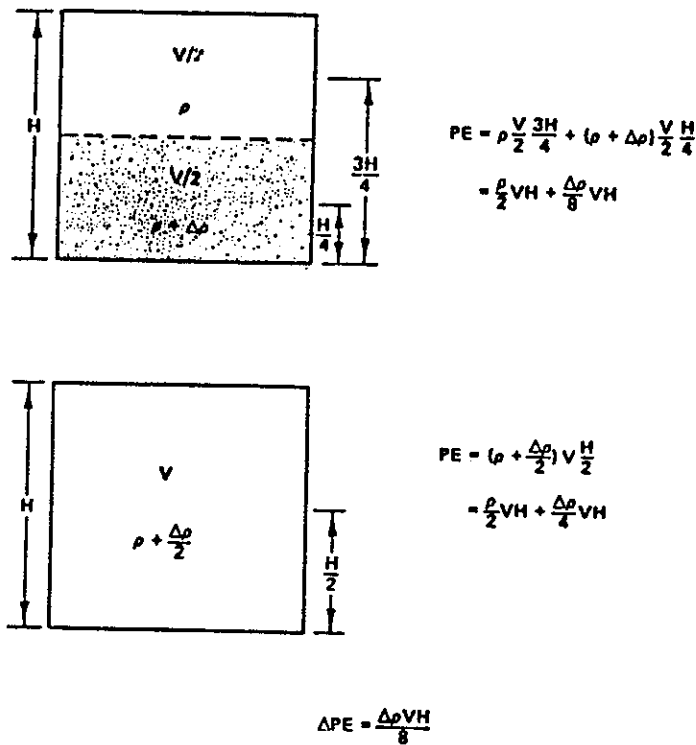


Figure 18. Change in potential energy resulting from destratification of a two-layered system

states computed from either Equation 1 or Equation 2 is the same (Ford 1976) but the signs are opposite.

The RPE's for DeGray and Ouachita Lakes, Arkansas, are shown in Figure 19. In February, the reservoirs are isothermal and the entire water column is mixed vertically. The center of mass is therefore located at the center of volume, and the RPE is small since the water density of the entire column is near  $\rho_m$ . The maximum RPE occurs in mid- to late-July and coincides with the time of maximum stratification. As the reservoirs cool, mixing occurs, and the RPE decreases.

Figure 19 also illustrates two features of Equation 2. First, the larger the lake, the larger the horizontal areas,  $A(z)$ , and the larger the RPE. In Figure 19, Lake Ouachita is significantly larger than DeGray Lake. Second, the weaker the stratification, the smaller the RPE. In 1976, DeGray Lake was operated with surface withdrawal and had

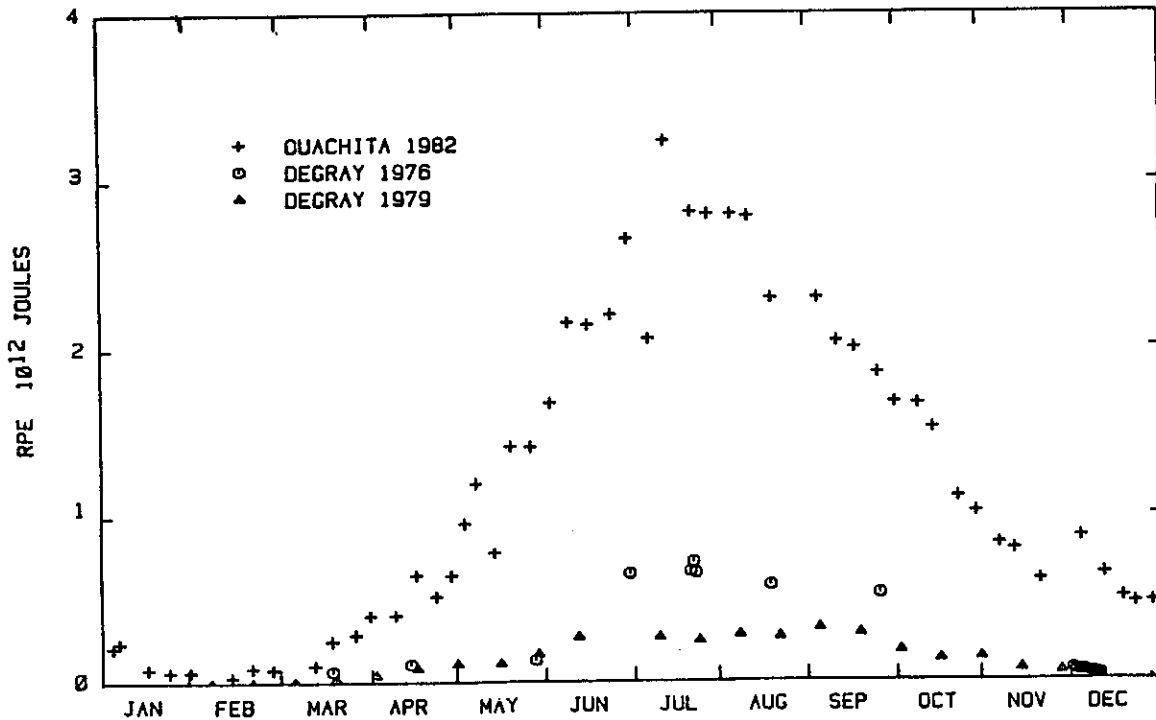


Figure 19. Seasonal variation in potential energy

a stronger stratification than in 1979 when it was operated with bottom withdrawal. The RPE was therefore greater for 1976 than for 1979.

To illustrate how the RPE can be used to explain the annual thermal stratification cycle, the RPE for DeGray Lake in 1979 is compared with the turbulent kinetic energy (TKE) input from the wind and inflows in Figure 20. Specifics concerning the computation of TKE from the wind and inflow rates are described in Sections 3.2.2 and 3.2.5, respectively.

In February, the reservoir was nearly isothermal. The RPE was small since water densities were nearly constant. With little or no stratification, the RPE was not large enough to prevent complete mixing by the TKE. As the water column warmed, stratification increased, RPE increased, and it became more difficult for the TKE to mix the entire water column. Stratification started to form in March at the bottom of the lake (Figure 6) because the density differences and the resulting RPE were small compared to the TKE input from the wind (Ford and Stefan 1980a). As the solar radiation increased, water temperatures increased

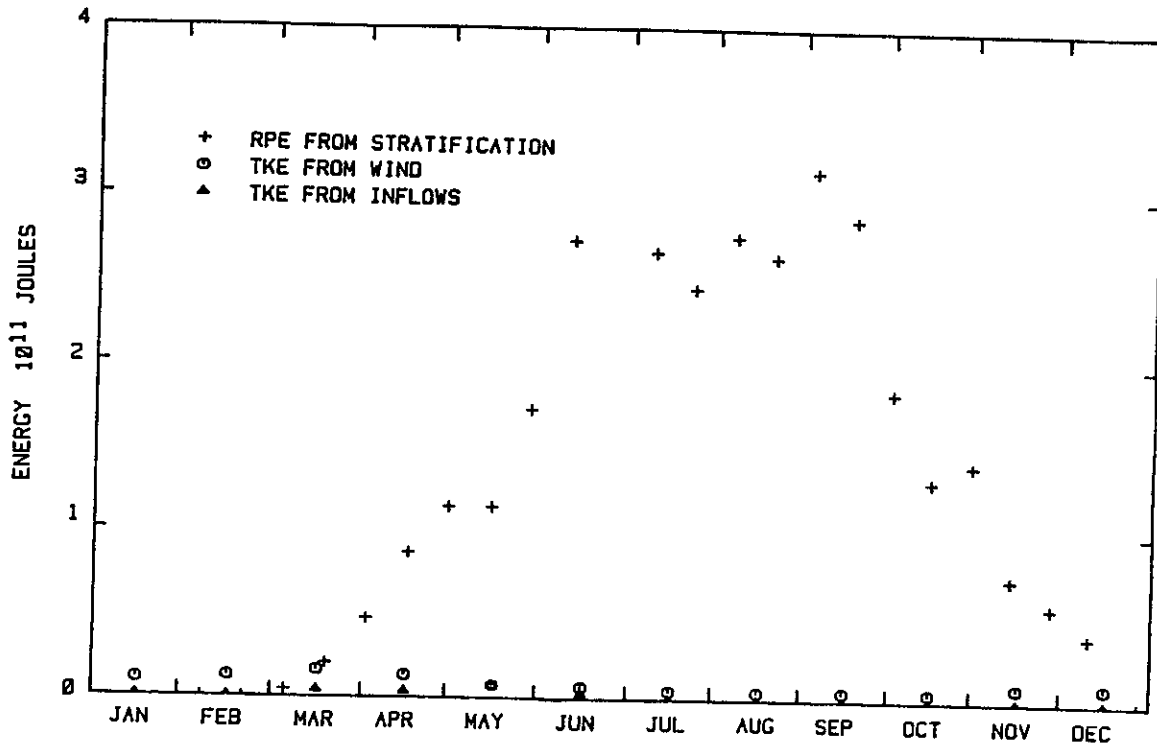


Figure 20. Comparison of RPE with the TKE from the wind and inflows, DeGray Lake, Arkansas, 1979

and the density differences increased; the thermocline moved upward because the TKE input could not overcome the ever-increasing RPE (i.e., buoyancy forces). The maximum RPE occurred in mid- to late-July and coincided with the time of maximum stratification. Once stratification formed, the hypolimnion temperature remained relatively constant until fall overturn. As the reservoir cooled, stratification decreased and the RPE decreased, allowing the available TKE to deepen the thermocline further, and eventually resulted in complete vertical mixing. When comparing the RPE of stratification with the TKE input it is important to note that the RPE varies significantly over the seasonal time scale (i.e., the time scale of stratification) while the TKE is introduced at much shorter time scales (i.e., passage of storms).

Figure 21 compares the TKE from the wind with the TKE from the inflows. Except in May (the wettest month), the TKE from wind is greater, indicating its dominance over advection (inflows) as a source of energy and as a mechanism for mixing.

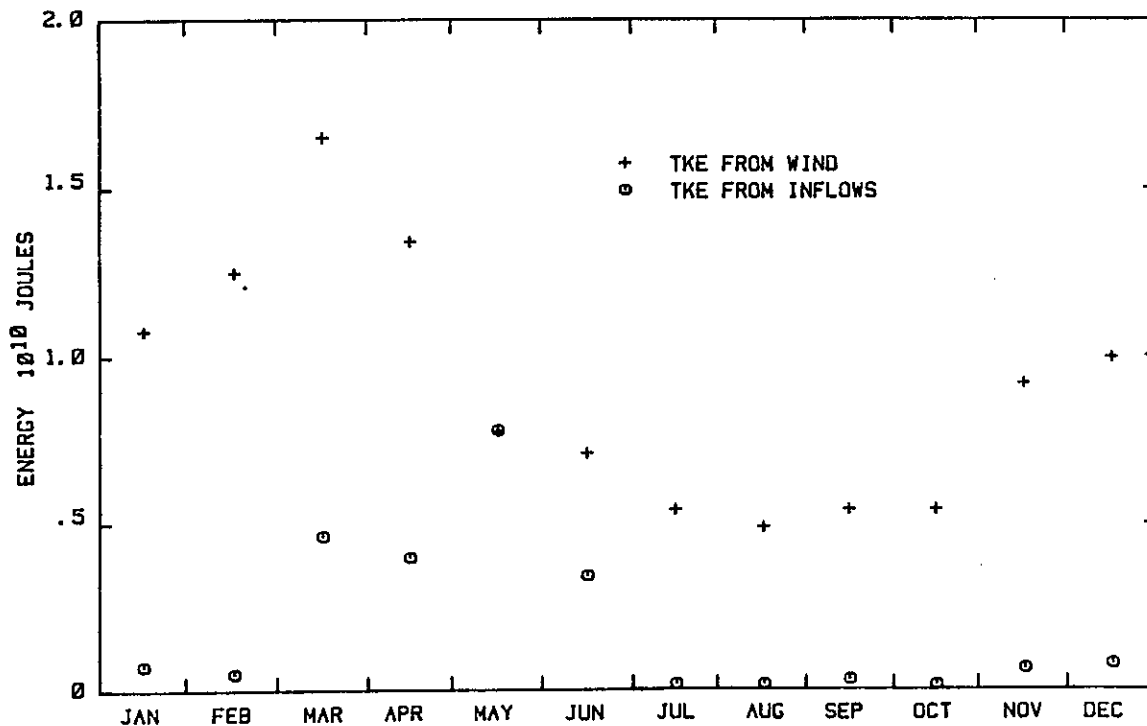


Figure 21. Comparison of TKE from the wind and inflows, DeGray Lake, Arkansas, 1979

#### 2.4 General Transport Processes

There are several fundamental transport or mixing processes which cause a parcel of fluid to blend with other parcels and which occur in any fluid system, including reservoirs. These are advection, shear, molecular diffusion, turbulence and turbulent diffusion, entrainment, convection, and dispersion. Each of these processes will be defined to form a common base for the remainder of the report. The nomenclature of Fischer et al. (1979) will be followed.

##### 2.4.1 Advection

Advection is transport by the mean motion of the fluid (Figure 22a). If the fluid is moving with velocity  $U$ , which has components of  $U_x$ ,  $U_y$ , and  $U_z$  in the  $x$ ,  $y$ ,  $z$  directions, respectively, then the advective transport in the direction of the velocity vector  $U$  is  $UC$  where  $C$  is the concentration of the

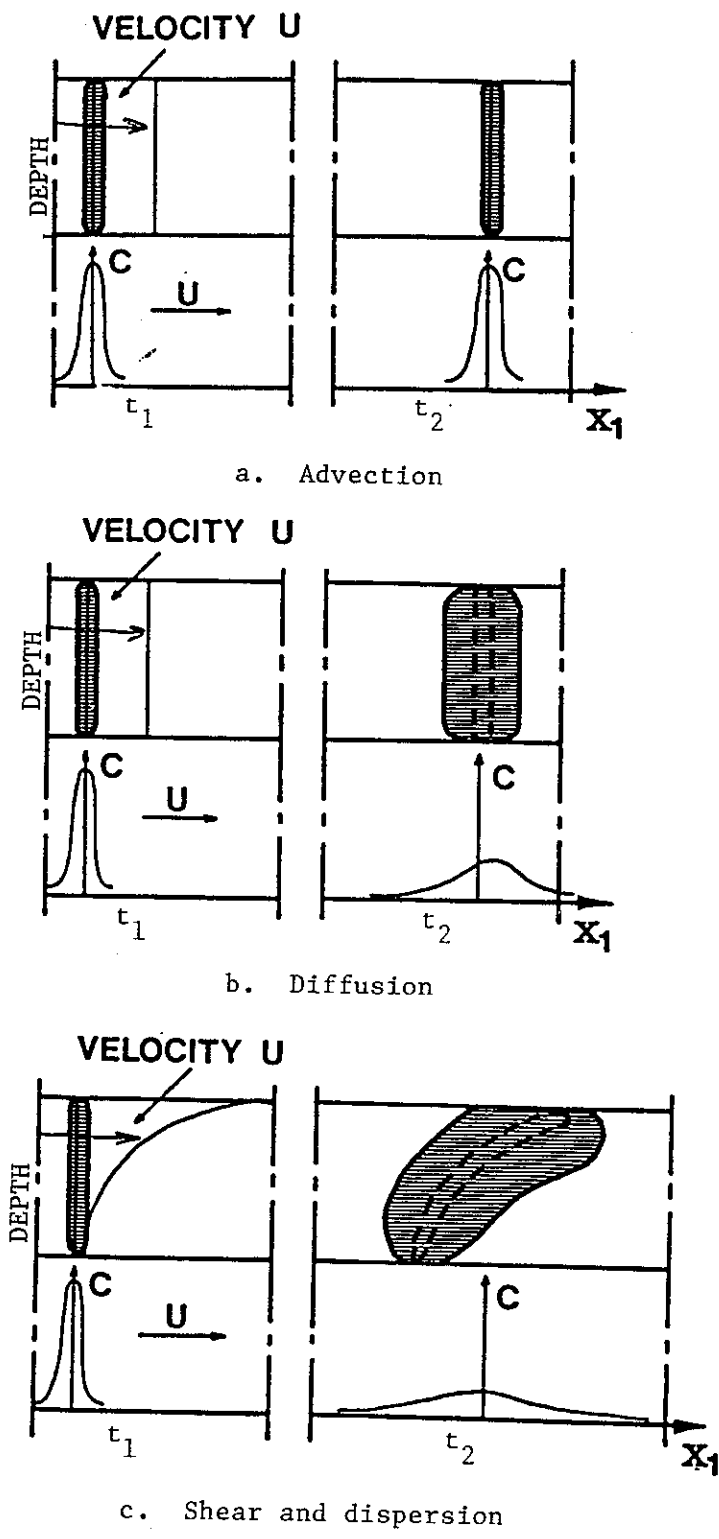


Figure 22. Comparison of advection, diffusion, and dispersion

solute. The advective transport in the x, y, and z directions is, therefore,  $U_x C$ ,  $U_y C$ , and  $U_z C$ , respectively. Since the units of  $U$  are  $L/t$  (length/time) and the units of  $C$  are  $M/L^3$  (mass/length<sup>3</sup>), the units of  $UC$  are  $M/L^2/t$ , which represents the rate of mass transport through the unit area  $L^2$ . For transport by advection only, there will be no change in the concentration  $C$  provided no other transport mechanisms act on the parcel of fluid.

To be transported by advection, a parcel of fluid must be acted upon by a force. For rivers, this force is gravity. In reservoirs, advection may be caused by inflows, outflows, and wind shear at the air/water interface.

#### 2.4.2 Shear

Shear is advection at different speeds at different locations (i.e., flows with velocity gradients are shear flows) (Figure 22c). Friction or shear forces at boundaries cause velocities to be less near the boundaries than in the center of the flow field. Shear flows vary from simple logarithmic profiles typically found in open-channel flow to complex flow patterns in lakes where velocity vectors vary temporally and spatially both in magnitude and direction. In shear flows, mixing or spreading in the direction of flow is caused primarily by velocity gradients. Since the variability in the velocity profile is proportional to the shear velocity  $w_*$  ( $w_* = \sqrt{\tau/\rho}$ , where  $\tau$  = shear stress and  $\rho$  = density) and independent of the mean velocity  $U$ , the longitudinal mixing in a shear flow depends on the shear velocity not the mean flow velocity (Fischer et al. 1979).

#### 2.4.3 Molecular Diffusion

Molecular diffusion is a process by which a certain property of a fluid is transferred down a concentration gradient by the random motion of molecules without any overall transport of the fluid taking place. It is important to understand molecular diffusion because molecular diffusion theory is the basis for the turbulent diffusion theory discussed in Section 2.4.4.

The flux or transport of mass or heat per unit cross-sectional area per unit time in a given direction by molecular diffusion is:

$$q_m = -K_m \frac{\partial C}{\partial x} \quad (3)$$

where

$K_m$  = molecular diffusivity or diffusion coefficient,  $m^2/sec$

$\frac{\partial C}{\partial x}$  = concentration gradient,  $mg/l/m$

The minus sign is required because the transport is from high to low concentrations. The molecular diffusivity is a function both of the solute and the solvent in which it is dissolved (Table 2).

Table 2  
Molecular Diffusion Coefficient of Solutes in Water at 20° C

<u>Substance</u>	<u>Diffusion Coefficient, <math>m^2/sec</math></u>
Temperature	$1.42 \times 10^{-7}$
Dissolved oxygen	$1.80 \times 10^{-9}$
Carbon dioxide	$1.77 \times 10^{-9}$
Nitrogen	$1.64 \times 10^{-9}$
Sodium chloride	$1.35 \times 10^{-9}$

SOURCE: "CRC Handbook of Tables for Applied Engineering Science"  
 (Bolz and Tuve 1976).

The diffusion equation:

$$\frac{\partial C}{\partial t} = K_m \frac{\partial^2 C}{\partial x^2} \quad (4)$$

describes how mass is transferred by molecular or Fickian diffusion. The solution of this equation for an initial slug of mass  $M$  released at a point results in a Gaussian distribution of concentration versus

distance at a fixed time. Two properties of this solution are important. First, differences in mean concentrations are always reduced. Second, the variance always grows linearly with time (Figure 22b).

#### 2.4.4 Turbulence and Turbulent Diffusion

Turbulence is the most important source for mixing in lakes (Ottesen Hansen 1978). It is therefore imperative that turbulence be understood before mixing in lakes (or reservoirs) can be understood.

Most flows occurring in nature (e.g., atmospheric and surface water flows) are turbulent. Two notable characteristics of these flows are: (a) velocities and concentrations at a point in a turbulent flow are unsteady, and (b) mixing is much faster in turbulent flow than in laminar flow.

Turbulence is sometimes described as a family of eddies (i.e., rotating regions of fluid). These eddies or scales of turbulence can range in size from the physical limits of the flow (i.e., physical dimensions of a reservoir) down to molecular motion. At the smallest scales of turbulence, viscosity is important and the motion dissipates into heat. One disadvantage of portraying turbulence as a family of eddies is that it is difficult to separate wave motions from turbulence. According to Steward (1959), a more precise definition of turbulence is:

A fluid is said to be turbulent if each component of the vorticity is distributed irregularly and aperiodically in time and space, if the flow is characterized by a transfer of energy from larger to smaller scales of motion, and if the mean separation of neighboring fluid particles tends to increase with time.

Turbulent flows are therefore irregular (random), diffusive (produce mixing), rotational (three-dimensional vorticity fluctuations), time varying, and dissipative (decay rapidly without a continual source of energy). Turbulent flows are characterized by large Reynolds numbers (order of  $10^6$  in lakes) where energy propagates slowly with the speed of the fluid motion. In contrast, waves can distort a density distribution

but cannot permanently change the stratification profile unless the waves break to produce mixing; waves are dispersive but not dissipative, and energy is transferred rapidly through the fluid (Turner 1973).

The energy associated with turbulence or TKE is defined as

$$\text{TKE} = \overline{(u_x^2 + u_y^2 + u_z^2)}/2 \quad (5)$$

where  $u_x, u_y, u_z$  = turbulent fluctuations in the x, y, and z velocity components, m/sec.

The fluctuating velocity components are related to the instantaneous and mean velocity components by

$$U_x = \bar{U}_x + u_x \quad (6a)$$

$$U_y = \bar{U}_y + u_y \quad (6b)$$

$$U_z = \bar{U}_z + u_z \quad (6c)$$

where

$U_x, U_y, U_z$  = instantaneous velocity components, m/sec

$\bar{U}_x, \bar{U}_y, \bar{U}_z$  = mean velocity components, m/sec

Tennekes and Lumley (1972) develop and discuss this concept in detail.

In lakes, turbulence can be generated directly at a boundary (external process) or internally through a shear instability. The only way a fluid element outside a turbulent region can become turbulent (i.e., acquire vorticity) is through viscous diffusion of vorticity. Once a fluid element is turbulent (i.e., possesses vorticity), its turbulence or vorticity can be amplified by the straining set up by neighboring turbulence. Because of this straining, the vorticity and energy of smaller eddies can increase at the expense of the energy of larger eddies. Energy, therefore, flows from large to small eddies. Without a continual source of energy at the larger scales, turbulence could not be maintained and would rapidly decay. Generally, the larger

eddies move slowly and last longer than the smaller eddies. The larger eddies are also responsible for most of the transport of momentum and mass. At the very small scales, viscosity smooths the velocity fluctuations by dissipating small-scale motion into heat.

Density stratification inhibits turbulence and mixing. The reason for the decreased mixing in a zone of stable density stratification is that turbulent eddies lose energy not only through viscous dissipation, as previously described, but also through the performance of work against gravity in the density gradient (Section 2.3). The Richardson number

$$Ri = \frac{g \frac{d\rho}{dz}}{\rho \left(\frac{dU}{dz}\right)^2} \quad (7)$$

compares the energy required to do work against the density gradient ( $d\rho/dz$ ) with the energy supply of the shearing form ( $dU/dz$ ).

The scattering of particles by turbulent motion can be considered analogous to molecular diffusion with a larger turbulent diffusion coefficient replacing the molecular diffusion coefficient. The turbulence flux  $q_t$  in the x direction is therefore given by

$$q_t = -K_t \frac{\partial C}{\partial x} \quad (8)$$

where  $K_t$  = turbulent diffusion coefficient,  $m^2/sec$ .

The turbulent diffusion coefficient is equivalent to the product of the Lagrangian length scale  $l_L$  and the intensity of turbulence  $\langle u \rangle^{2/3}$

$$K_t = l_L \langle u \rangle^{2/3} \quad (9)$$

where

$\langle \rangle$  = ensemble mean (i.e., mean over many trials)  
 $\langle u^2 \rangle^{1/2}$  = root mean square velocity, m/sec

The Lagrangian length scale is that distance a particle must travel before it forgets its initial velocity. This turbulent diffusion approach is not valid for lengths smaller than  $l_L$  or times less than the Lagrangian time scale (i.e., the time required for a particle to move  $l_L$ ). Individual clouds of dimension less than  $l_L$  grow at a rate that increases with size (i.e., Richardson diffusion) and varies from cloud to cloud. There is an intermediate range where clouds grow in proportion to the 4/3 law (i.e., proportional to  $l_L^{4/3}$ ), but this requires homogeneous turbulence and no boundary effects.

#### 2.4.5 Entrainment

When a nonturbulent body of water is stirred at a boundary, the turbulence generated at that boundary will advance into the nonturbulent regions of the fluid. Entrainment is the term used to describe this one-way advective type transport which is characteristic of most free turbulent shear flows. If the fluid is homogeneous, entrainment will proceed unhindered, and the thickness of the layer being stirred will increase linearly with time until another boundary is reached or another force becomes limiting (e.g., Coriolis effect).

Visual observations in laboratory experiments (Turner 1973) showed the interface between the turbulent and nonturbulent regions to be sharp but convoluted. In the stratified fluids where the densities of the stirred layer and nonturbulent regions differ, turbulence and convolutions at the interface are generally suppressed by buoyancy forces. Under these conditions, entrainment is the result of wisps or thin sheets of fluid being scoured into the turbulent region by turbulent eddies.

The rate at which the mean position of the interface advances into the nonturbulent fluid is usually expressed in terms of an entrainment velocity  $w_e$ . The entrainment velocity is usually assumed to be a

function of the overall Richardson number

$$Ri_* = \frac{g \Delta\rho h}{\rho w_*^2} \quad (10)$$

where

- $g$  = acceleration due to gravity,  $m/sec^2$
- $\Delta\rho$  = density difference between turbulent layer (i.e., layer being stirred) and nonturbulent layer (i.e., layer being entrained),  $kg/m^3$
- $h$  = depth of turbulent layer,  $m$
- $\rho$  = density,  $kg/m^3$
- $w_*$  = shear velocity in turbulent layer,  $m/sec$

such that

$$\frac{w_e}{w_*} = f(Ri_*) \quad (11)$$

There is little reason to expect Equation 11 to be a simple function because of the complex and different physical processes involved in entrainment. It is, however, appealing to assume

$$\frac{w_e}{w_*} = c Ri_*^{-1} \quad (12)$$

where  $c$  = proportionality constant, because the rate of increase of potential energy is then equal to the rate of mechanical energy input. This law, however, falls apart as  $Ri_* \rightarrow 0$  and as  $Ri_* \rightarrow \infty$  (Phillips 1977).

#### 2.4.6 Convection

In order to distinguish vertical transport induced by density instabilities from advective transport generated by other forces or sources of energy, convection is defined as a buoyancy-induced flow that occurs in a fluid when it becomes unstable due to density (temperature)

differences. If the mixed-layer depth increases as heat is removed but no changes occur in the thermal profiles below the mixed layer, the increase in thickness of the mixed layer is termed encroachment by Tennekes and Driedonks (1980) (Figure 23a). If instead, some of the TKE generated by cooling at the air/water interface is used to entrain stably stratified water into the mixed layer and thereby modify the thermal profiles below the mixed layer, the convective entrainment is termed penetrative convection (Figure 23b). Reviews of penetrative convection can be found in Turner (1973) and Denton (1978).

In order to explain the process of convection, Denton (1978) divided the water column into three zones (Figure 24). The thin layer at the water surface is the buoyancy production zone. This layer is a molecular diffusion boundary layer that builds up due to cooling at the air/water interface. At some critical point, the layer becomes unstable and breaks up. At the time of breakup, Denton (1978) observed the formation of long, irregular rolls that eventually broke into single clumps of fluid (thermals). Since these thermals are heavier than the ambient fluid, they sink into the mixed layer. After the breakup of the boundary layer, a new layer begins to form which, in turn, will eventually become unstable and break up. In general, the thickness of the production layer is negligible compared to the total thickness of the mixed layer.

The mixed layer, as implied by its name, is uniformly mixed with respect to all properties. Dye observations and continuous temperature measurements in the mixed layer indicate that the thermals generated in the production layer pass through the mixed layer as discrete elements (not plumes as sometimes described), the net effect being to keep the layer turbulent.

Below the mixed layer is the region of the stably stratified fluid. The density gradient is usually assumed to be discontinuous at the interface to be consistent with entrainment experiments that report a sharpening of the gradient. When the thermals encounter the interface, they penetrate a short distance and sometimes rebound (Linden 1973). Through various mechanisms that are not completely understood,

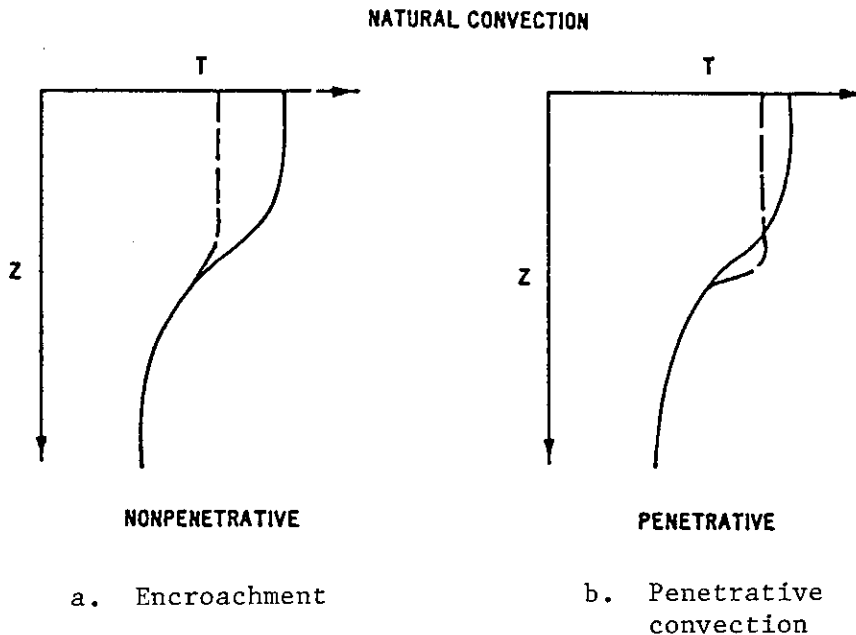


Figure 23. Comparison of encroachment and penetrative convection

some of the stratified fluid is entrained into the mixed layer. According to Tennekes and Driedonks (1980), 10 to 50 percent of the potential energy released during cooling is converted to TKE and used for entrainment. Denton (1978) concluded this fraction is not constant but attains a maximum at a Richardson number of 0.91 and decreases with increasing and decreasing Richardson number. The mixing and entrainment resulting from penetrative convection is restricted to the diffusive layer (Figure 24), which has a thickness of approximately 0.2 times the mixed layer depth.

#### 2.4.7 Dispersion

Dispersion includes the combined effects of shear and diffusion. Shear causes particles to move at different rates. Diffusion causes particles to move across the velocity gradient. After a certain period of time, a particle experiences all velocities and the longitudinal distribution appears Gaussian (Figure 25). The mixing can then be described by

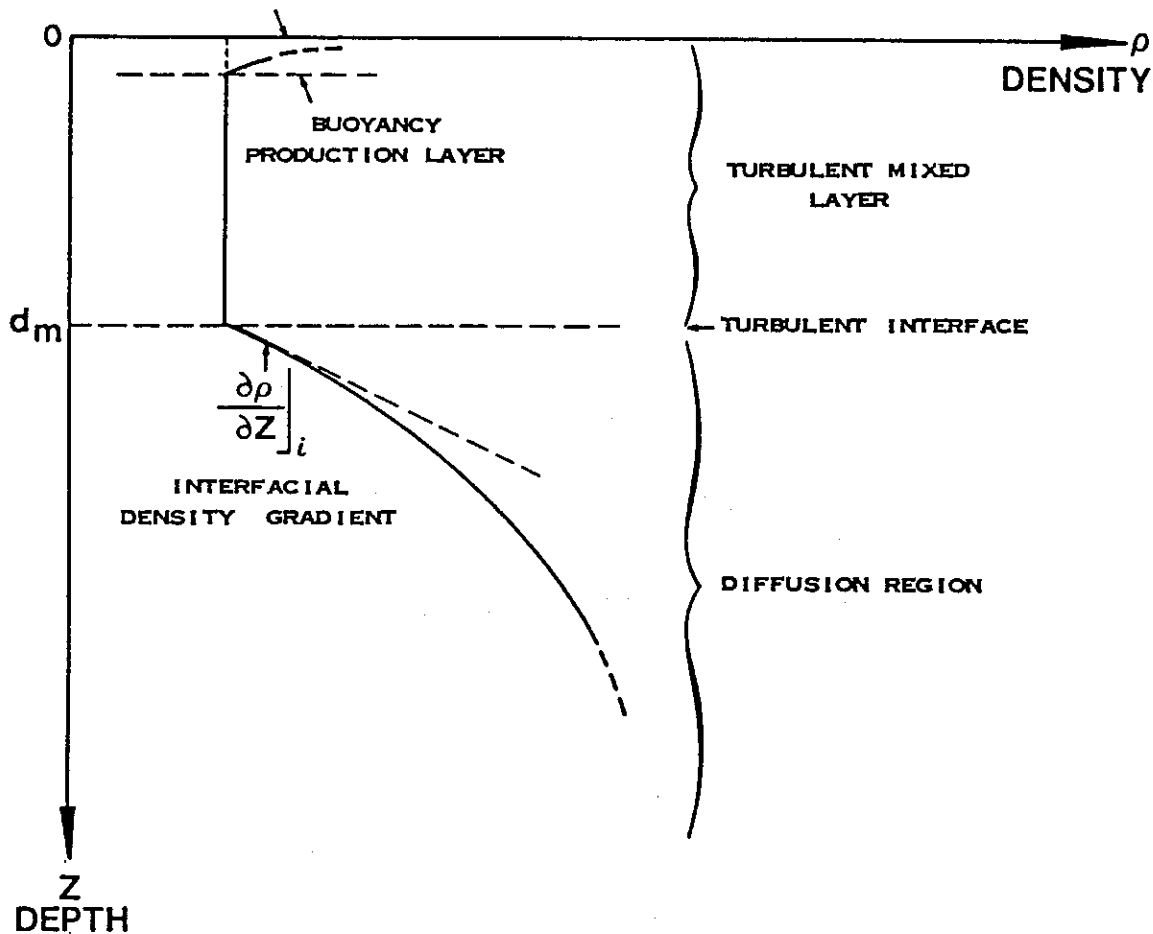


Figure 24. Schematic of convective zones

$$q_d = K_d \frac{\partial C}{\partial x} \quad (13)$$

where

- $K_d$  = dispersion coefficient,  $m^2/sec$
- $q_d$  = flux due to dispersion,  $kg/(m^2-sec)$

In riverine systems, the concentration is sometimes skewed (Figure 25) because of edge effects. Material is trapped along the banks and released at a later time, causing the longitudinal distribution to be skewed in an upstream direction. Fischer et al. (1979) discuss dispersion in detail.

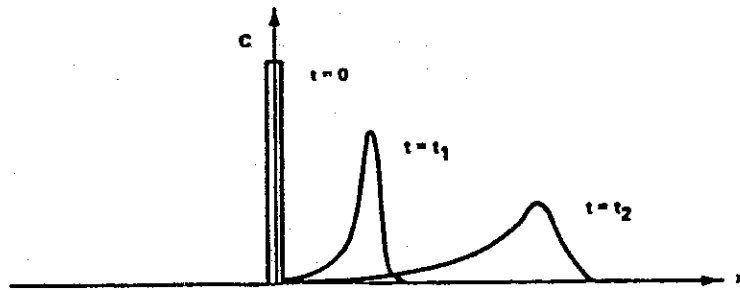
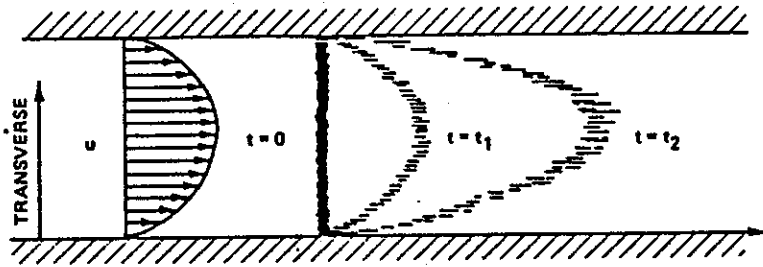


Figure 25. Longitudinal dispersion

## SECTION 3. RESERVOIR MIXING AND WATER QUALITY

### 3.1 Introduction

It was shown in Section 2.3 that energy is required to mix a stably stratified fluid. The energy is used to perform work and raise the center of mass. The major sources of energy potentially available to mix a reservoir are atmospheric heating (cooling), wind, inflows, outflows, barometric pressure, and gravity. Although several reviews have been published on lake mixing and hydrodynamics, these reviews tend to emphasize specific types of lakes or specific mixing processes. In general, these reviews do not consider all aspects of mixing and reservoir operation and their impacts on reservoir water quality. For example, Boyce (1974), Mortimer (1974), and Csanady (1975) reviewed the hydrodynamics of large lakes; Smith (1979) reviewed the hydraulics of isothermal lakes; Ottesen Hansen (1978), Fischer et al. (1979), and Imberger and Hamblin (1982) reviewed mixing mechanisms; Ford and Johnson (1983) reviewed inflow dynamics; Roberts and Dortch (1985) reviewed entrainment of pumped-storage inflow jets; and Imberger (1980) reviewed outflow dynamics and selective withdrawal. In addition, oceanographic reviews on internal waves by Garrett and Munk (1979), mixed layer dynamics by Kraus (1977), and microstructure by Gregg and Briscoe (1979) are directly applicable to mixing in reservoirs.

In this section, reservoir mixing will be reviewed and discussed with respect to energy inputs and water quality impacts. The section concludes with a summary of mixing processes that must be considered when developing a mathematical algorithm to predict water quality changes.

### 3.2 Description of Reservoir Mixing Processes

#### 3.2.1 Atmospheric Heating (Cooling)

The major surface heat exchange processes acting on a water body are summarized in Figure 26. The numbers in parentheses indicate the

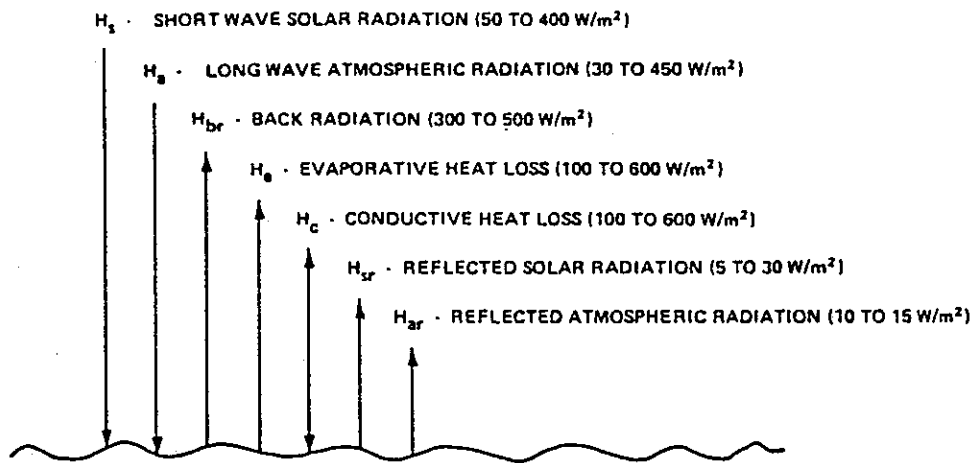


Figure 26. Major heat exchange processes  
(after Edinger, Brady, and Geyer 1974)

relative magnitudes and ranges of mean daily values at midlatitude. A complete description of these processes and their measurement and/or computation can be found in Tennessee Valley Authority (TVA) (1972); Edinger, Brady, and Geyer (1974); and other references. The relative magnitude of these processes depends primarily on the time of day and year, location on the earth's surface (i.e., latitude, longitude, and elevation), surrounding terrain and horizon angle, amount of water in the atmosphere, and meteorological conditions such as air temperature, cloud cover, wind speed and direction, and dew point temperature.

Atmospheric heating and cooling impact the mixing regime in reservoirs by: (a) adding and removing heat, thereby changing the water density and RPE, and (b) producing TKE during periods of heat loss and convective mixing. The seasonal variation in atmospheric heating for central Arkansas is shown in Figure 27. It indicates that periods of cooling and convective mixing typically occur during late summer, fall, and winter when heat losses exceed heat gains. Convective mixing can also occur during the other periods because of diurnal heating and cooling (Figure 28). Hirshburg, Goodling, and Maples (1976) analyzed this mixing process and developed a seasonal temperature model based on this concept. They showed that convective mixing due to diurnal cooling is an important mixing mechanism, but a short time increment ( $\sim 1$  hr) must be used to model convective mixing.

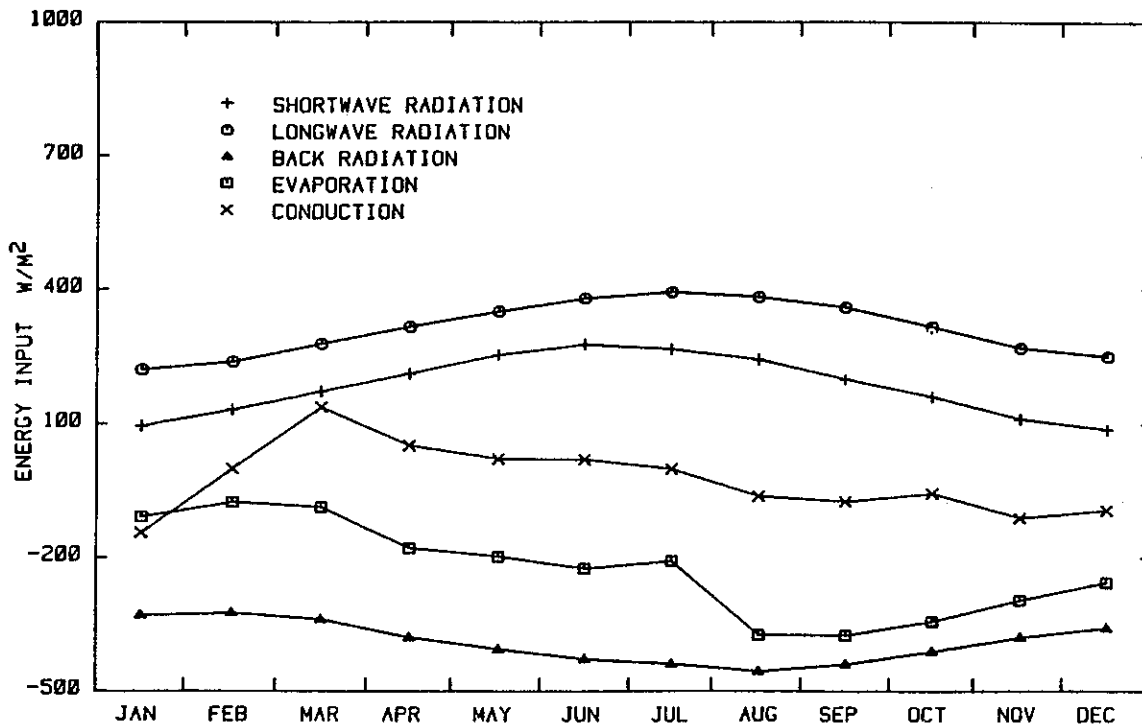


Figure 27. Seasonal variation in atmospheric heating, central Arkansas

### 3.2.2 Wind Processes

The wind is the major source of energy for many physical phenomena which either directly or indirectly cause mixing. These phenomena include surface waves, circulation currents, seiches, internal waves, turbulence, and Langmuir circulation.

Wind shear. When the wind blows across a water surface, it creates a shear stress that transmits energy to the water body (Figure 29). Part of this energy is used for surface waves, part for circulation currents, and part for the direct production of turbulence. The magnitude of the shear stress is determined from

$$\tau_s = \rho_a C_d W^2 \quad (14)$$

where

- $\tau_s$  = surface shear stress,  $\text{kg}/(\text{m}\cdot\text{sec}^2)$
- $\rho_a$  = density of air,  $1.177 \text{ kg}/\text{m}^3$
- $C_d$  = drag coefficient (order of  $10^{-3}$ ), dimensionless
- $W$  = wind speed at a specified elevation,  $\text{m}/\text{sec}$

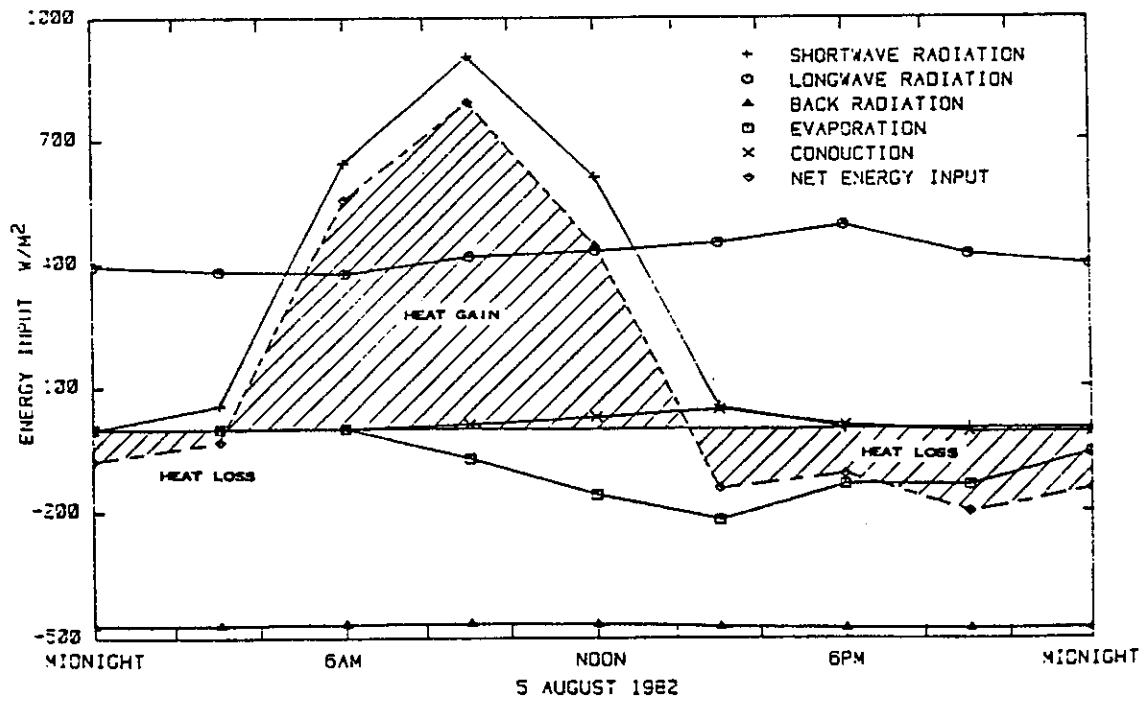
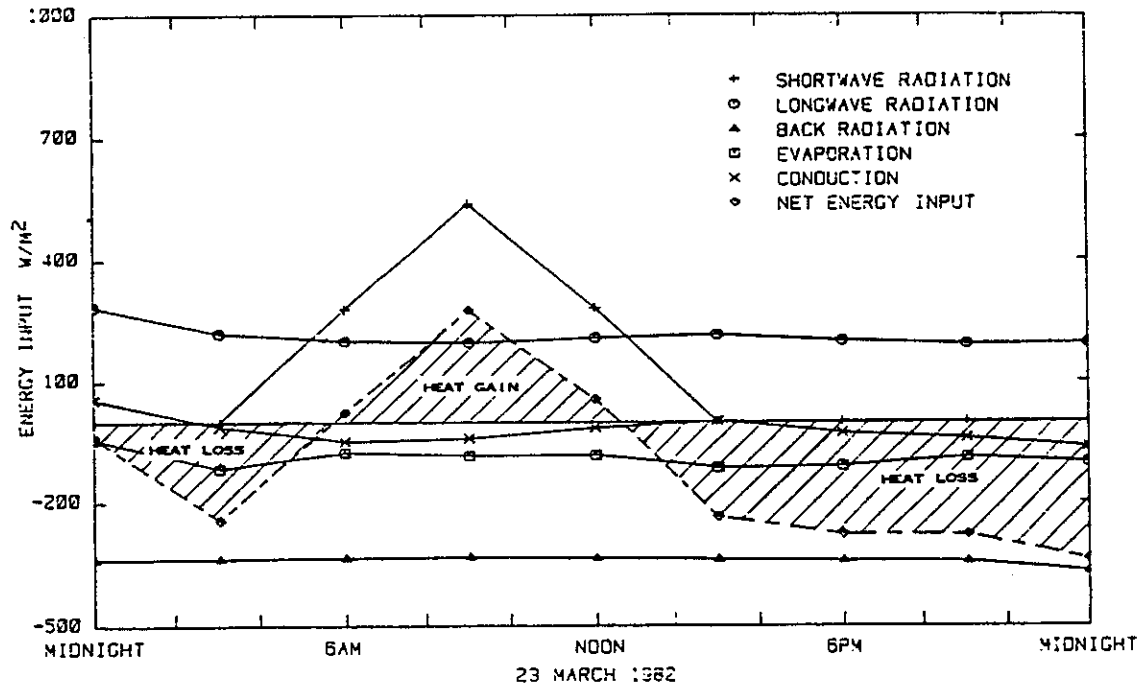


Figure 28. Diurnal heating and cooling cycles for central Arkansas (Continued)

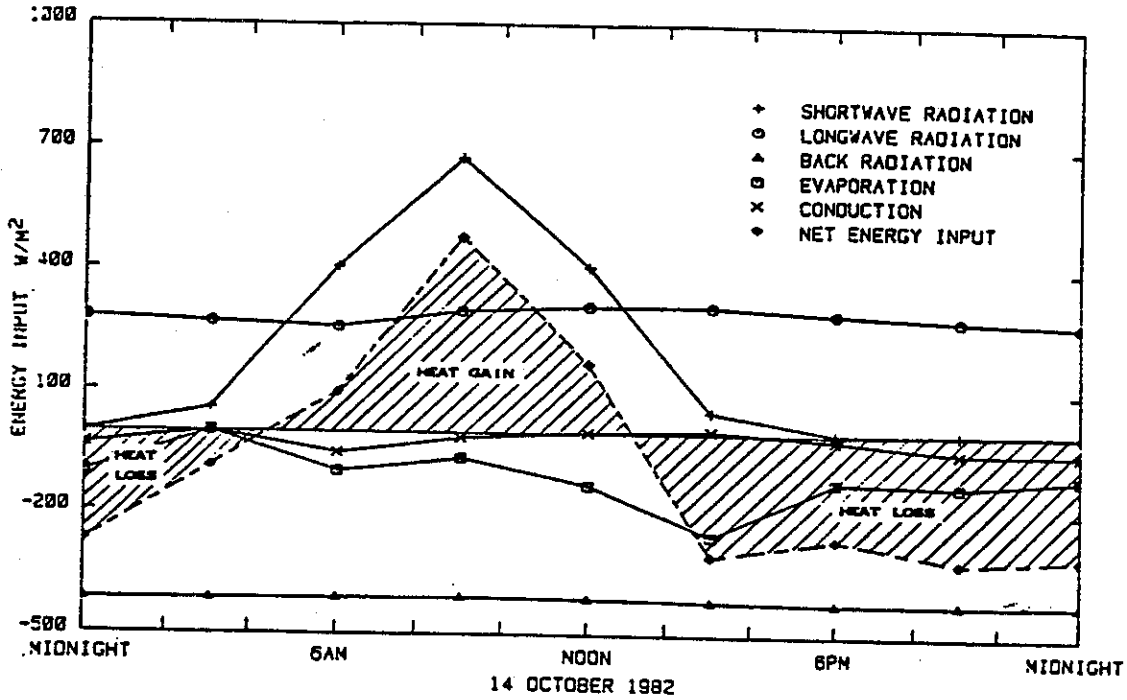


Figure 28. (Concluded)

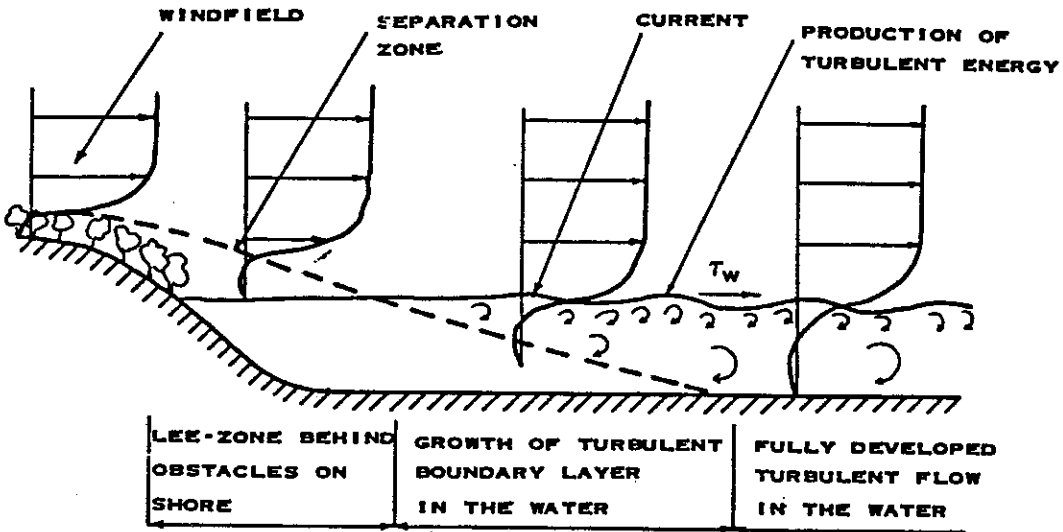


Figure 29. Wind shear on water surface  
(after Ottesen Hansen 1978)

The drag coefficient can be determined from empirical formulas developed by Safaie (1978), Wu (1980), and others. The rate of energy input to the water body is

$$\frac{d(\text{TKE})}{dt} = \int_{A_s} u_s \tau_s dA \quad (15)$$

where

$$A_s = \text{water surface area, m}^2$$

$$u_s = \text{surface drift velocity, m/sec}$$

The surface drift velocity is usually assumed to scale with the wind friction velocity in water ( $w_*$ ), which is defined by

$$w_* = \sqrt{\frac{\tau_s}{\rho_w}} \propto u_s \quad (16)$$

where  $\rho_w$  = water density,  $\text{kg/m}^3$ .

From Equations 14-16, it is evident that the energy available to create waves, turbulence, and currents and, hence, mixing is dependent on the wind speed to the third power and on the surface area of the reservoir. Depending on the surrounding terrain and shape of the reservoir, measured wind speeds and surface areas may not be appropriate for use in Equations 14 and 15. If the terrain surrounding a reservoir consists of high hills, trees, bluffs, etc., the terrain may shelter the water surface from the wind force. As a rule of thumb, the sheltering effects extend into the lake a distance of approximately eight times the vertical elevation (Ford 1976). The wind speed can also increase over a water surface because of the decrease in surface roughness going from land to water. Using boundary layer theory, Ford and Stefan (1980b) developed a relationship to predict the increase in wind speed based on fetch and roughness lengths. For complete reviews on this subject, the reader is referred to Haugen (1973) and Smith (1975). Dendritic reservoirs with many islands may experience funneling and variability in wind speed and direction which further complicate the determination of wind shear.

Surface waves. The significance of wave action with respect to mixing results from the orbital motion of water particles beneath the water surface (Figure 30). In isothermal lakes or in the mixed layer of a stratified lake, the depth of water affected by wave action is approximately one-half the wave length ( $\lambda$ ) (Smith 1979). This depth is also used to define the shore zone or that region of a lake where the wave form is distorted by bottom interference.

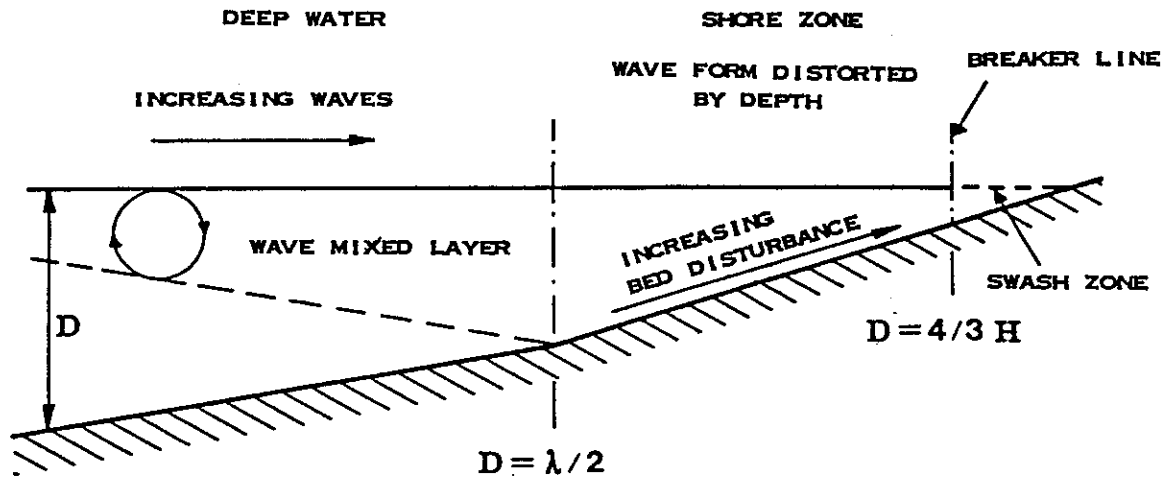


Figure 30. Schematic of surface waves (after Smith 1979)

The waves become unstable and break when the water depth is equal to four-thirds the wave height ( $H$ ). This point is the break line and defines the swash zone as the area where the waves break out of shore. Since the orbitals are not truly circular and do not completely close, there is a net transport by wave motion in the direction of the wind. This transport is usually negligible compared to the transport by currents (Smith 1979).

### 3.2.3 Circulation Currents

General. Circulation currents are averaged water movements controlled by Coriolis, external, and friction forces. Circulation patterns in reservoirs are complicated by basin configurations, density stratification, fluctuating wind speeds and directions, reservoir

operating plans (e.g., hydropower and flood control), and secondary circulations from differential heating and convective currents. In addition, the principle of continuity requires that any movement of water out of any part of a reservoir be balanced by the return of an equal volume of water or a change in water surface level.

Coriolis forces, which result from the earth's rotation about its axis, cause currents in the northern hemisphere to deflect to the right when looking in the direction of the flow. For example, Pharo and Carmack (1979) determined that Coriolis effects caused the Thompson River inflow to Kamloops Lake, British Columbia, to be deflected along the shore. According to Mortimer (1974), Coriolis forces or rotational effects become significant when the width of a lake is greater than  $5r$  and dominant when the lake width is greater than  $20r$ . The radius of the inertial circle  $r$  is defined by

$$r = \frac{U}{f} \quad (17)$$

where

$U$  = water velocity, m/sec

$f$  = Coriolis parameter ( $f = 2\bar{\omega} \sin \phi$ )

$\bar{\omega}$  = angular velocity of the earth's rotation  
 $(7.29 \times 10^{-5} \text{ rad/sec})$

$\phi$  = latitude

For a typical velocity  $U$  of 0.1 m/sec and a latitude  $\phi$  of 40 deg,  $r = 1.06$  km and rotational effects become significant for lakes with widths greater than 5 km. Because  $r$  is inversely related to the sine of the latitude  $\phi$ , rotational effects become significant at a smaller width with increasing latitude. In large lakes, which are dominated by rotational effects, the classical Ekman spiral can limit the depth of the upper mixed layer to the Ekman layer depth and thereby affect the mixing regime (Smith 1979).

The wind is a major external force governing circulation patterns in lakes and reservoirs. As previously discussed, the fraction of the

wind shear that is used to generate currents is unknown. It is, however, usually assumed that the surface current speed is 1 to 3 percent of the wind speed. Bengtsson (1978) and others have found that: (a) the percentage is not a constant even for a specific case, (b) the percentage decreases with increasing wind speed, and (c) the percentage increases with increasing lake dimensions. Figure 31 illustrates the complex surface current patterns that can develop in a lake. Although

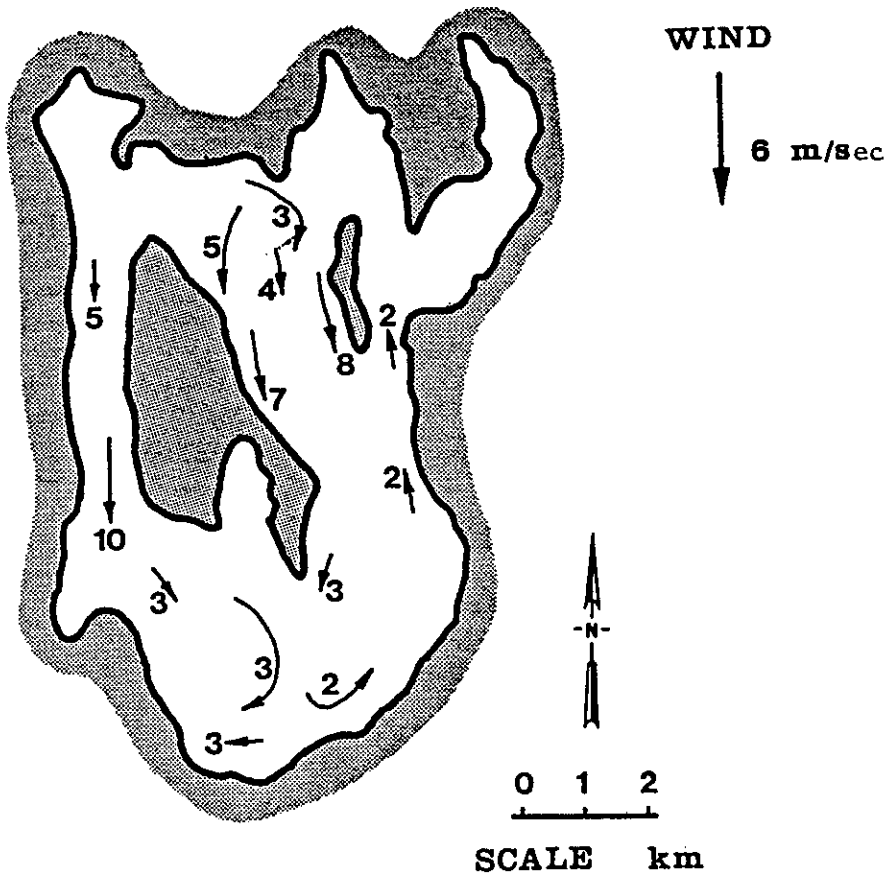


Figure 31. Surface currents in Lake Ivo, Sweden (after Bengtsson 1978)

it is usually assumed that the current speeds decline exponentially with depth, the actual shape of the current vertical profile will depend on the nature of all external forces, stratification, inflow and outflow distributions, and the location of all lake boundaries. Friction at the lake boundaries causes a boundary layer to form that can be described by

a logarithmic velocity profile such that the current speed at the bed is zero. The random variability of the wind and the geometrical complexities of reservoir basins result in a temporally changing and spatially nonuniform water. Smith (1979) discusses many of these and other factors controlling lake circulation in detail.

In reservoirs, the existence of well-defined inflow density currents (Ford and Johnson 1983), withdrawal zones (Bohan and Grace 1973, Imberger 1980), and possibly pumpback jets (Roberts 1981) probably significantly perturbs classical wind-generated circulation patterns, but little is known of these interactions. In addition, reservoir operating procedures that result in pool-level fluctuations also generate currents that must interact with the wind-generated current field. Again, little is known about the synergistic effects of these currents and mixing mechanisms except that, once water is set in motion, it cannot respond instantaneously to a change in flow regime.

Seiches. When a steady wind blows across a water surface, water is transported to the windward side of the lake and the water surface slope is determined by

$$S = \frac{\Delta D}{L} = \frac{\tau_s}{\rho g D} \quad (18)$$

where

- S = water surface slope
- $\Delta D$  = setup of water surface, L
- L = length of lake, L
- $\tau_s$  = surface shear stress,  $F/L^2$
- D = water depth, L

In this equation, the wind force is balanced by the change in hydrostatic pressure. If the water body is stratified such that it can be represented as a two-layered system, the interface responds to the wind force by tilting in the opposite direction (Figure 32) with a slope of

$$S_i = \frac{\tau_s S}{\rho g D_i} \quad (19)$$

where

$S_i$  = interface slope

$\Delta\rho$  = density difference between two layers,  $m/L^3$

$D_i$  = thickness of top layer, L

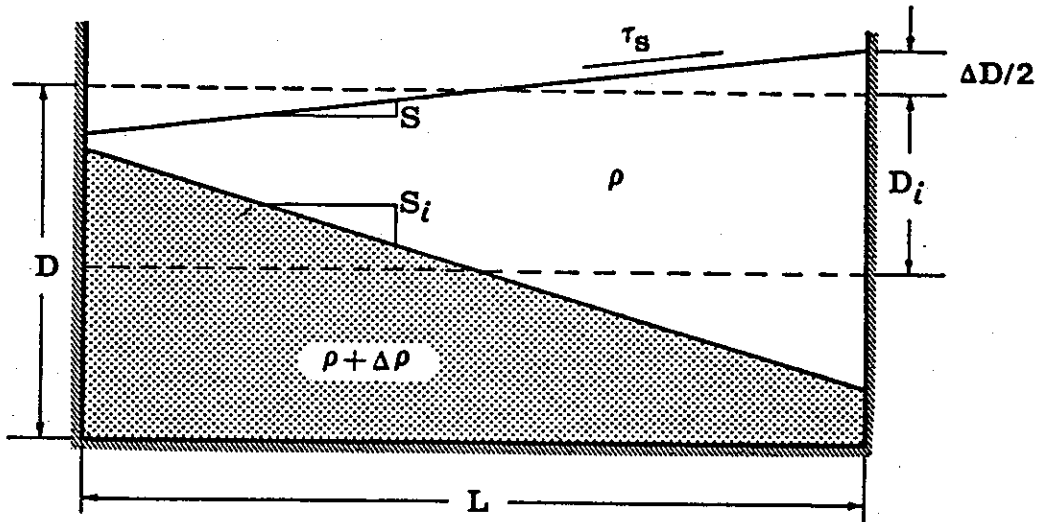


Figure 32. Nomenclature for an internal seiche

If the wind force ( $\tau_s$ ) is sufficiently large, the interface slope may become large enough so that the lower layer is exposed to the water surface. This phenomenon is termed upwelling and can result in the hypolimnetic water being mixed into the surface waters (Blanton 1973).

When the wind force is removed, the potential energy associated with the water surface and interface is converted into kinetic energy and flow. The result is an oscillating motion called seiching, which decays with time. The time for one cycle of the surface seiche (i.e., the seiche period) is

$$t_s = \frac{2L}{\sqrt{gD}} \quad (20)$$

where the terms are as previously defined. A seiche is one indirect mechanism for energy from the wind to become available for mixing in the hypolimnion of a lake. A more detailed review of seiches and upwelling is found in Monismith (1983).

#### 3.2.4 Internal Waves

All stably stratified fluids possess the ability to sustain internal wave motion. The waves can be generated locally by turbulence or externally by an outside perturbation such as hydropower operation. Internal waves transport momentum and can exist without breaking and forming turbulence. It is only after they break that turbulence is generated and mixing is possible.

Internal waves impact the mixing regime because they radiate energy away from the place where they were generated. They can reduce entrainment into the mixed layer by creating a local energy loss from the mixed layer (Kantha, Phillips, and Azad 1977). Internal waves can increase mixing by transporting energy into a region where it would not otherwise be available.

Turbulence. Part of the energy input from the wind shear is used to directly produce turbulence and TKE. This turbulence interacts with turbulence produced by breaking waves (surface and internal), cooling at the air/water interface, and current shear to keep the upper layer (epilimnion) well mixed and to entrain metalimnetic water into the epilimnion. If the turbulence is generated at a length scale less than the thickness of the mixed layer, viscous dissipation with depth will result in a negligible fraction of the energy being available for entrainment at the epilimnetic/metalimnetic interface. If there is a simultaneous heat (buoyancy) flux across the air/water interface, all of the wind-generated TKE may be used to maintain the well-mixed layer and not be available for additional entrainment.

Langmuir circulation. Langmuir circulations are counter-rotating concentric vortices in the surface layers of water bodies (Figure 33). Their existence is readily observed because materials accumulating in the zones of convergence appear as streaks or bands on the water

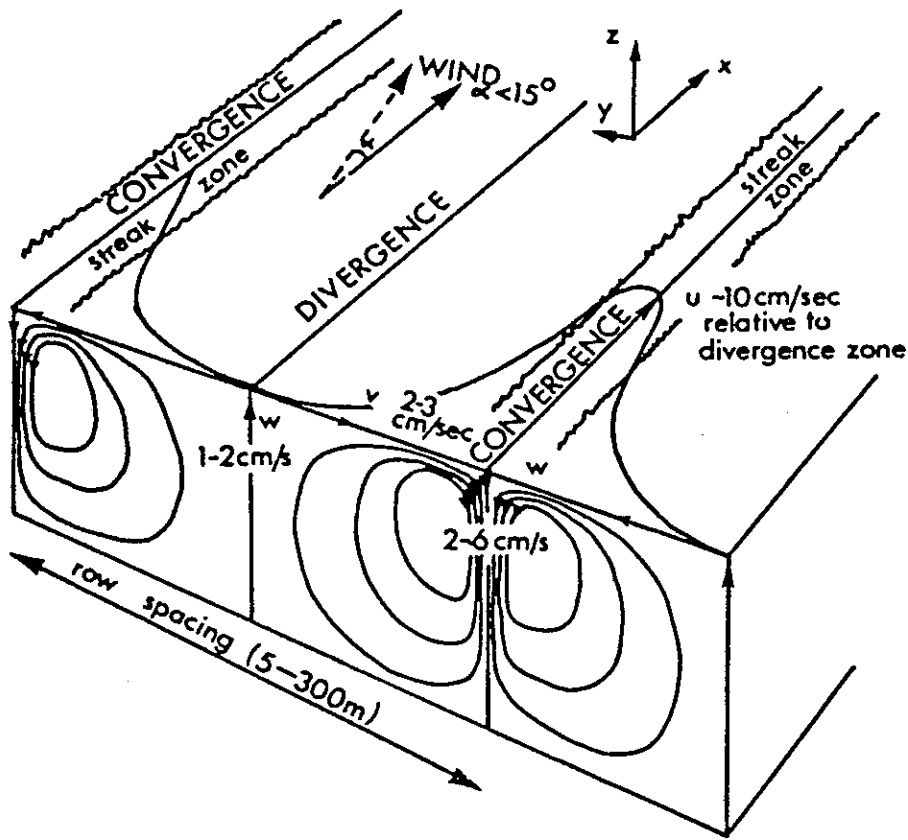


Figure 33. Schematic of a Langmuir circulation cell (after Pollard 1977)

surface. In some instances, compressed films dampen the capillary waves, giving the streaks a smoother appearance. Langmuir (1938) was the first to show that the commonly observed surface streaks or windrows were a manifestation of a more complex circulation pattern related to the wind. Langmuir also concluded that the vortices were responsible for the formation of stratification and the maintenance of a well-mixed layer. Recent laboratory and theoretical studies have shown that both waves and current shear are required for the Langmuir cells to form (Leibovich 1983). Earlier models that related the formation of Langmuir circulation to instabilities and thermal convection are now considered invalid. In a comprehensive review of Langmuir circulation, Leibovich (1983) summarizes the results from several field studies. These include:

- a. Langmuir cells form and align within a few degrees of the wind direction.
- b. Cells form within a few minutes of onset of a wind of 3 m/sec or faster.
- c. Spacing of windrows varies from 1 m to hundreds of metres.
- d. Depth of penetration of cells is limited to the first significant density gradient.
- e. The spacing between the largest windrows is approximately twice the depth of the cells.

Although there is evidence to suggest Langmuir cells are important mixing mechanisms in reservoirs, there is no direct proof (Leibovich 1983).

### 3.2.5 Inflows

Since tributary inflow density usually differs from the density of the reservoir surface waters, inflows enter and move through reservoirs as density currents. Depending on the sign and magnitude of this density difference, density currents can enter the epilimnion, metalimnion, or hypolimnion (Figure 34) and thereby modify the mixing regime in these regions since inflows are a source of both buoyant potential energy and turbulent kinetic energy. The rate of the PE input is dependent on the inflow density, the flow rate, and the in-lake density distribution:

$$\frac{d(PE)}{dt} = \frac{d}{dt} (mgH) = \Delta\rho_j Q_j g Z_j \quad (21)$$

where

- $\Delta\rho_j$  = density difference between inflow and reservoir surface waters,  $kg/m^3$
- $Q_j$  = inflow rate,  $m^3/sec$
- $Z_j$  = difference in depth between center of mass of inflow and center of mass of inflow placement, m

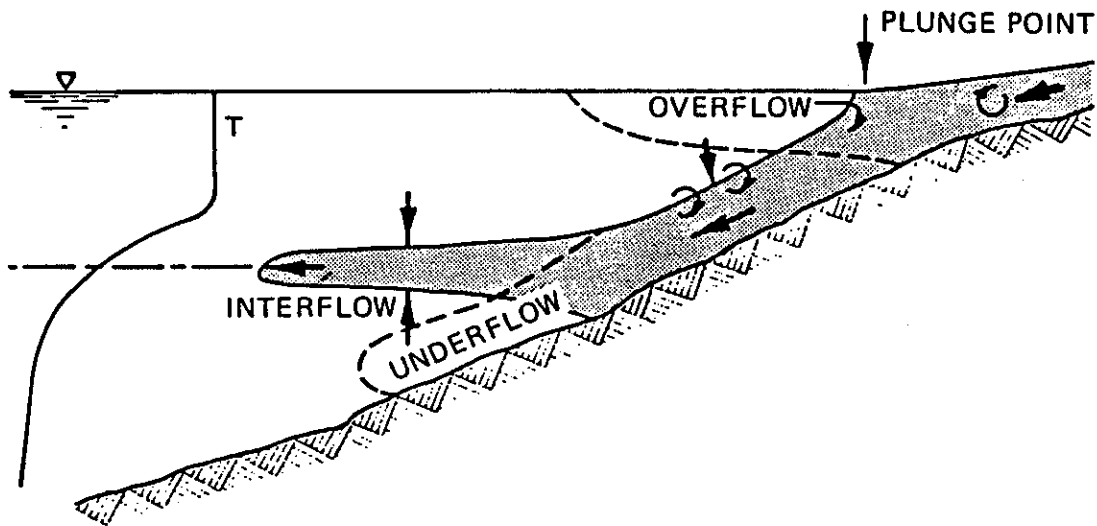


Figure 34. Inflow density currents

The rate of TKE input is also dependent on the flow rate:

$$\frac{d}{dt} (\text{TKE}) = \frac{d}{dt} \left( \frac{1}{2} m U_j^2 \right) = \frac{1}{2} \rho_j Q_j U_j^2 \quad (22)$$

where

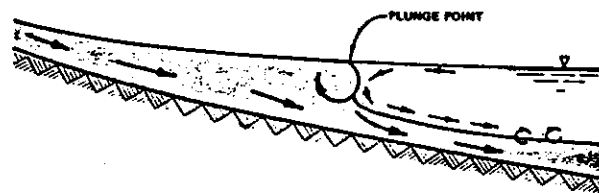
- $U_j$  = inflow velocity =  $Q_j/A_j$ , m/sec
- $\rho_j$  = inflow density,  $\text{kg/m}^3$
- $A_j$  = cross-sectional area perpendicular to inflow,  $\text{m}^2$

Since the mixing resulting from inflows is dependent on the energy input, the magnitude of inflow mixing is highly dependent on the flow rate. A complete analysis of reservoir inflows is found in Ford and Johnson (1983).

When the inflow density is less than the surface water density, the inflow will float on the water surface as an overflow. This condition typically occurs in the spring when inflows warm more rapidly than reservoirs. In an overflow, the excess hydrostatic pressure in the density current causes the current to flow in all directions not obstructed by boundaries. Overflows are susceptible to mixing from wind-induced mechanisms and diurnal heating and cooling processes. Wind

shear can direct the overflow into a cove or prevent it from moving downstream. Vertical mixing in the mixed layer can be enhanced with an overflow if the density difference is small and flow rate is large (i.e., large TKE input) or suppressed if the flow rate is small and density difference is large (this situation frequently exists with thermal discharges).

If the inflow density is greater than the water surface density, the inflow will push the reservoir water ahead until the buoyancy forces dominate and the inflow plunges beneath the water surface. The plunge point is sometimes made visible because of turbidity or the accumulation of floating debris, which may indicate a stagnation point. The location of the plunge point is determined by a balance between the stream momentum, the pressure gradient across the interface separating the river and reservoir waters, and the resisting shear forces. Some mixing (termed initial mixing) occurs at the plunge point because of the large eddies formed by flow reversals and pooling of the inflowing water (Akiyama and Stefan 1981). Ford and Johnson (1983) estimated this mixing to be on the order of 25 percent of the inflow volume. Knapp (1942) noticed that the flow in the vicinity of the plunge point occurred at the bottom of this pooled mixing zone (Figure 35). Ford, Johnson, and Monismith (1980) and Kennedy, Gunkel, and Carlile (1983) substantiated this pooling phenomenon during dye studies on DeGray Lake, Arkansas, and West Point Lake, Georgia, respectively, when the dye clouds appeared to have stalled at the plunge point. The location of the plunge point can also be influenced by morphological factors. Changes in the bed slope (e.g., due to sediment deposition), bed friction, and cross-sectional area may



MIXING AT PLUNGE POINT

Figure 35. Flow in the vicinity of the plunge point

affect location of the plunge point. For a river entering a wide lake, the plunge point may actually be a point rather than a line.

After the inflow plunges, it follows the old river channel (thalweg) as an underflow. The speed and thickness of the underflow is determined by a flow balance between the shear forces and the acceleration due to gravity (i.e., gradually varying flow theory). An underflow will entrain overlying reservoir water due to shear and turbulence generated by bottom roughness. Changes in the underflow density from entrainment must be quantified before a density interflow or intrusion can be analyzed, or estimates of the vertical placement of an interflow can be incorrect.

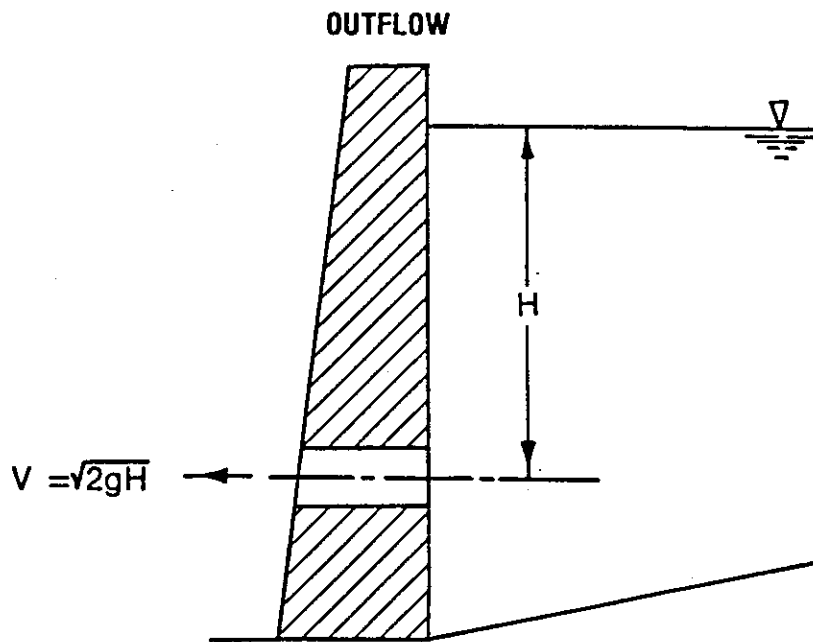
An interflow or intrusion occurs when a density current leaves the river bottom and propagates horizontally into a stratified body of water. Intrusions differ from overflows and underflows because an intrusion moves through a reservoir at a elevation where the intrusion and reservoir densities are similar. Intrusions require a continuous inflow and/or outflow for movement, or they stall and collapse (i.e., dissipate). Turbulence is usually quickly dissipated in an intrusion since the metalimnetic density gradient creates strong buoyancy forces which inhibit mixing. Mixing still occurs, however, because of the flow gradient.

### 3.2.6 Outflows

Manmade reservoirs differ from natural lakes in many respects, but especially with respect to the importance of outflows. In natural lakes, outflows are usually uncontrolled surface withdrawals with the outflow rate dependent on the water surface elevation. In reservoirs, outflows are usually regulated by gates and/or a structure, and the withdrawal depth is not necessarily near the water surface. For example, many flood control projects have bottom outlets while multipurpose projects may have multilevel outlets (i.e., selective withdrawal structures).

Outflows contribute to the in-lake mixing regime through withdrawal currents and turbulence associated with them. Withdrawal

currents are generated because the PE associated with the water level (i.e., the head) is converted into TKE and causes water to flow through an outlet (see Figure 36). The characteristics of the withdrawal currents will be dependent on the withdrawal rate (i.e., gate or structure setting), ambient in-lake stratification, outlet location, and lake geometry. If the outlet is located in the hypolimnion of a strongly stratified lake, the withdrawal zone may also be limited to the hypolimnion of the lake. Withdrawal zones can also be limited to the epilimnion or metalimnion of a lake depending on the outlet location, flow rate, and ambient stratification. Withdrawal zones can be computed using formulas provided by Bohan and Grace (1973), Imberger (1980), and Davis, Holland, and Wilhelms (1985).



$$\frac{d}{dt} (KE) = \frac{1}{2} V^2 \frac{dm}{dt} = \frac{1}{2} V^2 \rho Q$$

Figure 36. Energy conversion associated with an outlet

### 3.2.7 Barometric Pressure and Gravity

On large lakes, horizontal variations in barometric pressure can result in surface seiching. As indicated in Section 3.2.2., seiching

can impact the mixing regime as internal waves and seiches form and break. Tidal movement resulting from the gravitational attraction of the moon and the sun has been observed in very large lakes (e.g., Lake Superior, Minnesota and Wisconsin, and Lake Baikal, Siberia) (Wetzel 1983) but is probably negligible in most reservoirs.

#### 3.2.8 Summary

In the preceding discussion of reservoir mixing, it was shown that the observed thermal structure in a reservoir results from the cumulative effects of a number of complex, nonlinear, interdependent mixing processes. Although the sources of TKE for mixing are limited (i.e., solar and atmospheric heating, wind, inflows, and outflows (including outlet location)) and well known, quantitative knowledge of specific mixing mechanisms is limited. TKE budgets for the entire lake do, however, clearly expose the physical causes of observed motion and thermal stratification.

The observed temperature structure in a lake is actually a signature of past mixing events. The relative timing of these events is important. For example, the occurrence of spring floods after stratification forms can result in a significantly different thermal structure than if the floods occur prior to stratification. Identification of the mixing events is crucial to understanding the thermal structure of a lake.

### 3.3 Influence of Mixing on Reservoir Water Quality

While the mixing mechanisms of inflows and outflows, upwelling and seiches, turbulence, and others are highly interactive, the influence of each of these processes on chemical and biological processes will be discussed separately for convenience. It must be recognized, however, that reservoir water quality is a function of the interactions among the dynamic mixing processes and of the chemical and biological responses to mixing.

### 3.3.1 Inflows and Outflows

Reservoir inflows usually represent the major contributions of both dissolved and particulate constituents to the reservoir mass budget. Ground-water and atmospheric contributions are generally minimal.

As an inflow enters the lake, velocity and turbulence decrease, coarse particulate or suspended materials settle, and the water clarity increases. Turbulence generated through bottom shear generally is sufficient to maintain silt- and clay-sized particles in suspension. Nutrients, bacteria, and organic constituents may be transported into the reservoir since these constituents generally sorb to particles in the clay-silt size range (Frink 1969; Pita and Hyne 1974; Sharpley and Segers 1979; De Pinto, Young, and Martin 1982). Depending on the density structure of the lake and inflow, the inflow can enter the epilimnion, metalimnion, or hypolimnion (Figure 34).

An overflow situation may have the greatest initial influence on reservoir water quality by introducing oxygen-demanding material, nutrients, and bacteria directly into the surface waters or euphotic zone. Available nutrients can be assimilated by phytoplankton and may stimulate plankton blooms; bacteria concentrations may exceed body contact recreation standards; and oxygen-demanding material may depress mixed-layer dissolved oxygen (DO) concentrations. Even though the euphotic zone thickness would probably be decreased due to increased turbidity, circulation and mixing in the mixed layer would circulate phytoplankton between the nutrient-rich inflow and euphotic zone. With overflow conditions, phytoplankton concentration would probably attain a maximum in the headwater regions and decrease in the downstream direction (Kimmel, Lind, and Paulson 1984).

Interflows and underflows have similar influences on water quality. At the plunge point, the inflow waters sink to form a density current flowing along the bottom. Bottom-generated turbulence results in entrainment of surface waters into the density current. This also may

introduce nutrients, organic matter, and bacteria into the overlying surface water and euphotic zone.

Once the density current enters the metalimnion as an interflow, the inflowing constituents are temporarily isolated from the mixed layer. These constituents may be entrained into the mixed layer during storm events if wind gusts deepen the mixed layer or as the thermocline erodes due to penetrative convective mixing. Since the metalimnion is isolated from oxygen exchange with the surface, oxygen-demanding material in the interflow may depress metalimnetic DO concentrations. In most stratified reservoirs, a metalimnetic DO minimum typically develops with anoxic conditions developing in some systems (Hannan and Cole 1984).

Underflows not only introduce inflowing constituents into the hypolimnion but also increase turbulent diffusion across the sediment/water interface because of bottom shear. This can increase oxygen depletion by increasing oxygen transfer across the diffusion-limited sediment/water interface. It also can increase the transfer of reduced and resolubilized constituents such as ammonia, phosphorus, iron, manganese, and hydrogen sulfide from the sediment into the overlying water column.

Interflows and underflows have been proposed as major transport processes for reduced and resolubilized species such as manganese and phosphorus from the upper reservoir to downstream areas (Nix 1981, 1984; Davison, Woof, and Rigg 1982). Since anoxic conditions generally begin in the upstream area of the reservoir, inflow mixing processes can promote the movement of this anoxic front further into the reservoir. Many dissolved nutrient species are in a readily available form for phytoplankton assimilation.

Underflows also can improve reservoir water quality. Cold, well-oxygenated outflows from Lake Ouachita, Arkansas, maintain an aerobic hypolimnion in the old thalweg of Lake Hamilton, Arkansas, downstream, even though the Lake Hamilton coves become anoxic.

The above situation can be altered depending on how the project is operated (i.e., how water is released). If a reservoir has a multilevel

withdrawal structure, water may be released at a similar elevation as the inflow enters the reservoir. Under such conditions the inflow waters can be short-circuited through the reservoir. If the residence time of a density overflow is less than the response time (i.e., doubling time) of phytoplankton under natural conditions, phytoplankton blooms may be minimized. Lund, Mackereth, and Mortimer (1963) report natural doubling times for *Asterionella formosa* to be 5 to 7 days. Doubling times for other species under natural conditions are on the order of 5 to 30 days (Ford and Thornton 1979). Therefore, when the residence time or short-circuited residence time is less than approximately 5 days, phytoplankton washout is probable. For Lake Windermere, England, a natural lake, Lund (1950) concluded losses due to overflow were approximately compensated for by inflowing nutrients. Lund, Mackereth, and Mortimer (1963) found outflow losses to be the major loss for *Asterionella*. Residence times of 5 days or less for overflows imply that the inflow water quality will dominate the mixed layer quality.

If the outflow is released from a different level than the inflow enters, mixing within the reservoir may be increased. Transport of nutrients from the metalimnion to the epilimnion and euphotic zone, for example, can be increased when inflows enter as interflows or underflows and the project is operated with surface discharge. Bottom withdrawal may promote movement of interflows and underflows through the reservoir and minimize the interaction between the inflowing constituents and the euphotic zone. Bottom withdrawal also may purge an anoxic hypolimnion of reduced and resolubilized constituents. Dunst (1974) found that bottom discharge from several Wisconsin reservoirs with anoxic hypolimnia significantly reduced the hypolimnetic phosphorus load. During fall overturn, then, this phosphorus load would not be available for mixing throughout the water column and phytoplankton assimilation.

Many reservoirs are operated to store water for downstream flood control. The pool elevation therefore rises to accommodate the inflowing water. Water also flows into littoral zones and coves, carrying with it inflowing constituents. These constituents can remain within these zones and coves and impact water quality later in the season.

Nutrients, for example, may be assimilated by phytoplankton, and organic loadings may contribute to the onset of anoxic conditions. When there is a net outflow from a reservoir, there is also a net transport from the littoral zones and coves into the main body of the reservoir. Increased horizontal transport also results in increased vertical transport.

### 3.3.2 Upwelling, Seiches, and Internal Waves

The water quality significance of upwelling and seiches is severalfold. First, upwelling is one mechanism whereby the waters of the metalimnion, and possibly the hypolimnion, are temporarily exposed to the surface. Upwelling of anoxic hypolimnetic water near the dam in C. J. Brown Lake, Ohio, depressed surface DO concentrations to about 2 mg/l with increased surface nutrient concentrations and hydrogen sulfide odors. This upwelling occurred because of the passage of a large storm front. The colder, nutrient-rich water may initiate a phytoplankton bloom of different composition than previously occurred within the lake.

Second, seiches may alter the mixed-layer depth and light regime to which plankton are exposed. Horizontal variations are also expected because the wind may concentrate phytoplankton at the downwind end of the lake, creating differences in mixed-layer depths and light penetration within the mixed layer. The correlation between upwelling and phytoplankton blooms is well established for coastal zones (Fogg 1975, Rao 1977) and is also found in natural lakes (Coulter 1968). The high rate of production throughout the year in Lake Victoria, Africa, is attributed to efficient mixing resulting from seiche action (Fogg 1975).

Seiche motion may indirectly initiate hypolimnetic mixing. As the water oscillates in the reservoir, bottom shear may create turbulence that increases mixing in the hypolimnion. This mixing may increase transfer of DO and reduced constituents across the sediment/water interface.

Seiche motion may result directly from project operation, particularly in peaking hydropower reservoirs. During generation, water

movement is established toward the dam. When generation ceases, water continues to move toward the dam and piles up at the dam with the establishment of oscillations of this water as the water surface seeks equilibrium. Seiche activity may explain the observed hypolimnetic DO fluctuations in Lake Sidney Lanier, Georgia. Hypolimnetic DO concentrations at a given depth near Buford Dam increased about 2 mg/l around 1000 hr from Tuesday through Saturday but were not evident on Sunday or Monday. Over long weekends with no generation, the increase was delayed until the day following the initiation of generation. Apparently, a seiche was created through generation with a frequency in phase with the generation cycle. This seiche motion created by hydropower generation may also increase hypolimnetic mixing through bottom shear.

While internal waves do not promote mixing unless these waves break, the vertical displacement of water by internal waves can significantly alter the light regime of phytoplankton in the metalimnion. Metalimnetic nutrient concentrations may be higher than in the mixed layer due to interflow loadings and microbial decomposition of organic matter settling from the epilimnion. Light may be the factor limiting phytoplankton production in the metalimnion. Internal waves with an amplitude of 2 to 15 m and a period of 15 min to 12 hr have been observed in coastal areas (Reid 1956, LaFond 1962). Armstrong and LaFond (1966) have observed vertical displacements of nutrient layers by these waves. As the metalimnion is displaced by the internal waves, this layer may enter the euphotic zone where available light may stimulate plankton production (Denman and Gargett 1983). Plankton production may increase metalimnetic DO concentrations during the day, but increased respiration at night may deplete DO concentrations below acceptable thresholds for aquatic life. Metalimnetic plankton assemblages may be entrained into the mixed layer and initiate plankton blooms.

Breaking internal waves may increase metalimnetic and hypolimnetic mixing. Many reservoirs are not completely cleared of timber when impounded, so these trees act as barriers to wave movement. The turbulence generated through breaking waves can mix metalimnetic constituent

concentrations and increase diffusion across the epilimnetic/metalimnetic interface. An anoxic metalimnion may contribute dissolved nutrients; reduced species such as manganese, iron, and hydrogen sulfide; and organic compounds to the mixed layer.

Project operation has the potential to generate internal waves of varying amplitudes and periods. Hydropower generation may result in internal waves with relatively regular periods while storm flows can result in internal waves with relatively large amplitudes.

### 3.3.3 Turbulence, Turbulent Mixing, and Entrainment

In the vertical dimension, the turbulent mixing and the resulting constituent distributions are determined primarily by density stratification. During periods of turbulent mixing, the upper well-mixed layer is usually isotropic despite settling and vertical variations in light intensity. Fee (1976) gives several examples where in vivo chlorophyll was isotropic in the upper mixed layer.

Below the upper mixed layer, in the metalimnion, the density gradient is usually strong enough to inhibit turbulent mixing. Measurements of temperature microstructure in freshwater lakes (Simpson and Woods 1970; Neal, Neshyba, and Denner 1971) show that the density structure in the metalimnion is not smooth as traditionally thought, but rather is made up of a series of steps on very small length-scales (e.g., Figure 37). These isotropic layers of intense mixing separated by strong gradients can have significant ecological effects. For example, Whitney (1938) found microstratification on the scale of centimetres based on transparency in several inland lakes. Whitney also was able to relate these abrupt changes in transparency to organic content and bacterial counts. More recently, Fee (1976) found narrow bands of high chlorophyll concentrations in the metalimnion and hypolimnion of several small, clear, well-stratified inland lakes. Thornton, Nix, and Bragg (1980) found narrow bands of high coliform bacteria concentrations in DeGray Lake, Arkansas. Density stratification and turbulence can therefore greatly affect vertical constituent distributions.

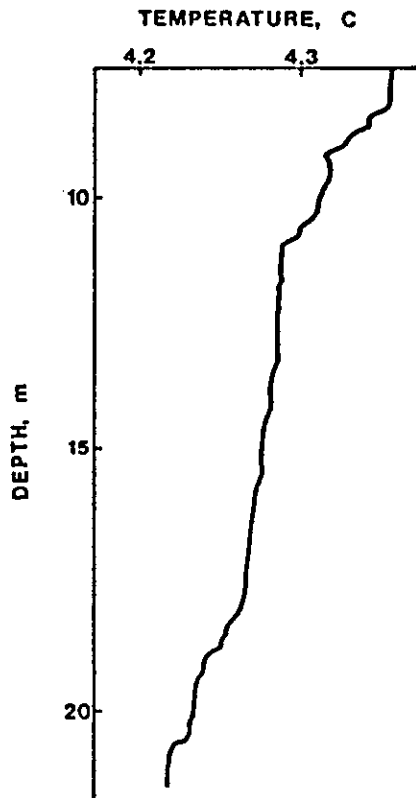


Figure 37. Example of temperature microstructure (after Neal, Neshyba, and Denner 1971)

Simultaneous measurements of chlorophyll a (a measure of phytoplankton biomass) and various physical parameters have been used to determine the importance of physical transport on phytoplankton distributions (Abbott et al. 1984). Using a time series of chlorophyll and temperature at a fixed location and fixed depth in the mixed layer, Platt (1972) found the power spectra of chlorophyll a followed a  $-5/3$  law which is characteristic of three-dimensional isotropic turbulence. Using the same data, Denman and Platt (1975) found significant coherence between temperature and chlorophyll a at each depth but not between depths. In summarizing these studies and others, Platt and Denman (1975b) concluded that for length scales between 100 m and 5 km, the observed variations in temperature and chlorophyll a resulted primarily from physical transport mechanisms including internal waves. For length scales less than 100 m, the fluctuations were damped out by turbulent diffusion. Powell et al. (1975) arrived at a similar conclusion using spectra of current speeds and chlorophyll a from the mixed layer of Lake

Tahoe, Nevada. This limit for turbulent diffusion is also consistent with the critical length scale of 50 m calculated by Platt and Denman (1975a) for the smallest patch of phytoplankton that can maintain itself against diffusion. Recently, Abbott et al. (1984) found the formation and dynamics of deep chlorophyll maxima were regulated by the interaction of three important processes: turbulent diffusion, nutrient supply rate, and light availability. Harris (1980) provides an excellent discussion of the important temporal and spatial scales in phytoplankton ecology and interaction of physical processes and plankton assemblages.

The case for a common physical mechanism controlling the distribution of both temperature and chlorophyll a at selected length scales was further substantiated by Denman (1976) and Fasham and Pugh (1976). In both studies, significant coherence was found between temperature and chlorophyll a measured at the same depth. The shapes of the power spectra of the two parameters were also similar. The gradual steepening of the power spectra at high frequencies was attributed to internal waves by Denman (1976). Denman (1976) also found that when the chlorophyll a variance was high (i.e., periods of high biological activity), the coherence between chlorophyll and temperature was low.

To investigate the vertical structure in more detail, Denman (1977) used a series of vertical profiles of chlorophyll a and temperature. The results suggested that most of the chlorophyll variation was due to horizontal advection of patches past the observation site and not to internal wave motion. Denman (1977) concluded that for a period characterized by little biological and physical activity, a single depth series of chlorophyll could depict changes in total chlorophyll only if the depth is located in an area of no appreciable vertical density gradient.

Closely related to turbulent diffusion is turbulent entrainment (Section 2.4.5). Entrainment is precisely what happens during the seasonal stratification cycle in temperate lakes. Examples of the onset and breakdown of stratification influencing phytoplankton blooms are numerous and well established (Lund 1954, Reynolds and Rogers 1976,

Kaeff and Knoechel 1978, etc.). Influences on the blooms include entraining cells living on the sediment surface at fall overturn (Lund 1954); entraining previously produced chlorophyll from the metalimnion and hypolimnion (Fee 1976); entraining nutrients from the metalimnion (Stauffer and Lee 1974); and diluting the food concentrations to a level too low for successful feeding (Fogg 1975). Turbulent entrainment also occurs at shorter time frames such as the passage of synoptic weather fronts. Gusting winds during storm events can increase the depth of the mixed layer and entrain constituents from an anoxic metalimnion and/or hypolimnion.

#### 3.3.4 Langmuir Circulation

A special case of turbulent mixing in the surface waters is Langmuir circulation (Section 3.2.4). Observations of Langmuir cells indicate that drift velocities are generally strongest in the zones of convergence. The cells are asymmetrical with downwelling velocities being larger than upwelling velocities. Downwelling velocities on the order of 5 cm/sec ( $4.3 \times 10^3$  m/day) are typical and are several orders of magnitude larger than typical settling velocities (i.e., 0.01 to 1 m/day). The currents in Langmuir circulations are more than sufficient to keep phytoplankton and other particulate constituents (i.e., bacteria) suspended (Denman and Gargett 1983).

Langmuir cells can transport phytoplankton, bacteria, and other constituents into and out of the euphotic zone. This transport can pass plankton and other cells through microstratification layers of higher nutrient or organic concentrations. Since nutrient uptake is usually much faster than growth, luxury uptake of nutrients by plankton as they pass through these microstrata can maintain or promote plankton growth.

### 3.4 Synthesis

The preceding review of reservoir mixing processes and the influence of mixing on reservoir water quality indicated that in order to achieve the second objective of this study (i.e., develop a

mathematical algorithm for one-dimensional water quality models which realistically represents all major mixing processes occurring in CE reservoirs), the mixing algorithm should be capable of accurately predicting the:

- a. Onset of stratification.
- b. Daily variations in mixed-layer depths and dynamics of short-term mixing events.
- c. Metalimnetic gradient.
- d. Variable mixing in the hypolimnion.
- e. Fall overturn.
- f. Inverse stratification during winter months.
- g. Effects of project operation.

An accurate representation of the onset of stratification is required to accurately predict, for example, the depletion of dissolved oxygen and the onset of phytoplankton blooms. As previously explained (Section 2.2), reservoir stratification starts at the bottom of a lake and moves upward, not from the water surface downward. The extent of metalimnetic and hypolimnetic DO depletion may depend on the relation between spring runoff and the onset of stratification. If spring runoff occurs prior to stratification, the nutrients and organic load may be distributed throughout the water column or proceed as a density overflow. If the onset of stratification has occurred before the spring runoff, an interflow may occur that can result in a significant load to the metalimnion or upper part of the hypolimnion. This load may exert an oxygen demand that results in the development of an anoxic metalimnion or hypolimnion. An accurate representation of the onset of stratification is also critical for simulating the water quality of lakes that exhibit weak or intermittent stratification.

Daily variations in mixed-layer depths are required to accurately simulate the entrainment of nutrient-rich metalimnetic waters into the epilimnion. This water, when released in the euphotic zone, may result in phytoplankton blooms. The depth of the mixed layer, relative to the

depth of the euphotic zone, can also impact the timing, magnitude, and composition of a phytoplankton bloom.

Materials tend to accumulate in the metalimnion because density gradients inhibit mixing. It is necessary to simulate this accumulation for entrainment into the epilimnion and to predict metalimnetic oxygen minima. An accurate representation of the metalimnetic gradient is also required to compute withdrawal zones and inflow placement.

Variable mixing in the hypolimnion is required to accurately simulate the depletion of dissolved oxygen and material exchanges across the sediment/water interface. It is also required to predict hypolimnetic temperatures required to meet downstream temperature objectives. Although little is known about hypolimnetic mixing, it is known that mixing levels increase with hydrometeorological forcing and use of bottom gates.

With fall overturn, complete vertical mixing returns and water quality problems associated with stratification are eliminated. If a significant oxygen demand builds up during the stratified period, oxygen levels may be depressed for a few days at overturn to satisfy the existing oxygen demand. Fall overturn also signifies the time when it is no longer possible to control release quality (e.g., temperature) through project operation (i.e., selective withdrawal).

Many CE reservoirs are located in cold climates and experience water quality problems during winter months when ice and snow covers isolate the lakes from exchanges across the air/water interface. During this period the lakes can become inversely stratified, and mixing is dominated by inflow and outflow processes.

Project operation influences both reservoir mixing processes and water quality. Bottom withdrawal can promote interflows and underflows, increase hypolimnetic mixing and mass transfer across the sediment/water interface, and decrease the buildup of anoxic constituents in the hypolimnion. Bottom withdrawal can also decrease the thermal stability of the reservoir by depleting the colder hypolimnetic water and hastening fall overturn. Since phytoplankton succession is dictated, in part, by the stratification pattern in the reservoir, the successional pattern

can be altered by project operation. Superimposing peaking hydropower generation and bottom withdrawal can create additional mixing through fluctuating water levels, Kelvin-Helmholtz instabilities, and epimetalimnetic and metahypolimnetic interfacial shear due to return currents established by project operation.

## SECTION 4. REVIEW OF ONE-DIMENSIONAL PREDICTIVE TECHNIQUES

### 4.1 Introduction

Since the early to mid 1960's, one-dimensional lake and reservoir models have been proven to be effective tools for analyzing in-lake and downstream temperature and water quality problems because temperature and many water quality parameters tend to vary more along a vertical distance of tens of metres than along a horizontal distance of thousands of metres. One-dimensional models solve a set of one-dimensional conservation equations for heat and mass. The major difficulty in solving these equations is finding expressions for the turbulent fluxes for heat and mass.

Following Niiler and Kraus (1977), one-dimensional material transport models for reservoirs can be grouped into four types depending on how the turbulent fluxes are expressed. These types include deterministic solutions, turbulence closure models, eddy coefficient models, and mixed-layer models. Deterministic solutions directly determine the fluctuating velocities from the primitive equations and thereby avoid the problem of specifying the turbulent fluxes. Since this approach requires a very fine space scale and correspondingly high time resolution, it is too expensive and time consuming for practical problems. An example of its use is found in Deardorff (1970). Turbulence closure models express the turbulent fluxes in terms of higher order moments (i.e., averaged triple products of the fluctuating quantities) which in turn must be parameterized in terms of empirical coefficients and computable (bulk) quantities or be represented by another set of equations involving fourth-order moments. Mellor and Yamada (1974) describe this process as a hierarchy of turbulent closure models with the classical eddy coefficient models at the lowest level. With the exception of this lowest level, the equations solved in these models are cumbersome and difficult to solve. Eddy coefficient models assume the turbulent fluxes can be expressed by the gradient of the transported quantity multiplied by an eddy diffusion coefficient which is a complicated function of

space and local stability. Mixed-layer models assume, as implied by the name, that the upper layer is well mixed. This assumption permits the vertical integration and solution of the turbulent energy equation in terms of the upper mixed-layer depth. According to Niiler and Kraus (1977), this approach is probably the most effective tool for prediction of upper ocean temperatures and heat storage.

In this section, the one-dimensional assumption and its implications are examined, and existing eddy coefficient and mixed-layer models are reviewed. Deterministic solutions and turbulence closure models were not considered cost-effective tools for the solution of practical problems.

#### 4.2 One-Dimensional Assumption

Vertical one-dimensionality assumes that forcing across the air/water interface and vertical variations (gradients) play a dominant role with transverse and longitudinal variations playing a secondary role. The one-dimensional assumption therefore assumes that reservoirs are represented by a vertical series of horizontal slices (Figure 38). Each horizontal slice is assumed to be well mixed laterally and longitudinally. Inputs to a horizontal layer are assumed to be instantaneously mixed throughout the layer. Since vertical density gradients (i.e., strong stratification) inhibit vertical motions (i.e., act to keep the isotherms horizontal), the use of a one-dimensional assumption for stratified systems is often justified.

Ford and Thornton (1979) analyzed the time and length scales characterizing the hydrodynamics, chemistry, and biology of lakes and showed that there is both an upper and lower bound to the lake size that can be characterized by a one-dimensional model. The lower bound was set at horizontal dimensions on the order of 0.05 to 0.5 km to minimize horizontal gradients caused by near-field effects such as local runoff and upwelling. The upper bound was set at horizontal dimensions on the order of 10 to 1.0 km to minimize horizontal variations caused by variations in the synoptic forcing functions.

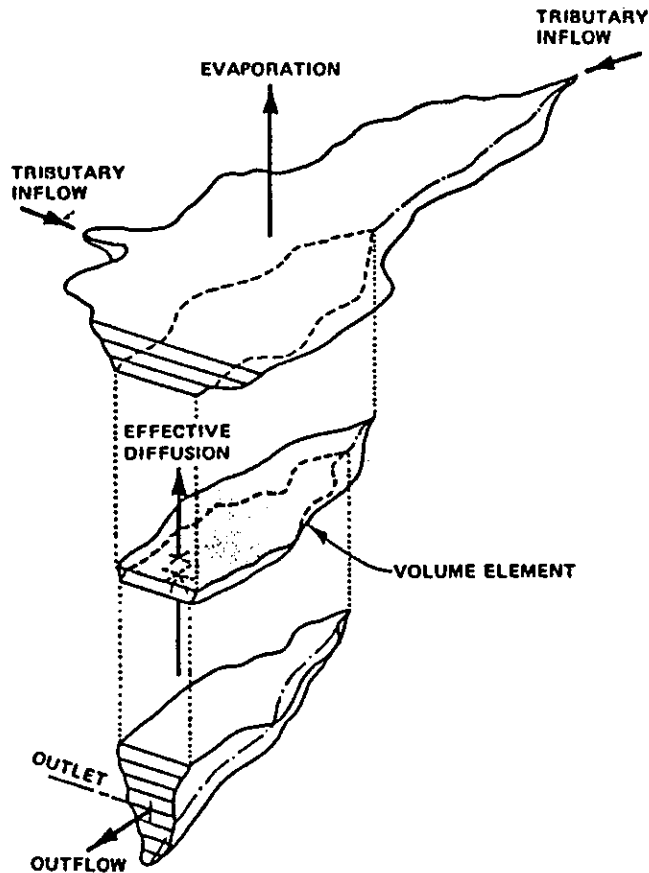


Figure 38. Vertical one-dimensional representation

When evaluating the appropriateness of the one-dimensional assumption for reservoirs, two physical factors must be specifically considered in addition to the ideas presented by Ford and Thornton (1979). These factors are the wind setup and the horizontal penetration of the inflow (i.e., plunge point). When the wind blows across the water surface, the resulting shear stress causes the isotherms to tilt (Section 3.2.2). If the wind is sufficiently strong, metalimnetic and hypolimnetic waters may become exposed to the surface (upwelling) and become mixed with epilimnetic waters. The magnitude of the wind setup at the water surface can be estimated by comparing the applied wind shear force

$$\tau_s A_s = \rho_a C_d W^2 A_s = \rho_w w_*^2 A_s \quad (23)$$

where

$$\begin{aligned} \tau_s &= \text{shear stress, kg/(m-sec}^2\text{)} \\ A_s &= \text{surface area, m}^2 \\ \rho_a &= \text{density of air, 1.177 kg/m}^3 \\ W &= \text{wind speed, m/sec} \\ \rho_w &= \text{density of water, kg/m}^3 \\ w_* &= \text{shear velocity in water, m/sec} \end{aligned}$$

with the pressure force (potential energy) that builds up

$$PE = \rho_w g \frac{dz}{dx} D \quad (24)$$

where

$$\begin{aligned} g &= \text{acceleration due to gravity, m/sec}^2 \\ \frac{dz}{dx} &= \text{slope of water surface, m/m} \\ D &= \text{depth of lake, m} \end{aligned}$$

This balance assumes no bottom shear. The slope of the water surface is

$$\frac{dz}{dx} = \frac{w_*^2}{gD} \quad (25)$$

and the slope of the thermocline

$$\frac{dz}{dx_i} = \frac{dz}{dx} \frac{\rho_w}{\Delta\rho} = \frac{w_*^2}{\Delta\rho Dg} \quad (26)$$

If  $(dz/dx)$  is approximated by  $\Delta D/L$ , Imberger's Wedderburn number ( $We$ ) is obtained

$$We = \frac{\frac{\Delta\rho}{\rho} g \Delta D}{w_*^2} \frac{\Delta D}{L} \quad (27)$$

The Wedderburn number therefore compares the slope of the interface with wind forcing. It can be used to determine if upwelling is significant. If  $We \gg 1$ , upwelling is not sufficient and the one-dimensional assumption is valid.

The plunge point location provides an indication of where the riverine zone stops and the lake begins (Section 3.2.5). If the riverine zone extends a significant distance into the reservoir, the reservoir is dominated by advective forces and cannot be considered to be vertically one-dimensional. Following the recommendations of Ford and Johnson (1983), the depth of the plunge point can be determined by

$$h_p = 1.6 \left( \frac{Q_j^2}{B_c^2 g \frac{\Delta\rho_j}{\rho}} \right)^{1/3} \quad (28)$$

where

- $h_p$  = hydraulic plunge depth, m
- $Q_j$  = inflow rate,  $m^3/sec$
- $B_c$  = width of zone of conveyance, m
- $\Delta\rho_j$  = density difference between inflow and reservoir,  $kg/m^3$

If  $h_p/Z_m$ , where  $Z_m$  is the maximum reservoir depth, is less than 1/3, the reservoir is one-dimensional.

### 4.3 Eddy Coefficient (Diffusion) Models

#### 4.3.1 Description

Eddy diffusion models were initially used in the mid-1960's to predict temperature changes in deep, stratified reservoirs. They have

been routinely used by the CE since the late 1960's and form the basis for many one-dimensional water quality/ecological models. Eddy diffusion models are based on the vertical one-dimensional thermal energy equation:

$$\begin{aligned}
 \frac{\partial T}{\partial t} + \frac{1}{A(z)} \frac{\partial}{\partial z} (Q_v T) &= \frac{1}{A(z)} \frac{\partial}{\partial z} \left[ (K_m + K_z) A(z) \frac{\partial T}{\partial z} \right] \\
 (1) \qquad (2) & \qquad (3) \\
 &+ \frac{B(z)}{A(z)} \left[ u_j(z) T_j - u_o(z) T \right] \\
 & \qquad (4) \\
 &+ \frac{1}{\rho_w c_p A(z)} \frac{\partial}{\partial z} \left[ H_z A(z) \right] \qquad (29) \\
 & \qquad (5)
 \end{aligned}$$

where

- T = water temperature, °C
- t = time, sec
- A(z) = horizontal area of reservoir at elevation z, m<sup>2</sup>
- z = vertical elevation, m
- Q<sub>v</sub> = vertical flow rate, m<sup>3</sup>/sec
- K<sub>m</sub> = molecular diffusion coefficient, m<sup>2</sup>/sec
- K<sub>z</sub> = global vertical diffusion coefficient, m<sup>2</sup>/sec
- B(z) = reservoir width at elevation z, m
- u<sub>j</sub>(z) = inflow velocity distribution, m/sec
- T<sub>j</sub> = inflow temperature, °C
- u<sub>o</sub>(z) = outflow velocity distribution, m/sec
- ρ<sub>w</sub> = density of water, kg/m<sup>3</sup>
- c<sub>p</sub> = heat capacity of water, J/(kg-°C)
- H<sub>z</sub> = heat flux at elevation z, W/m<sup>2</sup>

Term (1) on the left side is the time rate of change of temperature. Term (2) is the vertical advective transport term. It represents the flow between internal elements that is required to balance inflows and outflows and maintain continuity. If a Lagrangian or variable layer

scheme is used (Section 5.4.3), there is no flow between elements ( $Q_v = 0$ ), and term (2) is not required. Term (3) (the first term on right side of Equation 29) is the diffusion term. The molecular diffusion coefficient  $K_m$ , is usually neglected or incorporated into the turbulent diffusion coefficient  $K_z$ . Various formulations for  $K_z$  are discussed in Section 4.3.2. Term (4) of Equation 29 represents the heat input from tributaries and heat loss from outflows. The inflow and outflow velocity distributions are usually based on empirical relationships developed from laboratory experiments (e.g., Bohan and Grace 1973). Many diffusion models developed for natural lakes (e.g., Sundaram and Rehm 1973; Henderson-Sellers 1976; Walters, Carey, and Winter 1978) ignore the fourth term. For many CE reservoirs characterized by short residence times (i.e., less than 60 days), this term dominates Equation 29. Term (5), the last term in Equation 29, represents the local heat source which includes the internal heating from solar radiation. The various components of this term were discussed in Section 3.2.1.

Equation 29 can be solved by various computational techniques knowing the initial conditions, boundary conditions (i.e., heat transfer at air/water interface, inflow and outflow velocity distributions, heat transfer at sediment/water interface), and reservoir geometry (i.e.,  $A(z)$  and  $B(z)$ ). In addition to these requirements, the only major difficulties remaining to solve Equation 29 are the specifications of the internal absorption of solar radiation  $H_z$  and the eddy diffusion coefficient  $K_z$ . As indicated in Section 2.2.2, the specification of  $H_z$  requires knowledge of both dissolved and particulate materials in the water. Although thermal simulations in some systems are sensitive to the attenuation of shortwave radiation, it will not be discussed further. Reviews on light penetration can be found in Williams et al. (1981).

#### 4.3.2 Eddy Coefficient Formulations

Field measurements. Since the eddy diffusion coefficient includes the dynamics of all mixing processes, it is a complicated function of

time, space, and local stability. It is therefore informative to review results from field measurements of eddy diffusion coefficients prior to discussing the various formulations for  $K_z$ . According to Imberger and Hamblin (1982), there are no direct measurements of local values of vertical diffusion coefficients in either lakes or oceans, only basin averaged  $K_z$  values derived from global thermal budgets or tracer budgets. Since this study is concerned only with one-dimensional formulations, global- or basin-averaged coefficients are consistent with study assumptions.

In the global thermal budget approach, estimates of  $K_z$  are back-calculated from Equation 29, temperature data, and information on the internal absorption of solar radiation  $H_z$ , assuming no vertical and horizontal advective transport (i.e., terms (2) and (4) in Equation 29 are assumed to be 0). This assumption is usually valid for lakes and reservoirs with long residence times. If Equation 29 is integrated down the water column from depth  $z$  to the maximum depth  $Z_m$ , then

$$K_z = \int_z^{Z_m} \left( \frac{\partial T}{\partial t} - H_z \right) / \left( - \frac{\partial T}{\partial z} \right) \quad (30)$$

and  $K_z$  can be determined either graphically or with the aid of a computer. Typical results are shown in Figure 39, which illustrates decreased values for  $K_z$  in the metalimnion or regions of temperature gradient. The  $K_z$  values computed by the method represent an average value over the period between temperature profiles. Figure 40 illustrates that different values can be obtained if different integration periods are used. The smaller the period, the more variation in  $K_z$ . Computed  $K_z$  values may vary over several orders of magnitude from one day to the next. As discussed in Jassby and Powell (1975), it is essential that the internal absorption of solar radiation be considered when back-calculating  $K_z$ . For this reason and others,  $K_z$  should not be computed for the epilimnion using this method.

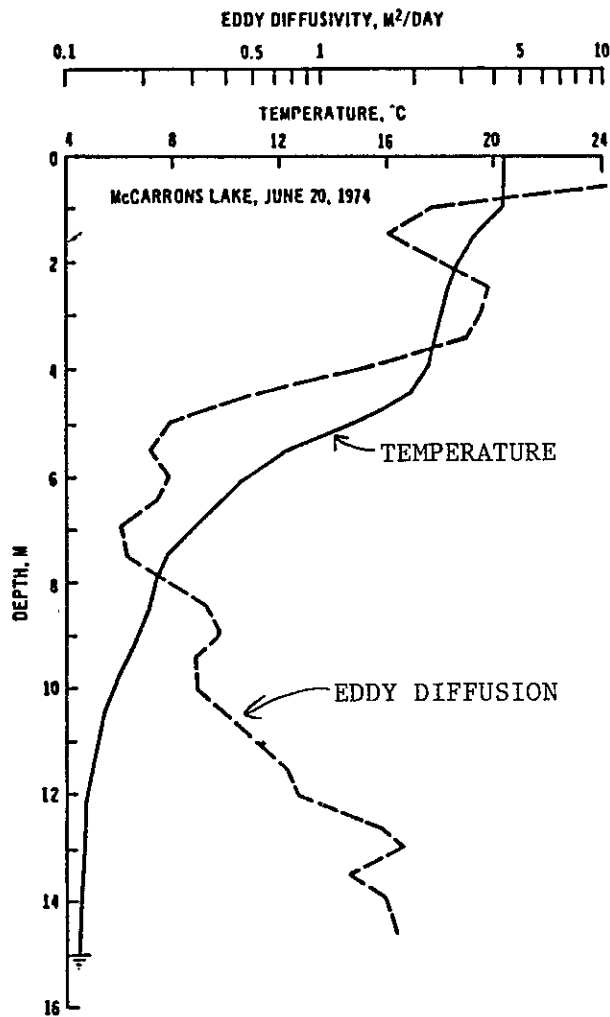


Figure 39. Vertical variation in eddy diffusion coefficients

Eddy diffusion coefficients can also be computed from passive tracer budgets using the one-dimensional, unsteady diffusion equation (i.e., a modified version of Equation 29) and/or the method of moments (Fischer et al. 1979). Examples of tracer studies include Kullenburg, Murthy, and Westerberg (1973) using dye; Imboden et al. (1977) using tritium; Imboden and Emerson (1978) using radon and phosphorus, and Quay et al. (1980) using tritium. The  $K_z$  values computed from these studies represent the time scale over which the study took place. In many instances this period is shorter than those computed by the thermal budget approach.

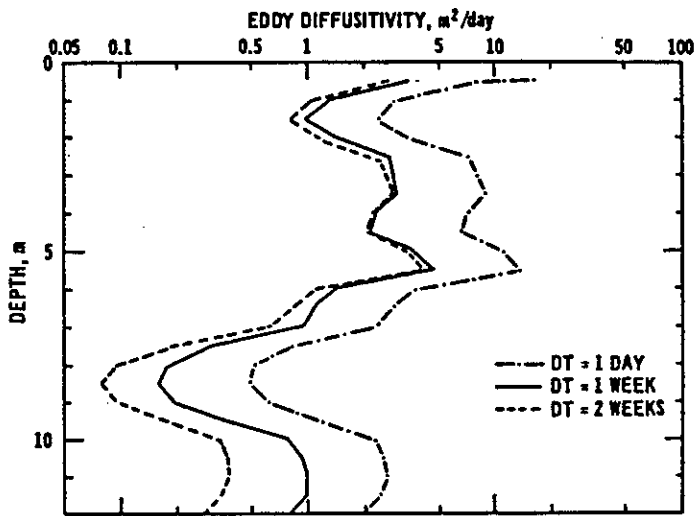


Figure 40. Variation in computed eddy diffusion coefficients with integration time, McCarrons Lake, Minnesota

Field studies using the thermal budget approach, tracers, or a combination of both substantiate the following conclusions concerning vertical diffusion coefficients. First, vertical diffusivities of heat range from molecular (i.e.,  $1.42 \times 10^{-7} \text{ m}^2/\text{sec}$ ) up to values of  $10^{-4} \text{ m}^2/\text{sec}$  (Figure 41). They are several orders of magnitude less than horizontal eddy diffusion coefficients but greater than molecular diffusion coefficients for gases and salts.

Second, vertical diffusion coefficients for heat and mass are about the same in the hypolimnion but differ in the metalimnion. Quay et al. (1980) found that heat diffuses faster than mass in the metalimnion, indicating molecular diffusion is important in determining the rate of vertical transport in the metalimnion. As shown in Table 2, the molecular diffusion coefficient for heat and mass differ significantly.

Third, the diffusivity is usually higher during periods of strong winds and large inflows or outflows. Bengtsson (1978) found an almost linear increase in  $\log K_z$  with wind speed (Figure 42).

Fourth, the diffusivity decreases with increasing stability (i.e., stratification) according to the following relationship

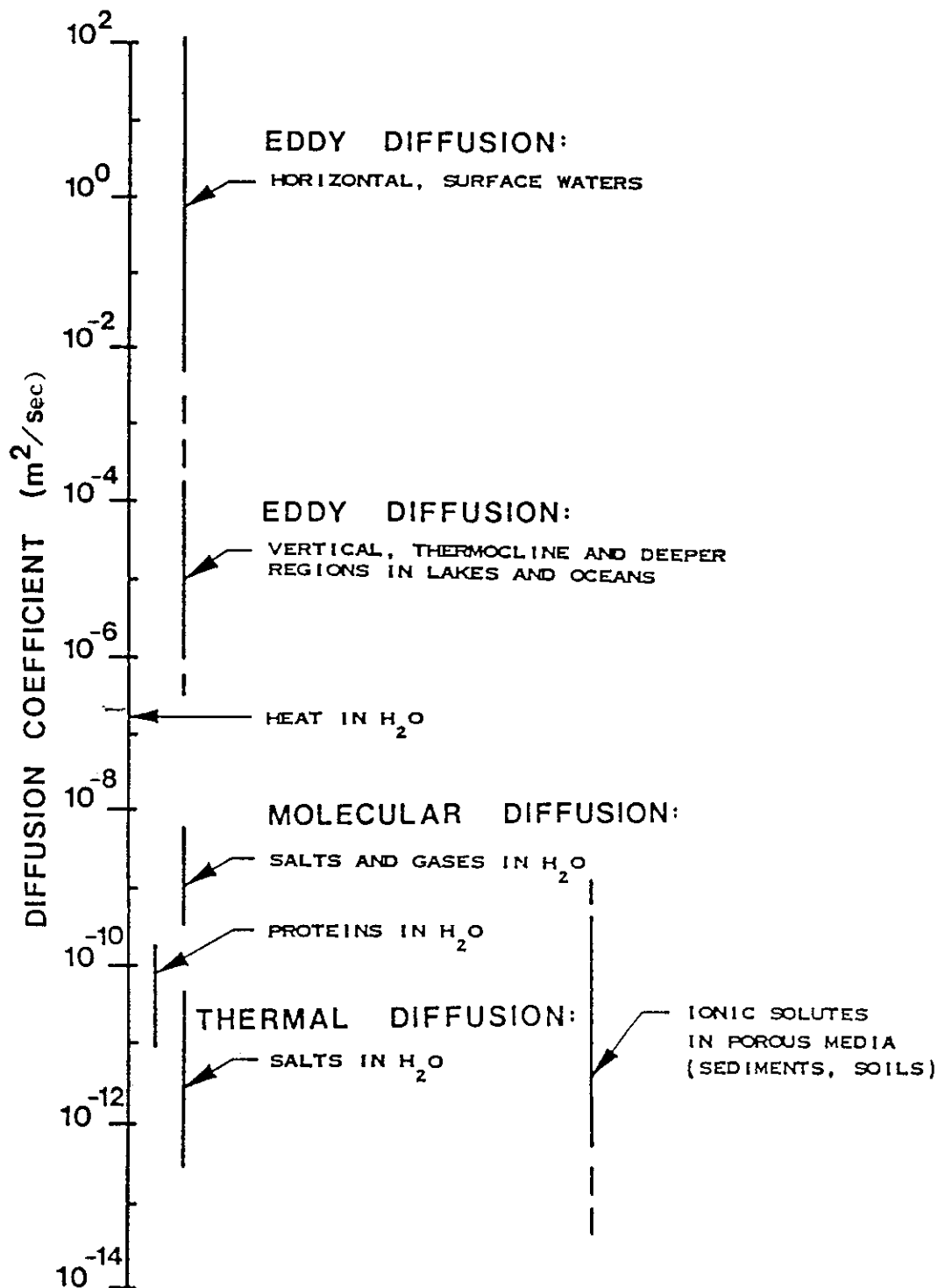


Figure 41. Comparative ranges for diffusion coefficients (after Lerman 1971)

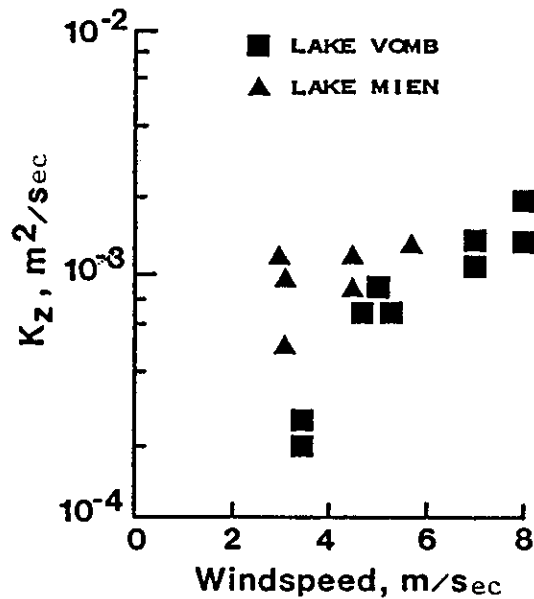


Figure 42. Increase in  $K_z$  with wind speed (after Bengtsson 1978)

$$K_z = a(N^2)^{-n} \quad (31)$$

where

$a$  = proportionality coefficient, units vary

$$N^2 = \frac{g}{\rho} \frac{\partial \rho}{\partial z} = \text{buoyancy frequency, sec}^{-2}$$

$n$  = coefficient, dimensionless

Values for  $n$  vary from 0.25 (Hutchinson 1941) to almost 2.0 (Blanton 1973). Using dimensional analysis, Welander (1968) attributed different coefficients to different physical processes. For example,  $n = 0.5$  is a local shear process and  $n = 1$  is for a cascade process. Figure 43 illustrates the variation in  $K_z$  with  $N^2$ .

Fifth, diffusion coefficients generally increase with lake size. Ward (1977) related  $K_z$  to the surface area of lakes

$$K_z = 3.3 \times 10^{-9} A_s^{1/2} \quad (32)$$

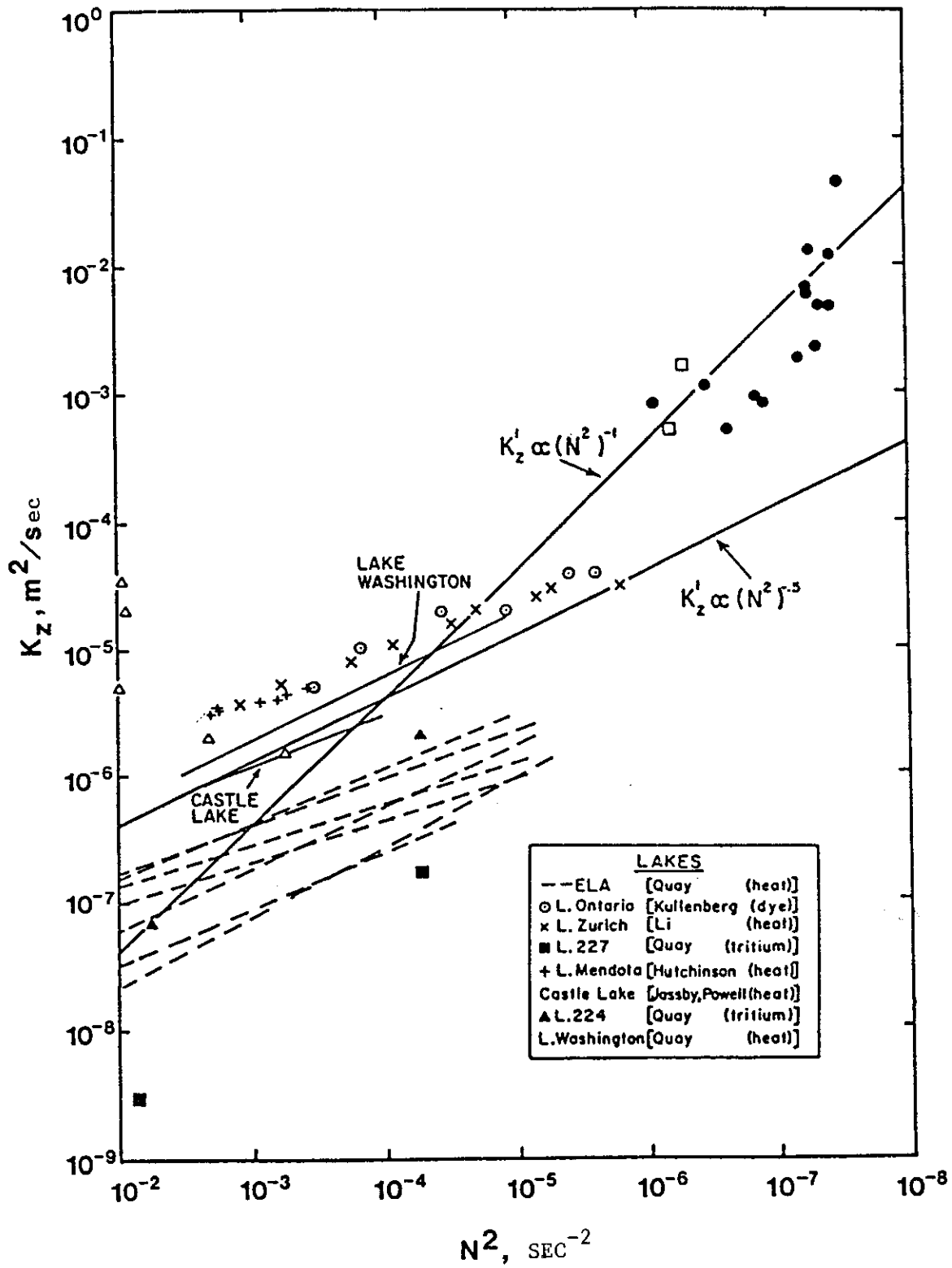


Figure 43. Variation in  $K_z$  with stratification stability  $N^2$  (after Quay et al. 1980)

where  $A_s$  = surface area,  $m^2$ .

This relationship is consistent with the data published by Ford (1978) (Figure 44).

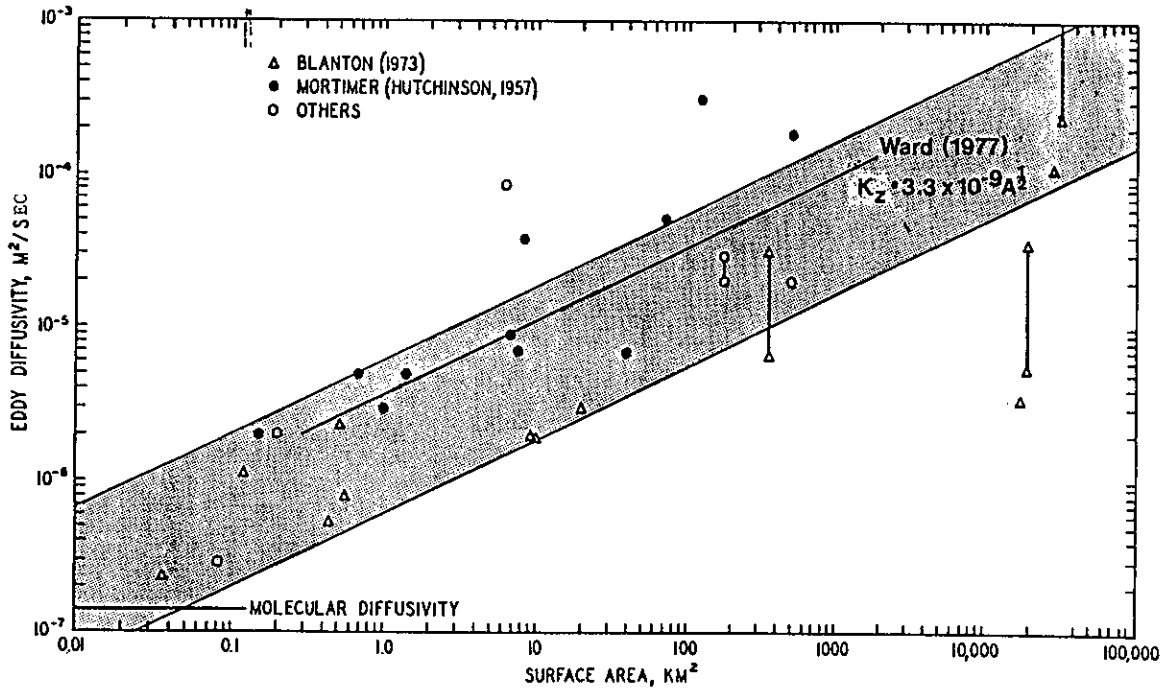


Figure 44. Variation in  $K_z$  with lake surface area  $A_s$

Formulations. The specification of  $K_z$  varies from model to model. If turbulent diffusion is assumed to be much larger than molecular diffusion, molecular diffusion can be incorporated into the turbulent term without any loss in precision. Some early thermal models (e.g., MIT model (Huber and Harleman 1968); Eiker Model (USAE District, Baltimore 1974)) considered the turbulent diffusivity to be constant with depth; others considered it to be dependent on the density structure and, therefore, depth dependent.

Historically, the steady-state model of Munk and Anderson (1948) was probably the first to provide insight into the interplay of turbulence, stratification, and heat flow. They assumed the eddy diffusion coefficient was related to the Richardson number by

$$K_z = K_{zo} (1 + a Ri)^{-3/2} \quad (33)$$

where

- $K_{zo}$  = eddy diffusion coefficient at neutral stability,  $m^2/sec$   
 $a$  = dimensionless coefficient  
 $Ri$  = Richardson number, dimensionless

Since then, variations of this formulation have been used by Sundaram and Rehm (1971, 1973); Henderson-Sellers (1976); Walters, Carey, and Winter (1978); and others. Specific differences between formulations centered around the specification of  $K_{zo}$ ,  $Ri$ , and the power (i.e.,  $-3/2$ ). Some specific models (e.g., Sundaram and Rehm) modify the formulation after stratification forms to account for the smaller eddy diffusivities that are normally found in the hypolimnion of stratified lakes.

Henderson-Sellers (1976) reviewed five expressions for  $K_{zo}$  :

$$K_{zo} = \frac{1}{Pr} \frac{w_*^2}{\left| \frac{\partial U}{\partial z} \right|} \quad (34)$$

$$K_{zo} = \frac{1}{Pr} k w_* (z_s - z) \quad (35)$$

$$K_{zo} = c w_* \quad (36)$$

$$K_{zo} = \frac{1}{Pr} k^2 (z_s - z)^2 \left| \frac{\partial U}{\partial z} \right| \quad (37)$$

$$K_{zo} = \frac{1}{Pr} k^2 \frac{\left| \frac{\partial U}{\partial z} \right|^3}{\left| \frac{\partial^2 U}{\partial z^2} \right|^2} \quad (38)$$

where

$Pr$  = Prandtl number = 1 for water, dimensionless

$w_*$  = shear velocity, m/sec  
 $\frac{\partial U}{\partial z}$  = vertical velocity gradient, (m/sec)/m  
 $k$  = von Karman's constant ( $\sim 0.4$ )  
 $z_s$  = elevation of water surface, m  
 $z$  = elevation, m  
 $c$  = empirical coefficient, m

and recommended Equation 34. The major difficulty with Equations 34, 37, and 38 is that they require a priori knowledge of the current structure. Although it is possible to assume a simple characteristic velocity profile such as parabolic or exponential under isothermal, steady-state conditions, stratification significantly modifies these profiles. In addition, the impact on the current profile of the time-varying inflow density currents, withdrawal zones, wind vectors, and complicated reservoir geometry is totally unknown. The practicality of formulations for  $K_{z0}$  which require the velocity gradient is therefore questionable. Physically, Equation 35 is questionable, since  $K_{z0}$  increases with depth, which is contrary to field observations. Equation 36 is desirable since the  $K_{z0}$  increases with wind shear velocity in water but undesirable since  $K_{z0}$  is constant with depth and  $c$  is not dimensionless.

The form of the Richardson number (Ri) in Equation 33 can be taken as

$$Ri = \frac{-g \left( \frac{\partial \rho}{\partial z} \right)}{\rho \left( \frac{\partial U}{\partial z} \right)^2} \quad (39)$$

or

$$Ri = \frac{-g \left( \frac{\partial \rho}{\partial z} \right)}{\rho \frac{w_*^2}{(z_s - z)^2}} \quad (40)$$

where

$g$  = acceleration due to gravity,  $m/sec^2$

$\frac{\partial \rho}{\partial z}$  = local density gradient

As with the formulations for  $K_{z0}$ , Equation 40 is preferable over Equation 39 since the velocity gradient is not known.

Substitution of Equation 36 and 40 into Equation 33 yields

$$K_z = \frac{c w_*}{\left[ 1 + a \frac{\left[ \frac{-g}{\rho} \left( \frac{\partial \rho}{\partial z} \right)}{w_*^2} \right]} \right]^b} \quad (41)$$

If a lake does not stratify (i.e.,  $Ri = 0$ ), Equation 41 reduces to

$$K_z = c w_* \quad (42)$$

and if a lake stratifies such that  $Ri \gg 1$ , Equation 41 reduces to

$$K_z = \frac{c_* w_* \left[ \frac{w_*^2}{(z_s - z)^2} \right]^b}{\left[ -\frac{g}{\rho} \left( \frac{\partial \rho}{\partial z} \right) \right]^b} \quad (43)$$

where  $c_* = c/a^b$ , in metres.

Ozmidov (1965) took a different approach to formulating an eddy diffusion coefficient. He assumed that mixing was done at the smaller length scales and that a local steady state existed such that the rate of turbulent energy input at larger length scales is in balance with

rate of dissipation at smaller scales. Ozmidov (1965) used an equation similar to Equation 43 with  $b = 1$

$$K_z = \frac{c_1 \bar{\epsilon}}{N^2} \quad (44)$$

where

$K_z$  = global vertical diffusion coefficient,  $m^2/sec$

$c_1$  = dimensionless calibration coefficient

$\bar{\epsilon}$  = dissipation rate of TKE,  $m^2/sec^3$

$N^2 = \frac{g}{\rho} \frac{\partial \rho}{\partial z}$  = buoyancy frequency,  $sec^{-2}$

If all of the TKE is derived from the wind, the local dissipation per unit volume is proportional to the TKE input per unit surface area (i.e.,  $\propto w_*^3$ ) (see Equations 53 and 54) divided by the water column depth  $z$ . That is,

$$\bar{\epsilon} \propto \frac{w_*^3}{z} \quad (45)$$

and Equation 45 is similar to the numerator of Equation 43 if  $b = 1$ .

Other formulations for eddy diffusion coefficients have been proposed, but they are all variations of the above relationships and therefore will not be discussed.

#### 4.3.3 Assumptions and Limitations

The major assumption of eddy diffusion models is that the effects of all mixing processes can be combined into a single diffusion coefficient  $K_z$ , which is coupled to the mean concentration gradient  $\partial C / \partial z$  (see Section 2.4.4). If the concentration gradient becomes small or goes to zero (i.e., as in the epilimnion), the diffusion coefficient must be made infinitely large to compensate for the decrease in gradient

and still result in a finite value of the flux,  $K_z \partial C / \partial z$ . The method, therefore, breaks down when vertical transport is under way. According to Tennekes and Lumley (1972), the concept makes sense only for flows with a single characteristic scale. Since mixing in reservoirs is characterized by many scales of motion, the validity of the concept is questionable. Since turbulence may be decoupled from the mean gradient, the concept is physically meaningless (Zeman 1981).

From a practical viewpoint, the one major limitation of the various empirical formulations for the  $K_z$  is lack of knowledge concerning the internal current structure (i.e.,  $\partial U / \partial z$ ) in reservoirs. Since the one-dimensional models under consideration in this study do not and are not capable of simulating the internal current structure of reservoirs (i.e., that is not their purpose), formulations for  $K_z$  that include  $\partial U / \partial z$  are not practically viable alternatives.

#### 4.4 Mixed-Layer Models

##### 4.4.1 Background

In reservoirs, mixing is primarily caused by turbulence (Sections 2.4.4 and 3.2.3). Since turbulence is highly dissipative, it requires a constant source of energy to be maintained. In addition, energy is also expended when mixing occurs (Section 2.3). It is therefore logical that a turbulent kinetic energy (TKE) budget be used to analyze mixing. TKE budgets have been used by atmospheric scientists to study entrainment at the inversion base (e.g., Tennekes 1973; Stull 1976a,b; Zeman and Tennekes 1977; Deardorff 1979; Mahrt 1979), by oceanographers to investigate entrainment into the upper mixed layer (e.g., Kraus and Turner 1967; Turner and Kraus 1967; Pollard, Rhines, and Thompson 1973; Niler 1975; Niler and Kraus 1977; Garnich and Kitaigorodskii 1977, 1978), and by physical limnologists to study entrainment in lakes and reservoirs (e.g., Stefan and Ford 1975a,b; Hurley-Octavio, Jirka, and Harleman 1977; Imberger et al. 1978; Bloss and Harleman 1980; Ford and Stefan 1980b; Imberger and Patterson 1981). Atmospheric scientists generally perform the energy budget at the density interface, while

oceanographers and engineers generally employ a vertically integrated energy budget. These models are therefore sometimes referred to as integral energy models or mixed-layer models. According to Tennekes and Driedonks (1980), there are no substantial differences in these two approaches. The differences deal primarily with notation.

Mixed-layer models have their origin with the laboratory experiments of Rouse and Dodu (1955). They studied mixing across a density interface by generating turbulence in the upper layer of a two-layered density-stratified fluid using an oscillating grid (Figure 45). The turbulence formed a well-mixed layer, bounded by a sharp interface which moved away from the stirrer as fluid was entrained from the underlying quiescent layer into the upper well-mixed layer. Since then, other experiments employing oscillating grids (e.g., Cromwell 1960; Bouvard and Dumas 1967; Turner 1968; Brush 1970; Wolanski 1972; Crapper 1973; Crapper and Linden 1974; Linden 1973, 1975; Thompson and Turner 1975; Wolanski and Brush 1975; Hopfinger and Toly 1976), moving screens at the water surface (e.g., Kato and Phillips 1969; Kantha, Phillips, and Azad 1977), wind (e.g., Wu 1973), and oppositely directed jets (e.g., Moore and Long 1971), have indicated:

- a. The turbulence produces and maintains a well-mixed layer.
- b. The turbulence sharpens the interface.
- c. The turbulence causes mixing across the interface.
- d. The entrainment velocity or advancement speed of the interface is a function of the Richardson number.
- e. Mixing takes place largely through a process which looks like the intermittent breaking of steep-faced internal waves which tend to thicken the interface, followed by the sweeping away of this fluid by the stirring in the layers, which sharpens the interface again.
- f. The turbulence reflects the characteristics of the generation mechanism (e.g., grid), and therefore the scale of the generated turbulence is smaller than the mixed-layer depth.
- g. The TKE generated by stirring mechanisms decays with distance from the mechanism.

The results from these experiments are summarized in Turner (1973); Sherman, Imberger, and Corcos (1978); and Pederson (1980).

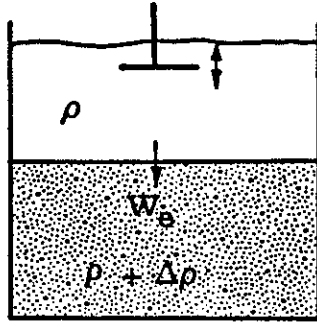


Figure 45. Schematic of an oscillating grid laboratory experiment

#### 4.4.2 Description

Results from the experiments described in Section 4.4.1 and others are used to parameterize and solve the TKE equation, which is the basis of mixed-layer models. The TKE equation is derived by scalar multiplication of the momentum equations with the turbulent velocity field and assuming: (a) the Boussinesq approximation; (b) the main flow is horizontal and in the direction of  $U$ ; and (c) the turbulence is homogeneous in the horizontal plane (see, e.g., Van Mieghem 1973, Ford 1976, and Phillips 1977):

$$\frac{\partial}{\partial t} \overline{q^2} + \frac{\partial}{\partial z} \overline{\left( u \left( \frac{p'}{\rho_0} + q^2 \right) \right)} = \overline{-u_x u_z} \frac{\partial \overline{U_x}}{\partial z} - \frac{g}{\rho_0} \overline{u_z \rho'} - \epsilon \quad (46)$$

(1)                      (2)                      (3)                      (4)                      (5)

where

$$\overline{q^2} = \overline{(u_x^2 + u_y^2 + u_z^2)} / 2 = \text{TKE per unit mass}$$

$u_x, u_y, u_z$  = turbulent fluctuations of the horizontal ( $x, y$ ) and vertical ( $z$ ) velocity components, m/sec

$p'$  = turbulent fluctuations of pressure, Pa  
 $\rho'$  = turbulent fluctuations of density,  $\text{kg/m}^2$   
 $\rho_0$  = mean density,  $\text{kg/m}^2$   
 $\epsilon$  = rate of dissipation of TKE,  $\text{m}^2/\text{sec}^3$   
 $\bar{U}_x$  = mean horizontal velocity,  $\text{m/sec}$   
 $t$  = time, sec  
 $z$  = vertical coordinate, m

In Equation 46, term (1) represents the temporal change in TKE; term (2) represents the redistribution in space of the TKE by turbulence; term (3) represents the rate of transfer of TKE from the mean flow by the Reynolds stresses; term (4) represents the gain or loss of TKE due to the release or increase of potential energy of the mean density (temperature) field; and term (5) represents the rate of dissipation of TKE.

In its present form, Equation 46 cannot be solved directly for any parameter of practical interest. The equation must therefore be parameterized in terms of variables of interest and practical significance. Following the parameterization scheme of Tennekes and Driedonks (1980), Equation 46 becomes

$$c_t \frac{\sigma w_e^2}{h} - c_f \frac{\sigma^3}{h} = -g w_e \frac{\Delta \rho}{\rho} - c_d \frac{\sigma^3}{h} \quad (47)$$

where

$c_t, c_f, c_d$  = constants determined from experimental data  
 $\sigma$  = velocity scale,  $\text{m/sec}$   
 $h$  = depth of mixed layer, m  
 $w_e = \frac{dh}{dt}$  = entrainment velocity,  $\text{m/sec}$

Early mixed-layer models (i.e., Kraus and Turner 1967; Stefan and Ford 1975a,b; Hurley-Octavio, Jirka, and Harleman 1977; Imberger et al. 1978) assumed the temporal and shear terms (terms (1) and (3) in Equation 46) were zero and that the local dissipation equaled local

production such that Equation 47 reduced to:

$$\frac{w_e}{w_*} \propto \frac{\rho w_*^2}{g \Delta \rho h} = Ri^{-1} \quad (48)$$

when  $\sigma$  was assumed to scale with  $w_*$ . This dependence of the entrainment speed on the inverse of the Richardson number was found in many of the laboratory experiments previously discussed in this section. Models based on Equation 48 did an excellent job of simulating mixed-layer dynamics during periods of strong stratification but overpredicted mixed-layer depth during periods of weak stratification (Bloss and Harleman 1980).

Bloss and Harleman (1980) corrected this deficiency by using the parameterization of Zilitinkevich (1975) for the transient term (term (1) in Equation 46). Assuming shear was still small and using the constant from Zeman and Tennekes (1977), Bloss and Harleman (1980) expressed Equation 47 as a function of Richardson number,

$$f(Ri) = 0.057 Ri \left[ \frac{29.46 - \sqrt{Ri}}{14.20 + Ri} \right] \quad (49)$$

where  $Ri = \frac{g \Delta \rho h}{\rho w_*^2}$ .

This function (Figure 46) is actually an efficiency factor for the conversion of TKE into potential energy. This modification significantly improved model predictions during periods of weak stratification.

Another deficiency of mixed-layer models was noted by Imberger and Patterson (1981). They observed that mixed-layer models always cause the metalimnetic gradient to sharpen, while field observations indicated times when the gradient was more diffuse. This prompted Imberger and Patterson to include shear (term (3) in Equation 46) in their

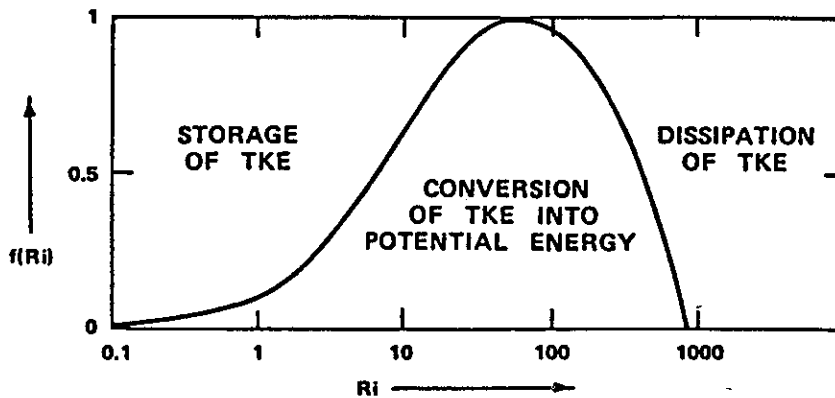


Figure 46. Efficiency factor for mixing  
(after Bloss and Harleman 1980)

formulation. This improvement requires computing the slope of thermocline under wind forcing.

#### 4.4.3 Assumptions and Limitations

TKE or mixed-layer models assume that a well-mixed layer overlies a region of density gradient. The depth of the upper mixed layer is determined by the TKE input at the air/water interface and the retarding buoyancy force of the underlying, density-stratified layer. The models predict averaged parameters for the mixed layer but do not consider the dynamics of the underlying density-stratified layer. Its major limitation is, therefore, that it does not simulate the lower density-stratified layer.

#### 4.5 Summary

The review of diffusion and TKE models indicates that both approaches have significant advantages and limitations. More important, however, is the fact that the two approaches model different physical mixing processes (i.e., diffusion and entrainment) and, since both of these processes are important reservoir mixing processes, both should be included in the recommended algorithm.

## SECTION 5. ALGORITHM DEVELOPMENT

### 5.1 Introduction

The second objective of this study was to develop a mathematical algorithm that realistically represents all major mixing processes occurring in CE reservoirs. Since this algorithm is intended to be used in a generalized one-dimensional water quality model (e.g., CE-QUAL-R1 (Environmental Laboratory 1982)) to predict changes in reservoir water quality resulting from changes in hydrometeorological conditions and project operation, several requirements had to be considered during algorithm development.

First, the algorithm had to be generalized with respect to CE reservoirs. Sizes of CE reservoirs range over four orders of magnitude (Ford 1978). Some reservoirs are small and round (e.g., Eau Galle Lake, Wisconsin, and C. J. Brown Lake, Ohio) while others are large and dendritic in shape with many islands (e.g., DeGray Lake, Arkansas). Elevations and proximity to major cities (i.e., a source of meteorological data) also vary. Since there is no typical CE reservoir or location, the algorithm must therefore not be constrained by extensive morphometric and hydrometeorological data requirements. In addition, it is highly unlikely that similar mixing processes dominate in all reservoirs.

Second, the algorithm is to be used in a one-dimensional water quality model (CE-QUAL-R1). The one-dimensional assumption (Section 4.2) not only limits model applicability to certain types of lakes and problems but also limits the types of formulations that can be used. For example, one-dimensional models do not generally compute the internal current structure. Water quality is defined to include the kinds and amounts of dissolved and suspended matter in water, the physical-chemical characteristics of the water, and the ecological relations with and among aquatic organisms; therefore, the algorithm must be capable of accurately describing the vertical transport of all water quality parameters and yet not be sensitive to concentration gradients.

Historically, temperature predictions have been relatively insensitive to diffusion formulations when compared with other water quality parameters because temperatures are physically constrained between 0° and 35° C by heat transfer at the air/water interface, and gradients are usually no more than a few degrees Celsius per metre. In contrast, the magnitudes and gradients of other water quality parameters may vary over several orders of magnitude and may not be as physically constrained to a specific range. Model simulations of these parameters can therefore be sensitive to changes in diffusion coefficients (Thornton et al. 1979).

Third, the algorithm must be able to predict changes in the mixing regime resulting from changes in hydrometeorological conditions and project operation. As previously stated (Section 3.2), mixing in reservoirs results from hydrometeorological forcing. Superimposed on the seasonal variation in hydrometeorological forcing are short-term fluctuations. The mixing regime responds to both of these forcing scales. Different mixing regimes result depending on the timing of the forcing mechanism and the formation of stratification. A change in project operation also results in a change in the mixing regime. For example, increasing the pool level may change the mixing regime from an advective-dominated to a buoyancy-dominated regime. Lowering the outlet depth from the surface to the bottom increases hypolimnetic mixing. The algorithm must be able to simulate these changes in mixing regime, without coefficient changes, in order to be used for evaluation of management alternatives.

## 5.2 Evaluation Procedures

Two approaches were used in this study to evaluate alternative mixing algorithms:

- a. Investigation of physical basis.
- b. Applications to different reservoirs.

Although our knowledge of reservoir mixing is more qualitative than quantitative, the potential sources of TKE for mixing and the basic

functional relationships are well known (Section 3.2). Based on the review of reservoir mixing processes in Section 3.2, the important sources of TKE were identified to be the wind, inflows, and outflows (including location) and solar and atmospheric heating and cooling (i.e., convective mixing). It is also shown that mixing increases non-linearly with increases in wind speed and inflow rate. Improvements to existing formulations and/or alternative formulations were therefore first evaluated on how realistically they approximated the physical phenomena to be modeled. For example, several of the formulations for eddy diffusion coefficients (i.e., Equation 32) were discarded since they did not accurately portray mixing processes and/or did not support field observations (Section 4.3.2).

After the proposed improvements or alternative formulations were determined to be physically viable, they were evaluated by applications to a number of different reservoirs and hydrometeorological conditions. When comparing model simulations with field data, it is important to consider the previous discussion on data interpretation (Section 2.2.5), especially the uncertainty associated with field measurements. For example, in Figure 47 there is up to a 3° C difference in metalimnetic temperature during a 3-day period. Since this was a period of calm weather and low, steady inflows and outflows, there is little reason to expect seiching and internal waves that could cause larger temperature deviations in the metalimnion. The difference in temperatures is probably representative of field measurement errors and should be considered when comparing field data with model predictions.

Based on the review of the influence of mixing on reservoir water quality (Section 3.3), it was determined that the mixing algorithm should be able to accurately predict the onset of stratification, mixed-layer depth dynamics, metalimnetic gradient, variable mixing in the hypolimnion, fall overturn, inverse stratification during winter months, and effects of project operation to adequately address reservoir water quality problems.

An accurate representation of the onset of stratification includes not only the timing but also the depth and gradient. As explained in

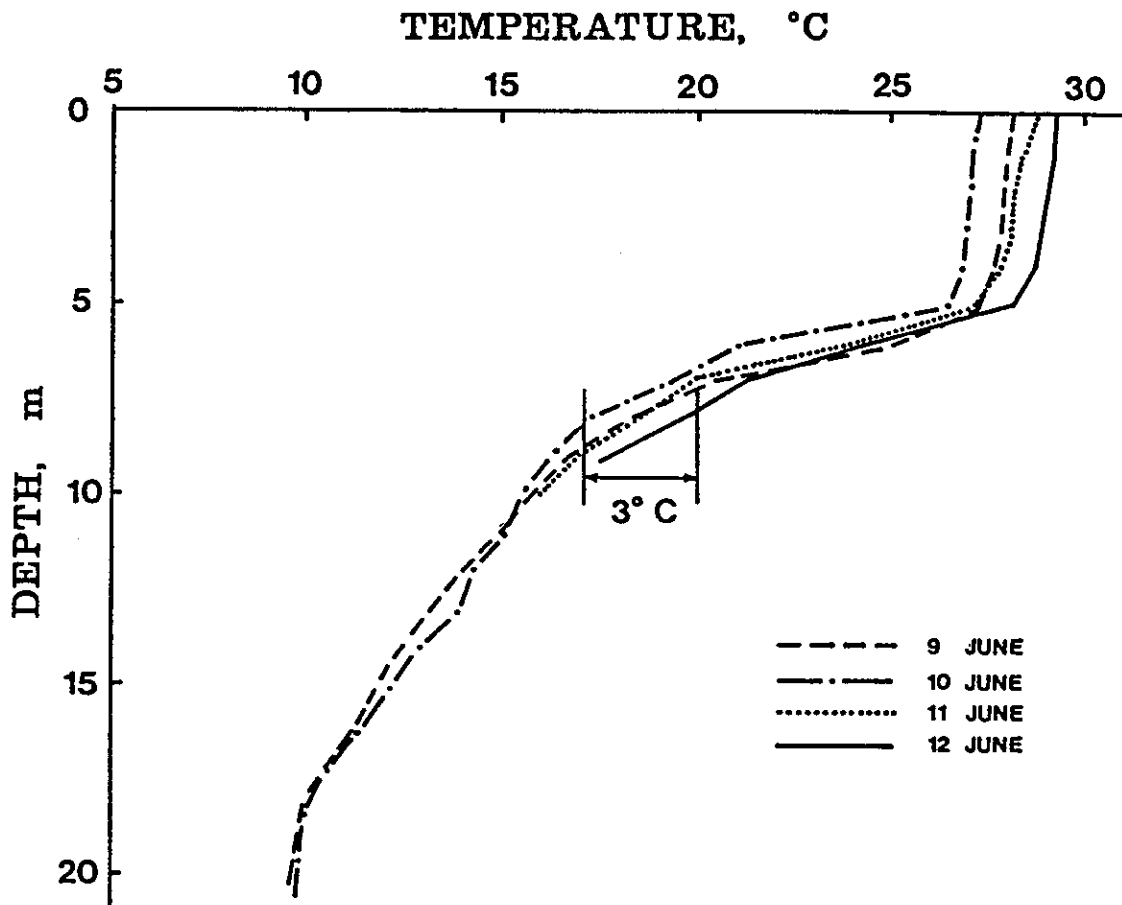
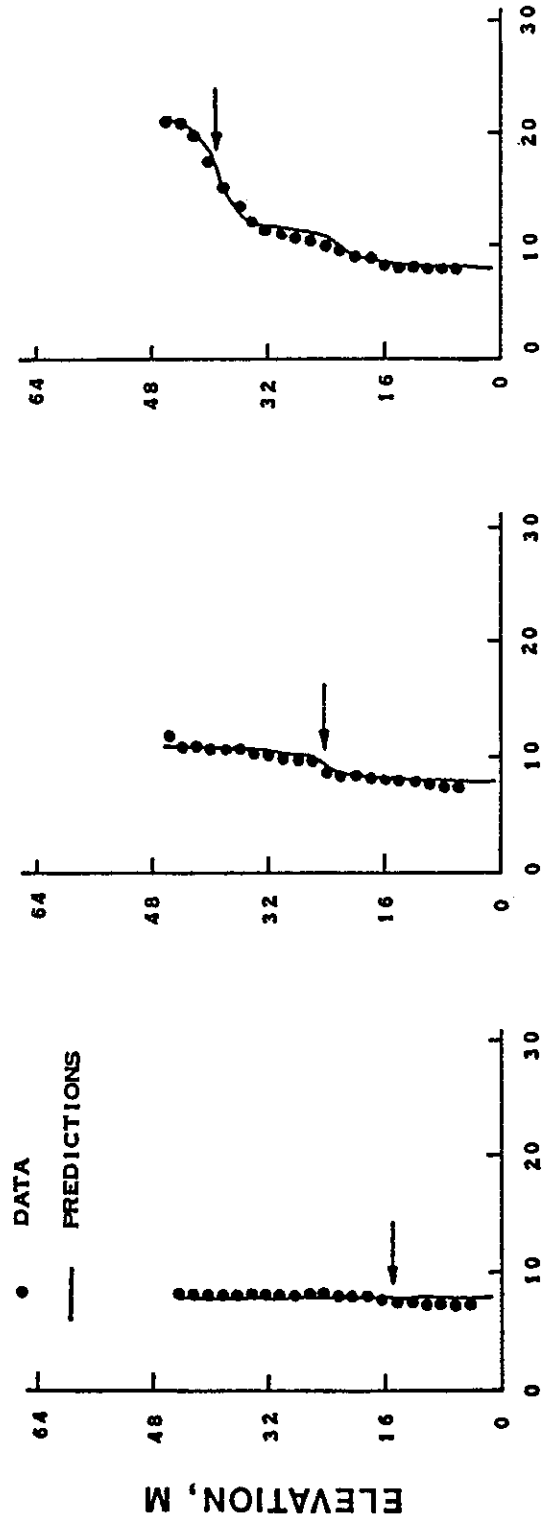


Figure 47. Daily variation in temperature profiles, DeGray Lake, Arkansas

Section 2.2 and shown in Figure 48, reservoir stratification starts at the bottom of a lake and moves upward, not from the water surface downward as some older diffusion models predict. In many shallow reservoirs, it is possible for stratification to form and break up several times prior to the permanent summer stratification forming.

Daily variations in mixed-layer depths result from synoptic variations in hydrometeorological forcing as well as diel variations (Section 2.2.3). Since the one-dimensional assumption limits the computational time interval to 1 day (Section 4.2), it is not possible to simulate diel variation in mixed-layer dynamics. Daily variations in mixed-layer depths and temperatures resulting from synoptic variations in hydrometeorological forcing are, however, significant. As indicated

LAKE GREESON, 1975



TEMPERATURE, °C

Julian Day 125

Julian Day 91

Julian Day 56

Figure 48. Simulation of the onset of stratification in Lake Greeson, Arkansas

in Section 2.2.5, it is sometimes difficult to separate diel variations from synoptic variations because most temperature data are collected at midday, not in the early morning hours.

Since density gradients inhibit mixing in the metalimnion, the dynamics of the metalimnion are sometimes ignored. An accurate representation of the metalimnetic gradient requires first an accurate portrayal of the onset of the stratification and, second, the inclusion of mixing from synoptic hydrometeorological forcing. It is important to simulate the sharpening of the metalimnetic gradient due to entrainment (Figure 49) as well as the weakening of the gradient due to advection and shear (Figure 50).

Variable mixing in the hypolimnion is dependent on hydrometeorological forcing and project operation. Although little is known about hypolimnetic mixing, it is known that mixing levels increase with hydrometeorological forcing and use of bottom gates. Because hypolimnetic temperatures can remain relatively constant, it is difficult to determine the significance of hypolimnetic mixing using only temperature data.

With fall overturn, complete vertical mixing returns to the lake. Consideration must be given to both the water temperature (i.e., heat transfer, Section 3.2.1) and the magnitude of entrainment (Figure 51). Accurate simulation of this process may require the inclusion of penetrative convection (Section 2.4.6). Because of the triangular longitudinal profile of most reservoirs (Figure 52), fall overturn appears to start at the upstream end of the reservoir and move downstream toward the dam.

Many CE reservoirs are located in cold climates and experience ice and snow covers that isolate the lakes from exchanges across the air/water interface. The lakes then become inversely stratified, and mixing is dominated by inflow and outflow processes. The actual formation of complete ice cover may take as little time as a few hours during a cold, calm night in small reservoirs, to several weeks in large reservoirs. Some reservoirs may never experience complete ice cover. To accurately simulate mixing during the period of ice formation, a measure of the

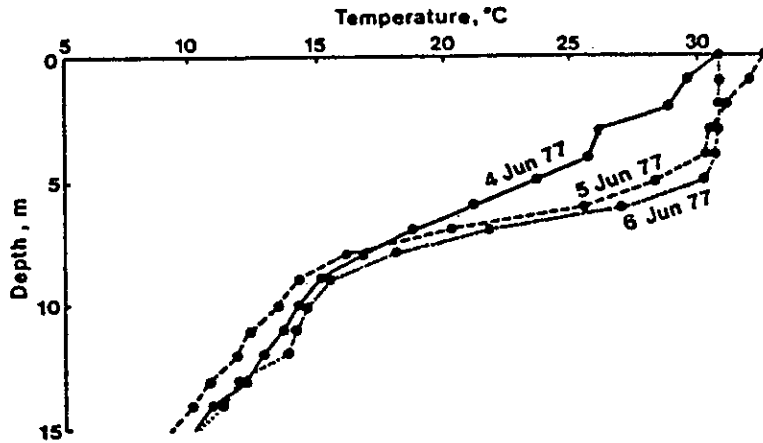


Figure 49. Sharpening of the metalimnetic gradient due to entrainment, DeGray Lake, Arkansas

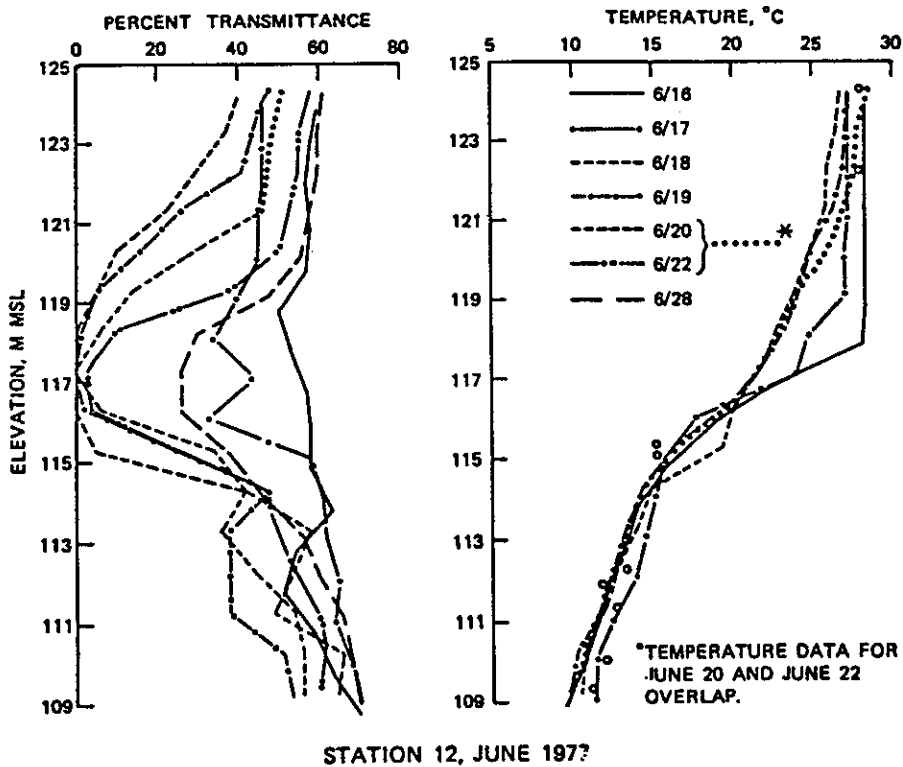


Figure 50. Weakening or diffusion of the metalimnetic gradient due to shear (inflow), DeGray Lake, Arkansas

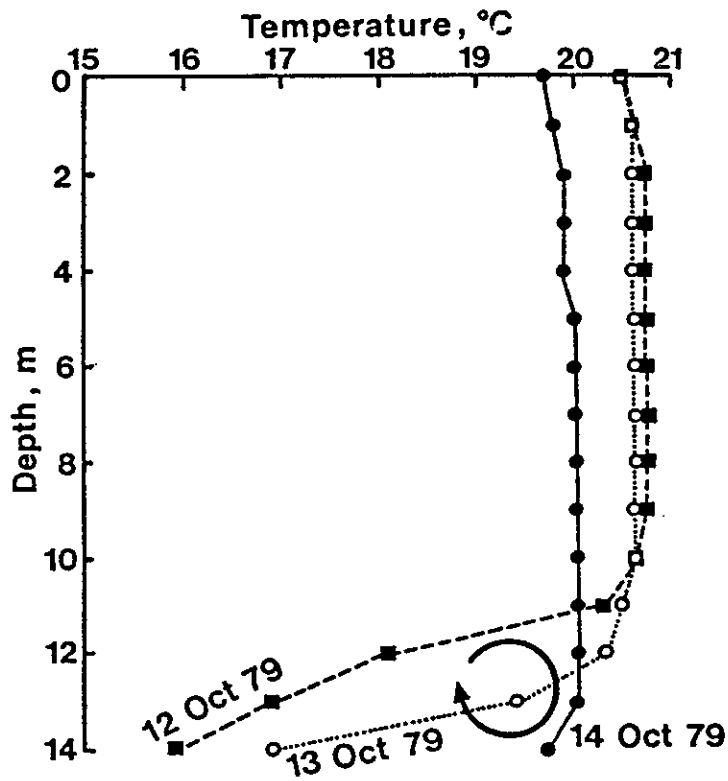


Figure 51. Fall overturn in DeGray Lake, Arkansas

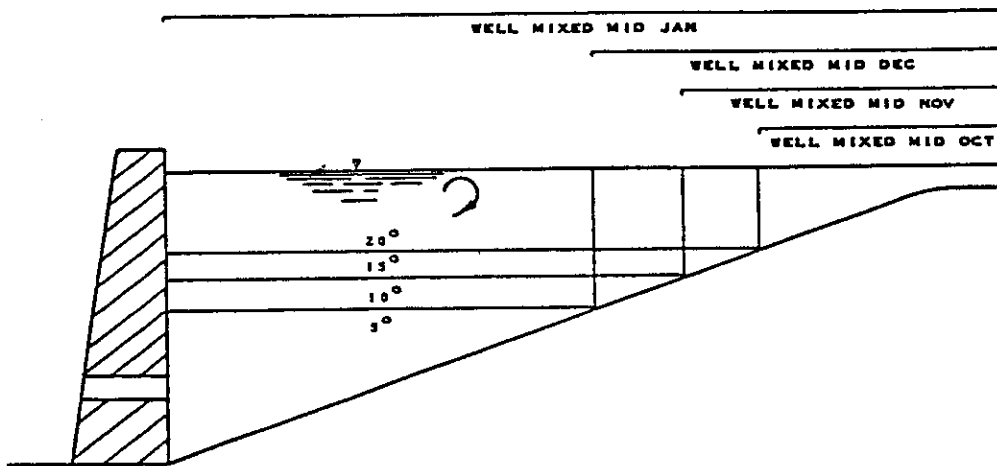


Figure 52. Triangular shape of a reservoir

size of ice-free water is required, necessitating the use of partial area ice cover algorithm (Schultz International, Ltd. 1984).

As previously described (Section 3.2.6), project operation can alter the mixing regime in a reservoir. In addition to considering the nonlinear effects of localized TKE input and its interactions with density stratification, an accurate representation of the mixing regime must consider other algorithms that compute effects of project operation such as selective withdrawal zones.

### 5.3 Historical Development

#### 5.3.1 WQRRS

Initial work on the mixing algorithm began with the 1974 version of the Water Quality for River-Reservoir Systems model (WQRRS) (Hydrologic Engineering Center 1974.) WQRRS was the basis from which CE-QUAL-R1 evolved (Environmental Laboratory 1982). WQRRS used the eddy diffusion coefficient formulation shown in Figure 53. Eddy diffusion coefficients were constant and equal in both the epilimnion and hypolimnion. Metalimnetic coefficients were decreased based on the density gradient and a calibration coefficient, A3. The metalimnion was distinguished from the epilimnion and hypolimnion using a user-specified stability criterion, GSWH. The major limitations of this formulation were the assumptions of equal, constant eddy diffusion coefficients in the epilimnion

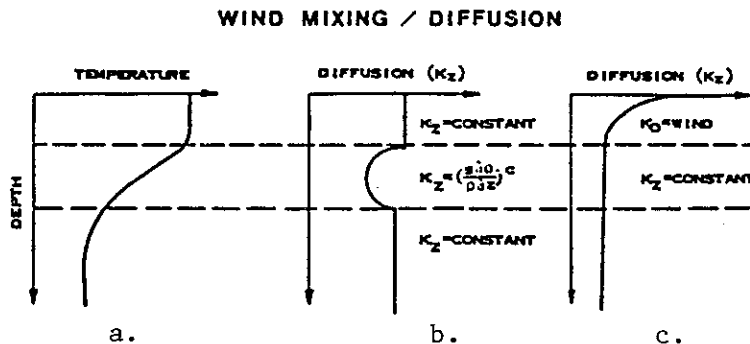


Figure 53. WQRRS diffusion coefficient formulations

and hypolimnion and no consideration of the wind as a mixing mechanism (Figure 53b).

WQRRS did contain an alternative formulation that considered the wind (Figure 53c), but in this formulation the dependence on the wind speed was linear and therefore not physically correct. This formulation also did not consider the reduced mixing in the metalimnion resulting from density gradients. As discussed in Section 4.3.2, the need for reduced mixing in the metalimnion is critical, and models that do not reduce metalimnetic eddy diffusion coefficients with increasing density gradients characteristically predict a metalimnetic gradient that is too weak even if the simulations are started with a measured temperature profile after stratification forms (e.g., Figure 54).

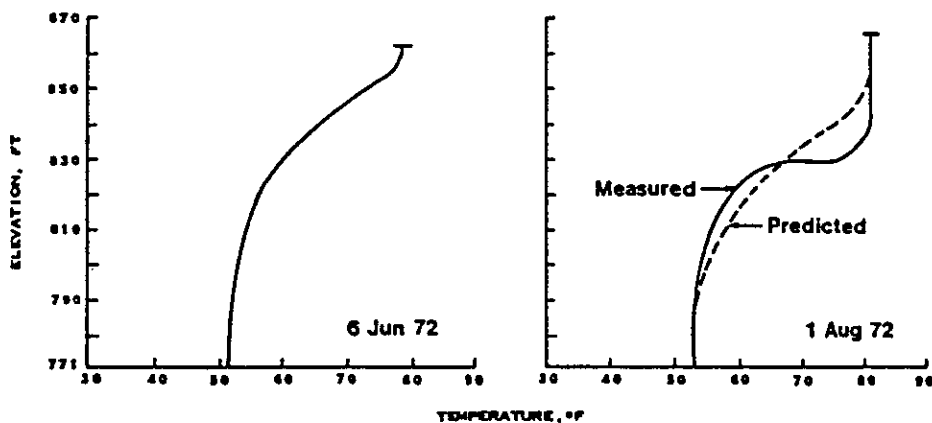


Figure 54. Diffused metalimnetic gradient resulting from using a constant diffusion coefficient

Both of these formulations received numerous applications and, for the most part, did an adequate job of representing the thermal regime in reservoirs. In many simulations (e.g., Figure 55), hypolimnetic temperatures were too low in the spring and too high in late summer, indicating insufficient mixing during spring turnover and too much hypolimnetic mixing during the summer stratified period.

In order to eliminate these deficiencies and improve model simulations, the formulation in WQRRS was modified to include the effects of

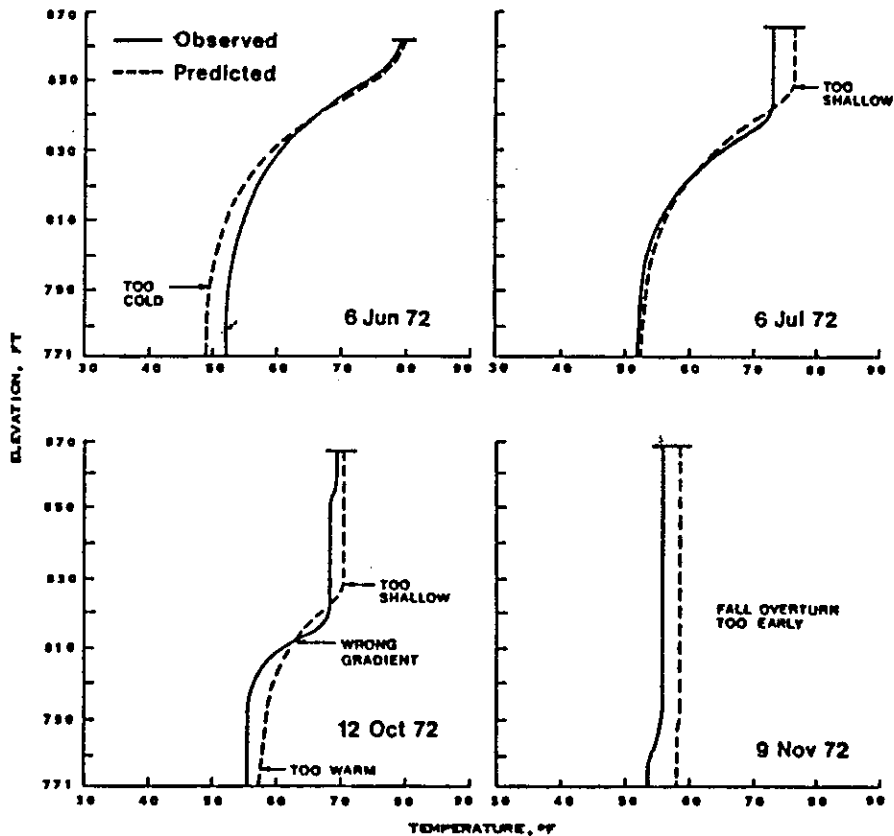
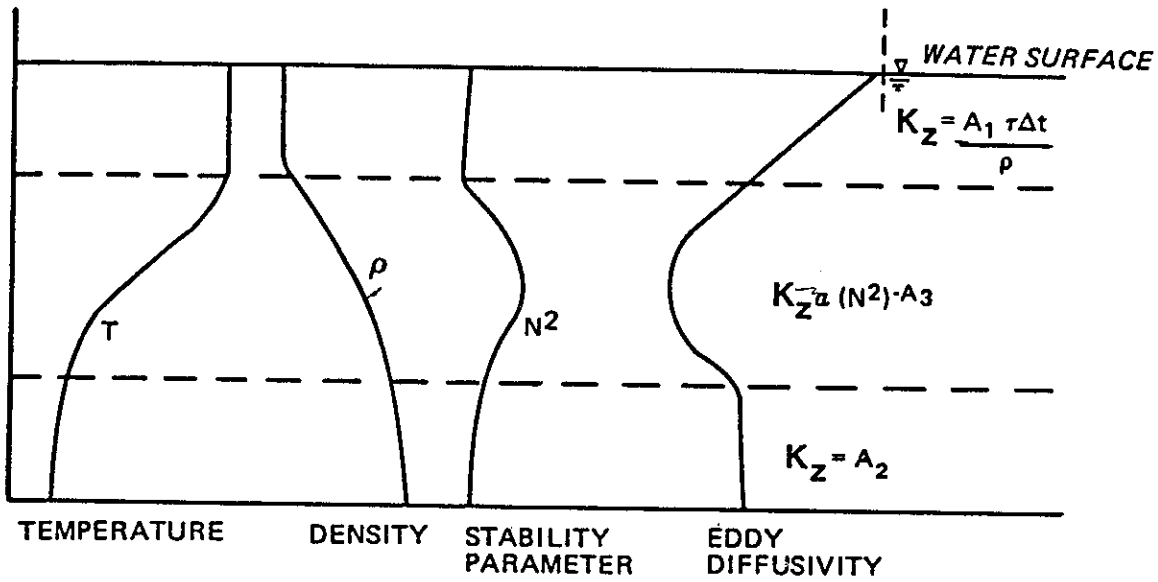
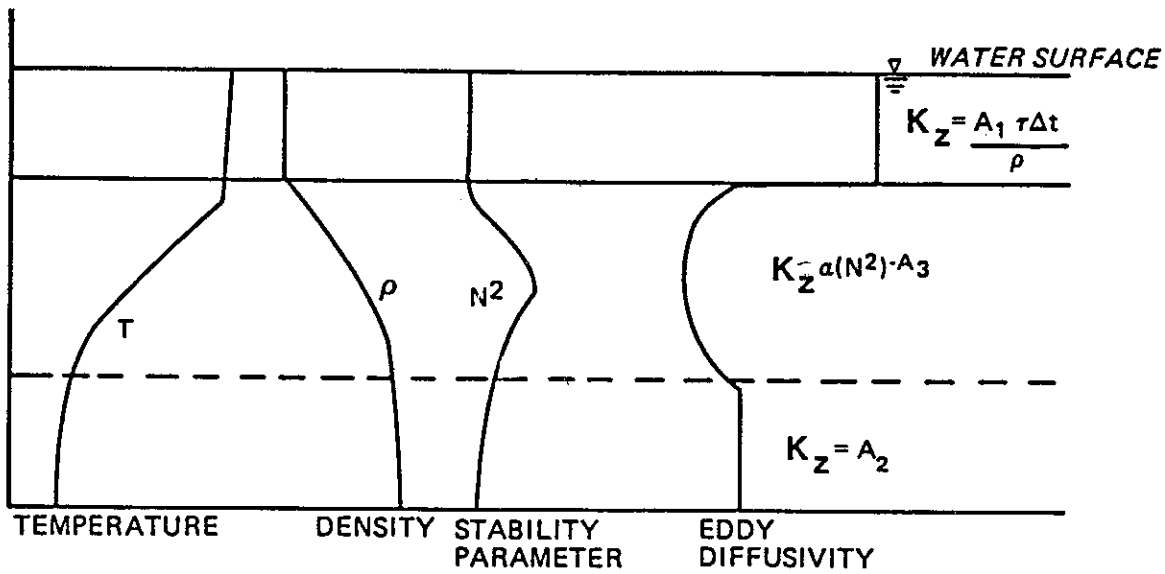


Figure 55. General characteristics of predictions using WQRRS, Stockton Lake, Missouri (to convert feet to metres, multiply by 0.3048; to convert degrees Fahrenheit to degrees Celsius, use the following formula:  $C = (5/9)(F - 32)$ )

the wind and to separate mixing in the epilimnion from mixing in the hypolimnion (Figure 56). The formulation retained the stability criteria and metalimnetic formulation from WQRRS. The hypolimnetic mixing coefficient was a separate user-specified diffusion coefficient that was considered constant throughout the simulation period; the epilimnetic mixing coefficient was dependent on the wind shear stress (i.e., wind speed squared) and either decreased linearly with depth to the hypolimnetic diffusion coefficient value (Figure 56a) or was constant with depth (Figure 56b). Simulations of a number of different reservoirs indicated the linear decreasing formulation was preferable.



a. Linear with depth



b. Constant with depth

Figure 56. Modified WQRRS diffusion coefficient formulation

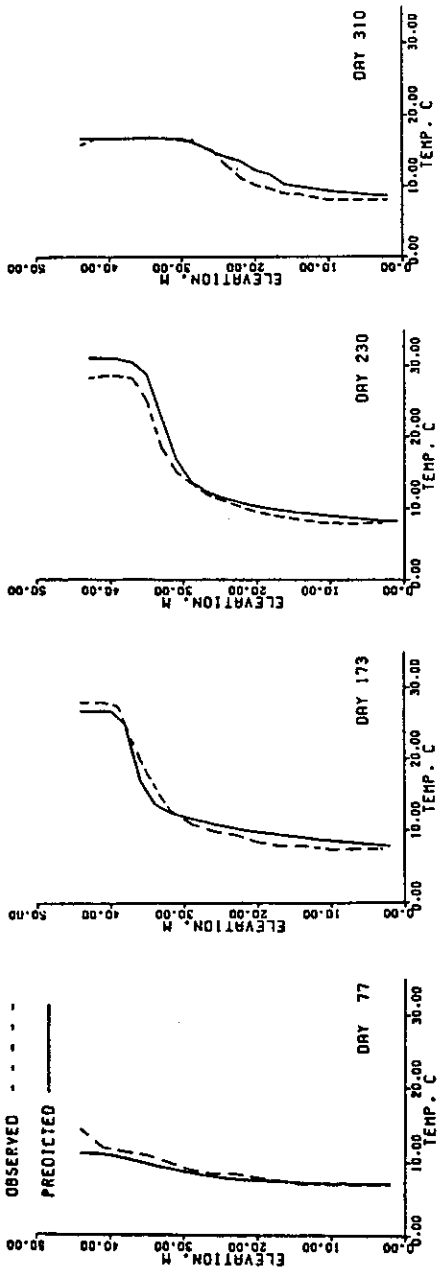
As with WQRRS, the stability criterion GSWH was used to define the density-dependent metalimnion.

This eddy diffusion coefficient formulation considered similar physical processes to those in the Richardson number formulations discussed in Section 4.3.2 but had more coefficients to calibrate to match field data. Stafford (1978) showed that although he could match the temperature structures of Lakes Greeson, Arkansas, and Sardis, Mississippi, for any single year, it was not possible to match temperature structures for 5 consecutive years using the same calibration coefficients. Selected calibration profiles from Lake Greeson (from 1972) are compared with verification simulations from 1974 in Figure 57. It is readily apparent from Figure 57 that the formulation was either not correctly calibrated or not capable of simulating different hydrometeorological conditions without recalibration. Simulations using other Richardson number-based formulations produced similar results, indicating that a Richardson number-type formulation for the diffusion coefficients, alone, was not adequate to accurately simulate changes in a lake's thermal structure resulting from hydrometeorological conditions.

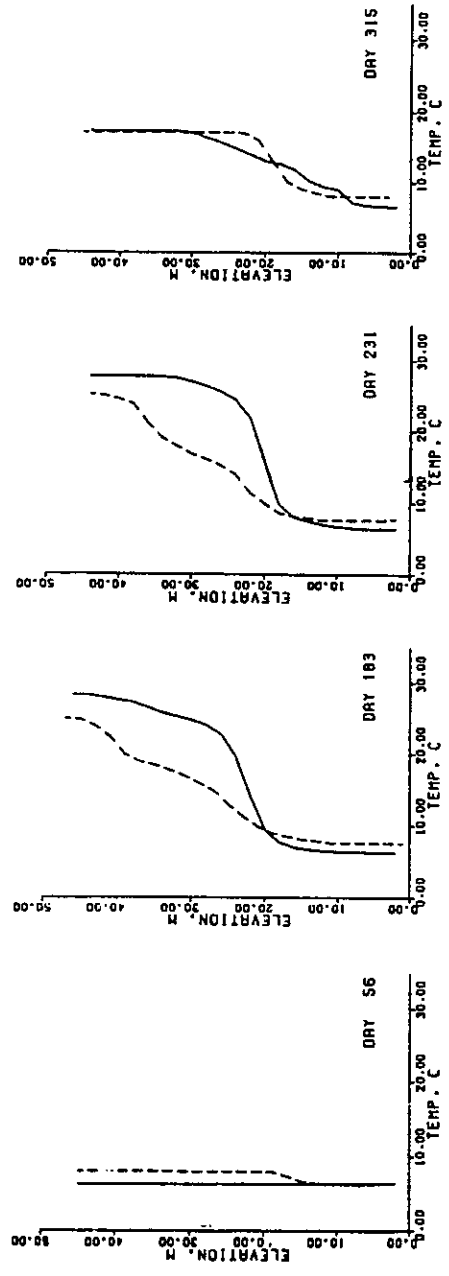
### 5.3.2 Variable Layer Formulation

One of the problems associated with the 1974 Lake Greeson predictions (Figure 57) was excessive metalimnetic mixing. This mixing resulted, in part, from the vertical advective term (term (2)) in Equation 29 for two reasons. First, reduction of the mixing coefficients to produce molecular diffusion in this region did not improve model predictions. Second, the outlet was located in the metalimnion at the same elevation where excessive mixing was observed.

To reduce this numerical mixing, the variable layer concept or Lagrangian approach of Imberger et al. (1978) was incorporated into the model. With this approach there is no vertical advection term and the layers are allowed to expand or contract with layer inflows and outflows. A simple example illustrating the differences between the fixed layer model and variable layer model is shown in Figure 58. With the fixed layer model, the net result of the mass inflow to the top layer and withdrawal from the bottom layer is an increase in bottom layer



a. 1972



b. 1974

Figure 57. Calibration and verification simulations from Lake Greeson, Arkansas (after Stafford 1978)

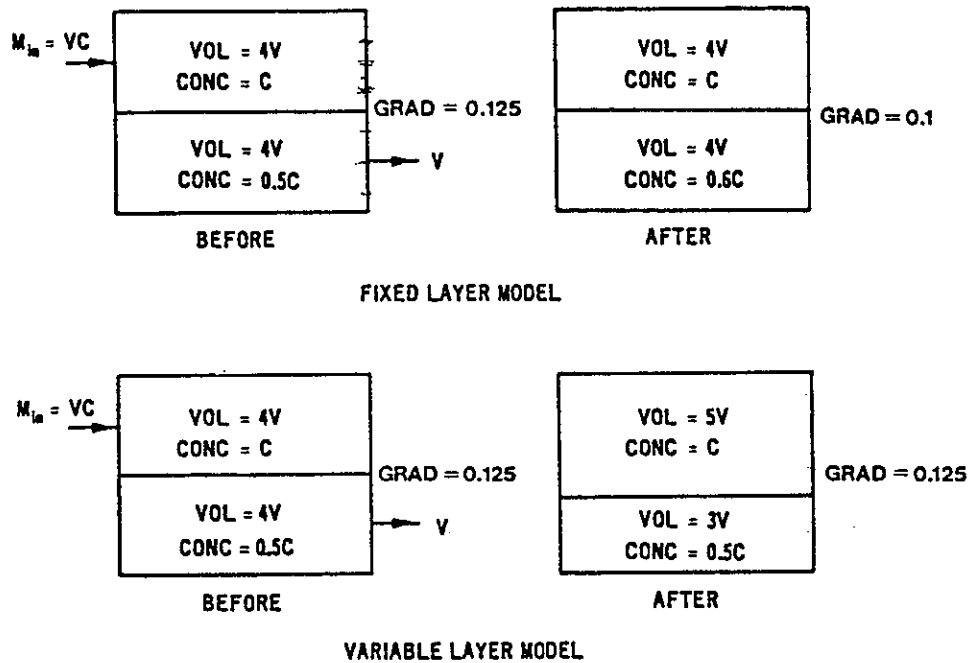


Figure 58. Schematic comparing fixed and variable layer formulations

concentration (0.5C to 0.6C) and decrease in the vertical concentration gradient between the two layers. The volumes or sizes of the two layers remain constant. In contrast, with the variable layer model, the top layer increases in size and the bottom layer decreases in size while the layer concentrations and the gradient remain unchanged.

A comparison of model predictions using the variable and fixed layer formulations is shown in Figure 59. As expected, there was less metalimnetic mixing with the variable layer formulation.

### 5.3.3 Mixed-Layer Dynamics

In addition to problems associated with simulating consecutive years on Lake Greeson, the modified WQRRS formulation also did not accurately portray the onset of stratification and mixed-layer dynamics. Since Ford (1976) showed that a simple TKE formulation (Section 4.4) was able to accurately reproduce the onset of stratification and mixed-layer dynamics in small natural lakes and Hurley-Octavio, Jirka, and Harleman (1977) and Imberger et al. (1978) were able to simulate the thermal

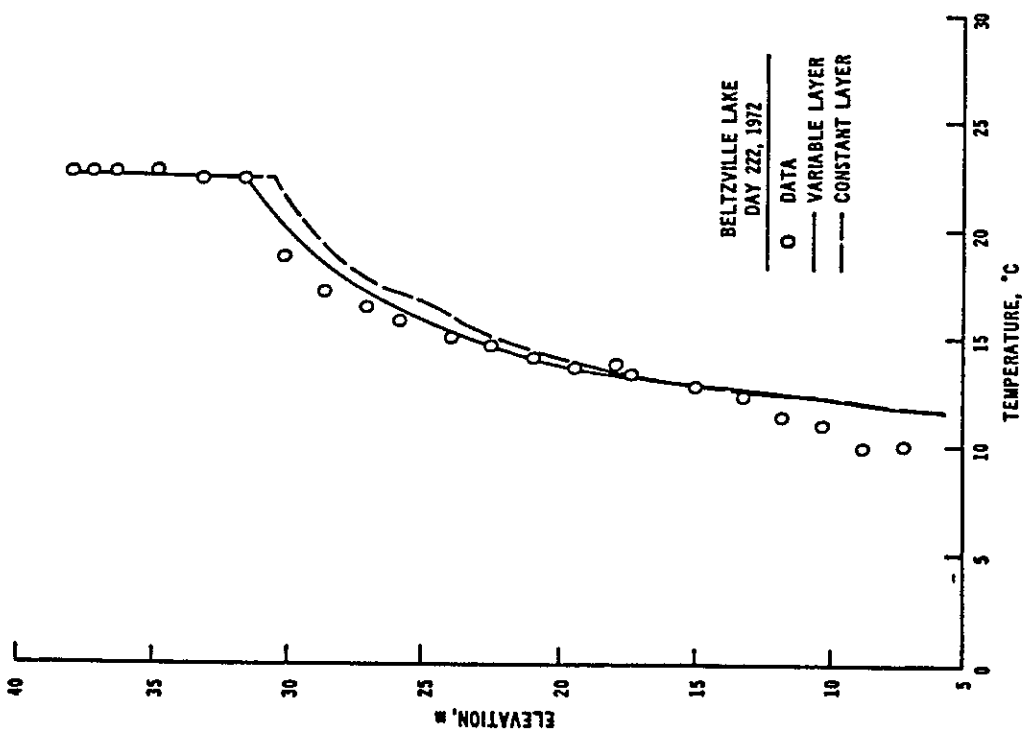
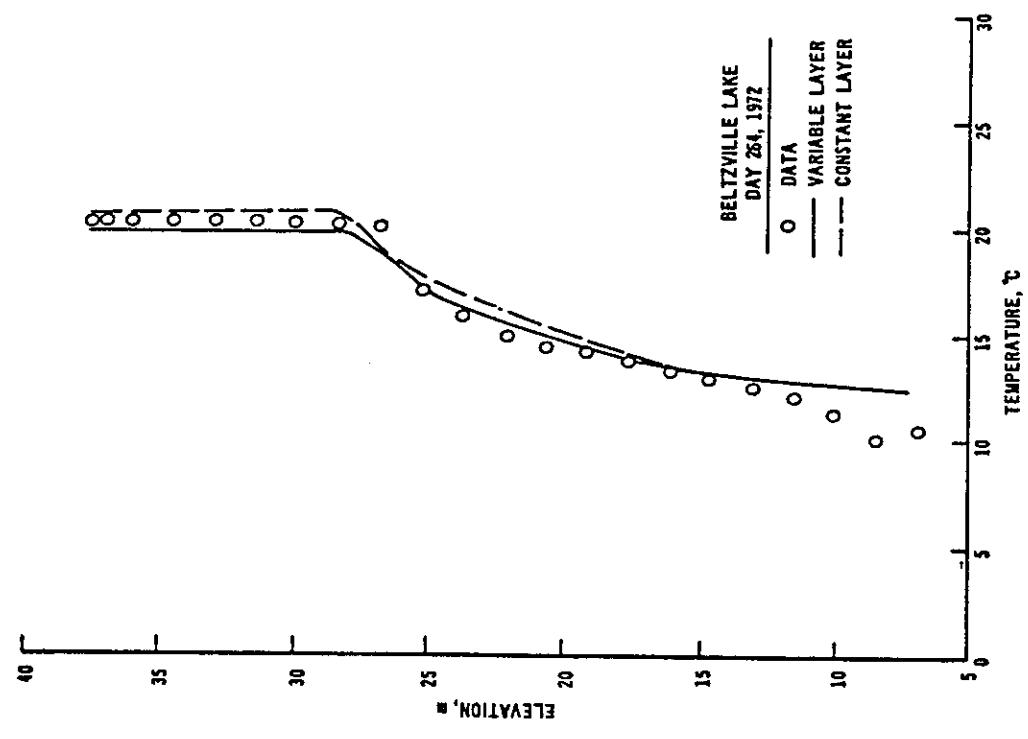


Figure 59. Comparison of thermal predictions using fixed and variable layer formulations

structure of larger reservoirs using similar formulations, a TKE formulation or mixed-layer formulation was incorporated into the mixing algorithm.

Initially, the mixed layer formulation followed the approach of Ford (1976) and Hurley-Octavio, Jirka, and Harleman (1977) and did not consider dissipation of TKE with depth. Although the simulations of the onset of stratification improved (Ford et al. 1981), there was too much entrainment during periods of weak stratification (i.e., the predicted mixed-layer depths were too deep) (Figure 60). Imberger et al. (1978) avoided this problem by dissipating the TKE with depth using a cubic function. There was, however, no physical basis for the function. Noting the same problem with the Hurley-Octavio model, Bloss and Harleman (1980) developed an efficiency function for entrainment based on the Richardson number (Section 4.4). This function significantly improved

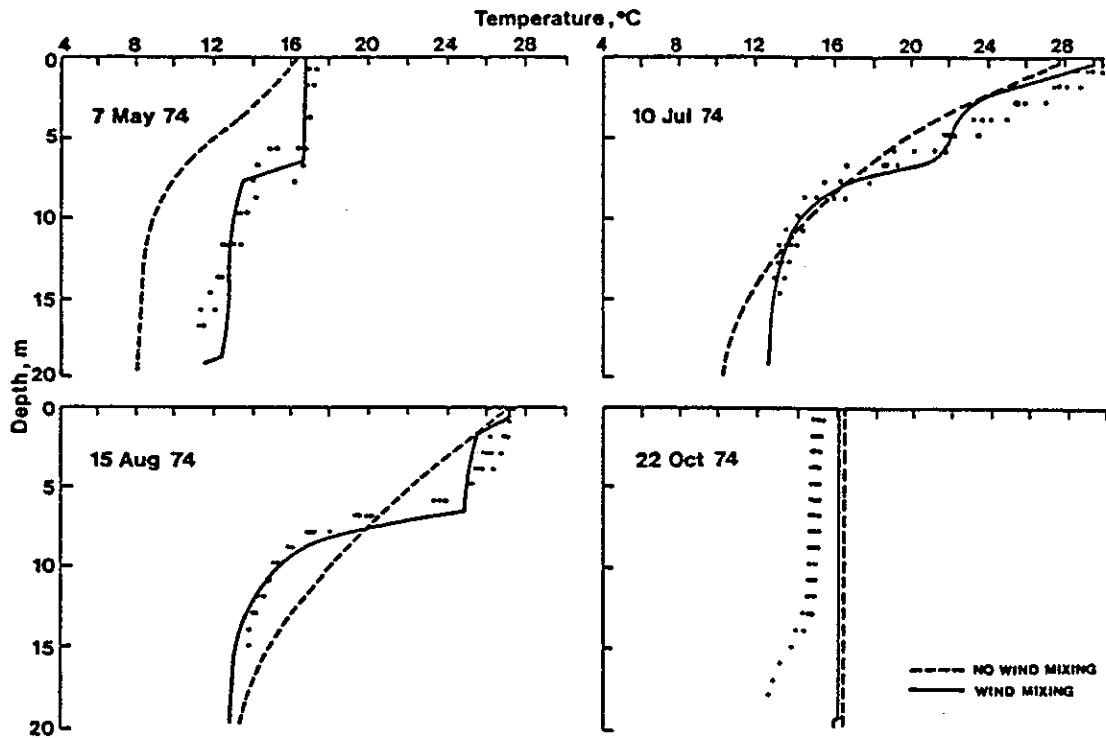


Figure 60. Comparison of simulation results from a diffusion and TKE model, Lake Anna, Virginia (after Hurley-Octavio, Jirka, and Harleman 1977)

model simulations (Figure 61). Johnson and Ford (1981) were able to simulate 6 years of data at DeGray Lake, Arkansas, and 5 years at Lake Greeson, Arkansas (including the years Stafford (1978) had problems with). Figures 62 and 63 compare Stafford's results using a diffusion model with Johnson and Ford's results using the TKE formulation in a diffusion model.

In the 1975 simulations (Figure 62), the onset of stratification (Julian Day (JD) 91), mixed-layer depths, metalimnetic gradients, and hypolimnetic temperatures (JD 167, 251, and 321) were all more accurately simulated with the mixed-layer formulation. The 1973 simulations (Figure 63) were also significantly better with respect to these parameters. As shown in Figure 64, the mixed-layer depth or TKE formulation was able to accurately predict differences in metalimnetic gradients resulting from hydrometeorological forcing. As previously indicated

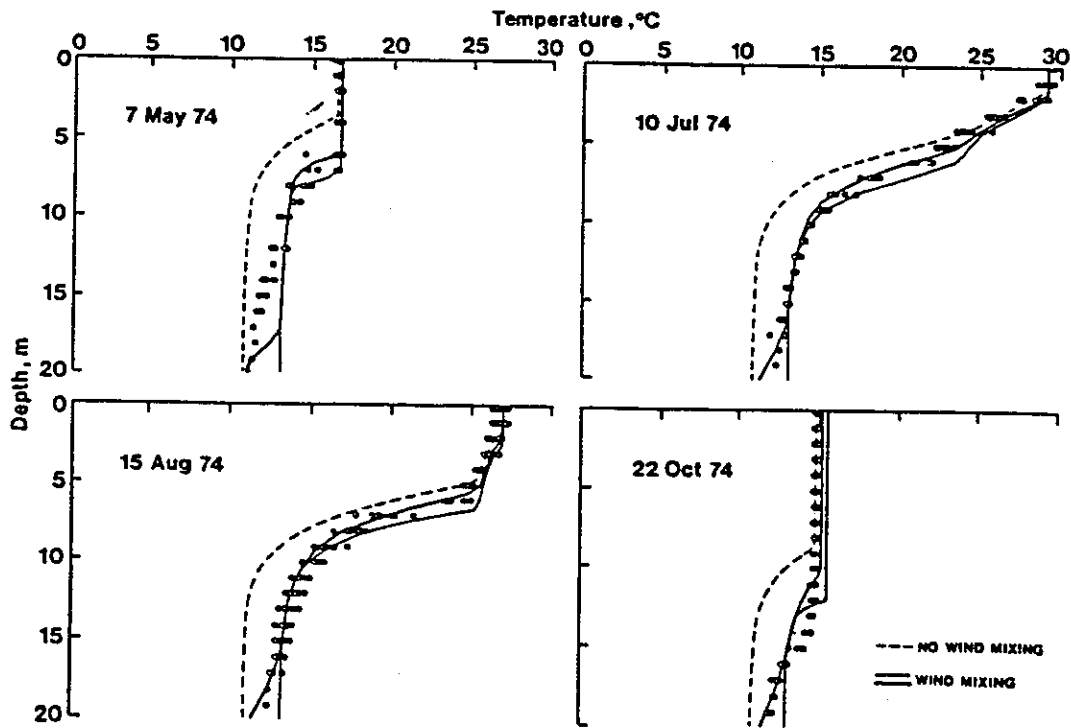
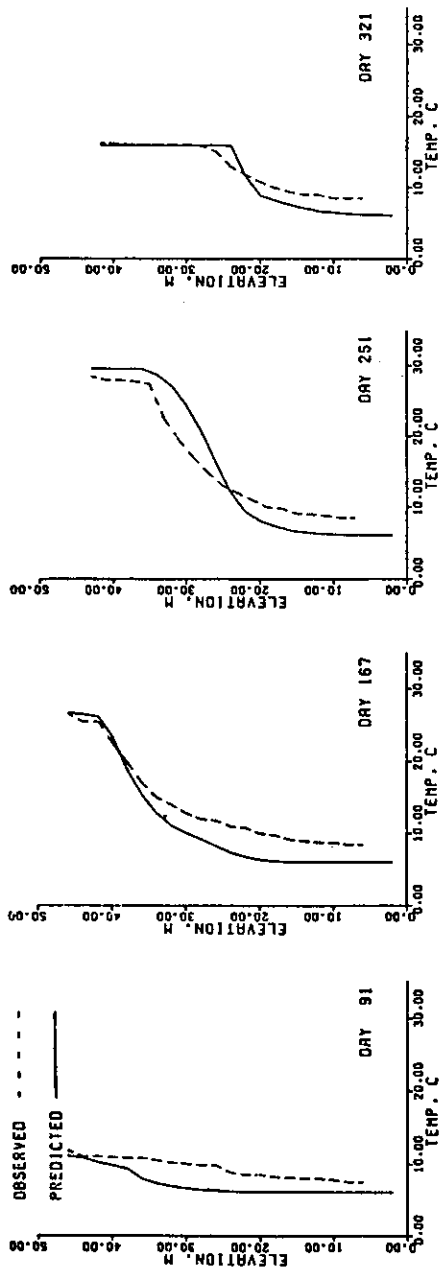
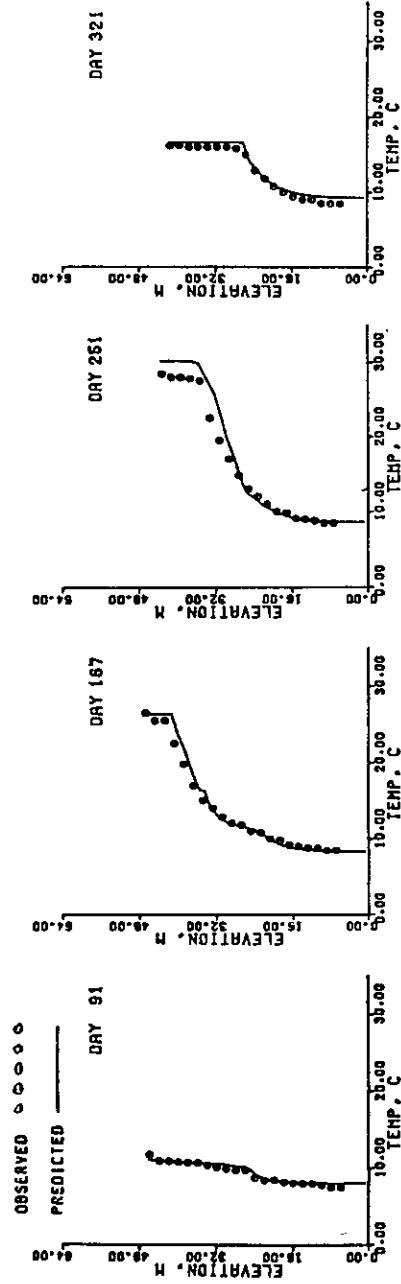


Figure 61. Comparison of simulation results with and without dissipation function, Lake Anna, Virginia (after Bloss and Harlemann 1980)

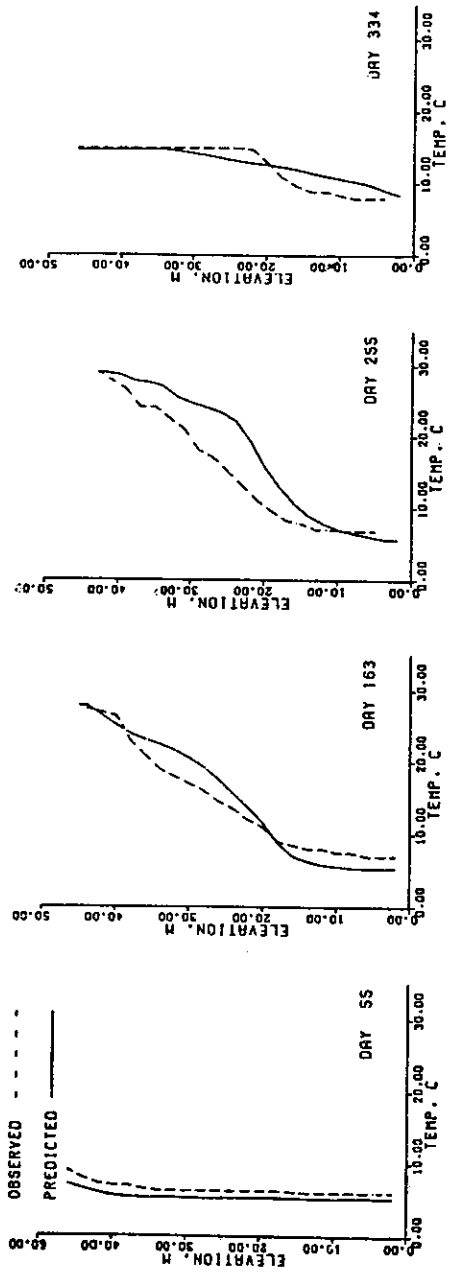


a. Diffusion model only

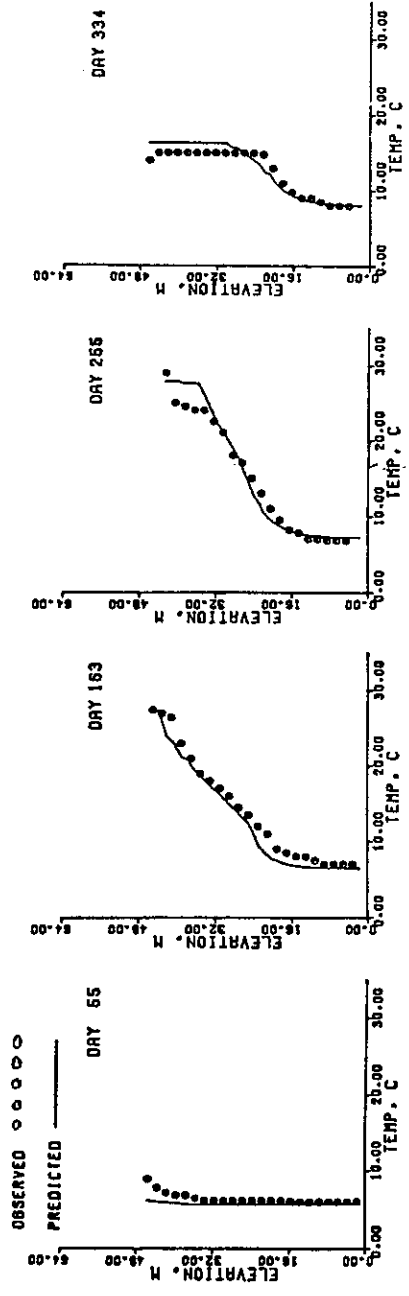


b. TKE formulation included

Figure 62. Comparison of diffusion and TKE model results, Lake Greesson, Arkansas, 1975

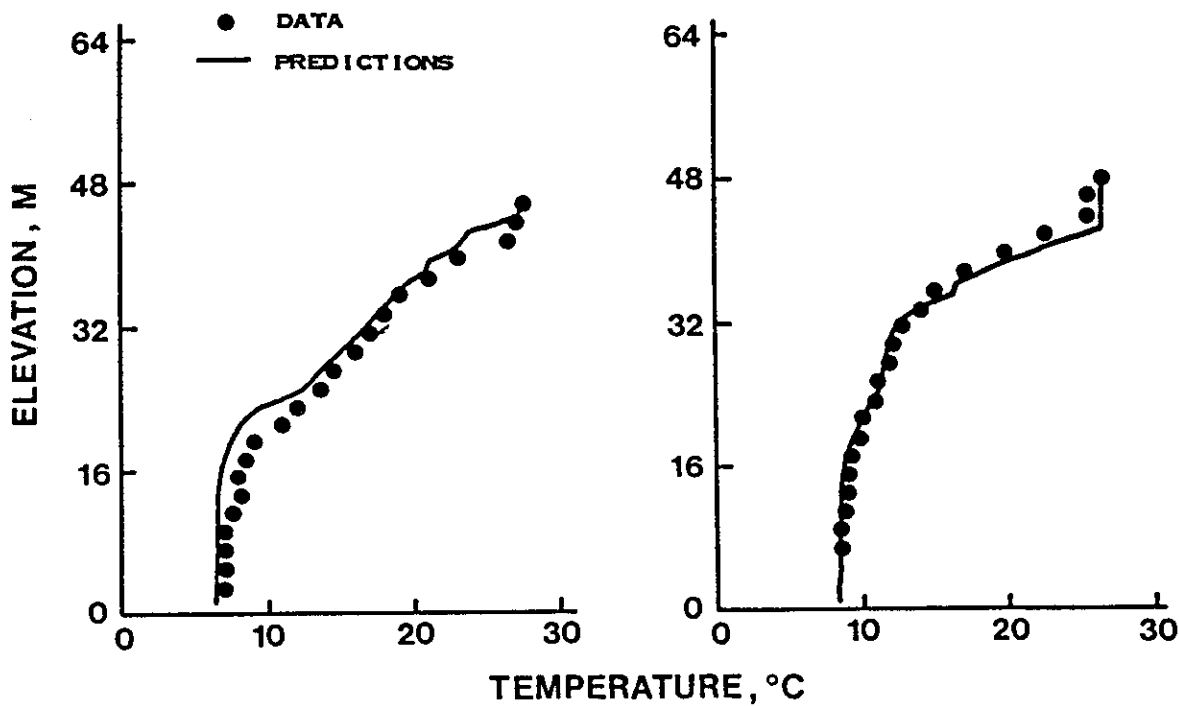


a. Diffusion model only



b. TKE formulation included

Figure 63. Comparison of diffusion and TKE model results, Lake Greesson, Arkansas, 1973



JD 163, 1973

JD 167, 1975

Figure 64. Simulation of metalimnetic gradient, Lake Greeson, Arkansas (Section 5.3.1), pure diffusion models based on Richardson number formulations were not able to reproduce these differences.

#### 5.3.4 Diffusion Coefficient Formulation

The incorporation of the variable layer concept and mixed-layer dynamics into the model reduced numerical dispersion (Section 5.3.2), improved mixed-layer depth predictions (Section 5.3.3), and identified the need to modify the diffusion coefficient formulation. Model simulations using the modified formulation indicated that mixing from inflows and outflows was not being adequately considered and that the hypolimnetic mixing coefficient should be variable and dependent on the wind speed.

Analysis of storm event data from DeGray Lake, Arkansas, clearly showed that mixing from inflows diffuses or weakens the metalimnetic temperature gradient (Figure 50). In the fixed layer formulation, mixing from inflows and outflows was introduced through the numerical dispersion introduced from the vertical advection. Elimination of this

dispersion with the incorporation of the variable layer concept also eliminated much of the mixing associated with inflows and outflows in the model. Since Ozmidov (1965) related the eddy diffusion coefficient to the dissipation rate of TKE (Equation 44), mixing from inflows and outflows was incorporated into the eddy diffusion coefficient by computing the TKE input associated with advection in a horizontal layer  $i$  :

$$\text{TKE}_a = \frac{1}{2} \rho_w Q_i U_i^2 \quad (50)$$

where

$Q_i$  = flow rate in layer  $i$ ,  $\text{m}^3/\text{sec}$

$U_i$  = flow velocity in layer  $i$ ,  $\text{m}/\text{sec}$

Equation 44 was used to incorporate variable mixing into the hypolimnion of a lake. Since wind-generated TKE can indirectly enter the metalimnion and hypolimnion via seiche motion and breaking of internal waves, the wind-generated TKE was assumed to be dissipated throughout the entire reservoir.

These formulations were incorporated in CE-QUAL-R1 and used by Johnson and Ford (1983) to simulate the thermal structures of Lakes DeGray and Greason.

#### 5.4 Recommended Algorithm

Based on an investigation of the physical basis for a number of algorithms and applications to reservoirs representing different regions of the country, different hydrometeorological conditions, and different operating conditions, it is recommended that the generalized, one-dimensional model capable of simulating changes in the mixing regime include:

- a. Variable layer formulation.

- b. Mixed-layer dynamics using the efficiency function of Bloss and Harleman (1980) and considering penetrative convection.
- c. Variable diffusion coefficient that depends on wind, inflows, outflows, and density differences.

#### 5.4.1 Variable Layer Formulation

A Lagrangian or variable layer formulation is recommended to reduce numerical diffusion and to allow calibration of the mixing resulting from inflows and outflows. Although the details and advantages of the variable formulation using power functions for the area  $A(z)$

$$A(z) = a_1 z \exp(a_2) \quad (51)$$

and the volume  $V(z)$

$$V(z) = \frac{a_1}{a_2 + 1} z \exp(a_2 + 1) \quad (52)$$

are fully described in the CE-QUAL-R1 User's Manual (Environmental Laboratory 1982), experience has shown that these simple power functions do not always provide a sufficiently accurate representation of reservoir geometry for water quality simulations. It is therefore recommended that a polynomial function or a lookup table of actual areas and volumes be used in future versions of CE-QUAL-R1.

#### 5.4.2 Mixed-Layer Dynamics

A mixed layer of TKE formulation is recommended to accurately simulate the onset of stratification and mixed-layer dynamics. This type of formulation ensures that stratification starts at the bottom of the lake and moves up, and that the dynamics of hydrometeorological forcing determine the shape of the metalimnetic temperature gradient. An accurate representation of mixed-layer dynamics during periods of cooling requires consideration of penetrative convection.

Wind. The TKE available for possible entrainment from the wind shear can be estimated by

$$\text{TKE}_w = \int_{A_s} c_t w_* \tau_s \Delta t \, dA \quad (53)$$

where

$\text{TKE}_w$  = wind shear turbulent kinetic energy,  $(\text{kg}\cdot\text{m}^2)/\text{sec}^2$   
 $A_s$  = water surface area,  $\text{m}^2$   
 $c_t$  = empirical coefficient  
 $w_*$  = shear velocity of water,  $\text{m}/\text{sec}$   
 $\tau_s$  = shear stress at the air/water interface,  $\text{kg}/(\text{m}\cdot\text{sec}^2)$   
 $\Delta t$  = time step,  $\text{sec}$

The shear velocity  $w_*$  is defined by

$$w_* = \sqrt{\frac{\tau_s}{\rho_w}} \quad (54)$$

in which  $\rho_w$  = water density,  $\text{kg}/\text{m}^3$ .

The shear stress at the air/water interface is given by:

$$\tau_s = \rho_a C_d W^2 \quad (55)$$

where

$\rho_a$  = air density ( $1.177 \text{ kg}/\text{m}^3$ )  
 $C_d$  = dimensionless drag coefficient  
 $W$  = wind speed,  $\text{m}/\text{sec}$

The drag coefficient is taken from Safaie (1978):

$$C_d = 0.00052 W^{0.44} \quad (56)$$

In many lakes, the wind stress does not act on the entire surface area because of sheltering effects from the surrounding terrain. The  $\text{TKE}_w$  (Equation 53) is therefore modified by a site-dependent sheltering

coefficient that is the ratio of the water surface area exposed to the wind to the total water surface area. The coefficient has a maximum value of 1 when sheltering is insignificant. It may also be necessary in some regions to modify Equation 56 for the drag coefficient to consider nonneutral atmospheric conditions.

Penetrative convection. TKE produced by convection currents during periods of cooling is assumed to be proportional to the net heat flux  $H_n$ , when  $H_n$  is negative. The energy available for entrainment from overturn convection can be estimated by:

$$TKE_c = -c_c H_n A_s h g \alpha \Delta t / c_p \quad (57)$$

where

- $TKE_c$  = turbulent kinetic energy,  $(kg \cdot m^2) / sec^2$
- $c_c$  = empirical calibration coefficient
- $H_n$  = net heat flux across the air/water interface,  $W/m^2$
- $h$  = depth of mixed layer, m
- $g$  = acceleration due to gravity,  $m/sec^2$
- $\alpha$  = coefficient of thermal expansion for water, per  $^{\circ}C$
- $c_p$  = specific heat of water,  $J/(kg \cdot ^{\circ}C)$

In Equation 57,  $TKE_c$  equals 0 when  $H_n$  is positive. The total TKE available for entrainment is:

$$TKE = TKE_w + TKE_c \quad (58)$$

Mixing efficiencies. Because mixing processes are dissipative and not efficient and because different processes dominate at different times, Equation 58 must be modified. Based on parameterization of the TKE balance at a density interface, Bloss and Harleman (1980) determined a Richardson number function  $f(R_i)$  to modify the TKE:

$$f(R_i) = 0.057 R_i \frac{29.46 - \sqrt{R_i}}{14.20 + R_i} \quad (59)$$

where

$$R_i = \text{Richardson number} = \frac{hg\Delta\rho}{\rho_w w_*^2}$$

$\Delta\rho$  = density difference across the interface

The total TKE available for entrainment is

$$\text{TKE} = \text{TKE} * F(R_i) \quad (60)$$

Entrainment. Prior to calculating entrainment, a temporary temperature (density) structure is computed for the computation interval. This structure considers internal absorption of solar radiation, net heat transfer at the air/water interface, inflows, and outflows. It does not consider mixing between layers.

The work  $W_L$  required to entrain or lift the mass  $\Delta\rho\Delta V$  from its position immediately below the mixed layer to the center of mass of the mixed layer is

$$W_L = \Delta\rho \Delta V g (h - h_g) \quad (61)$$

where

$W_L$  = entrainment work,  $(\text{kg}\cdot\text{m}^2)/\text{sec}^2$   
 $\Delta\rho$  = density difference between the mixed layer and underlying layer,  $\text{kg}/\text{m}^3$   
 $\Delta V$  = incremental volume to be entrained,  $\text{m}^3$   
 $g$  = acceleration due to gravity,  $\text{m}/\text{sec}^2$   
 $h_g$  = depth of the center of mass of the mixed layer, m

The depth of the mixed layer is calculated after comparing Equations 60 and 61. If the TKE is larger than  $W_L$ , entrainment occurs and  $h$  increases. Entrainment continues until TKE is no longer larger than  $W_L$ .

As indicated in Section 4.4.2, this type of formulation always sharpens the metalimnetic gradient. Diffusion or weakening of the gradient is discussed in the next section.

### 5.4.3 Diffusion Coefficient Formulation

Following the work of Ozmidov (1965), the recommended form of the diffusion coefficient for stratified conditions is

$$K_z = c_1 \frac{\bar{\epsilon}}{N^2} \quad (62)$$

where

$K_z$  = global vertical diffusion coefficient,  $m^2/sec$

$c_1$  = dimensionless calibration coefficient

$\bar{\epsilon}$  = local dissipation rate of TKE,  $m^2/sec^3$

$N^2 = \frac{g}{\rho} \frac{\partial \rho}{\partial z}$  = buoyancy frequency,  $sec^{-2}$

This equation assumes a local steady state or equilibrium such that the rate of input of TKE at larger scales is in balance with the rate of dissipation at smaller scales. Equation 62 has been theoretically justified by Weinstock (1978), who assumed mixing was done in the inertial subrange. These assumptions are acceptable since turbulence is highly dissipative. Values for  $c_1$  vary from 0.8 (Weinstock 1978) to 0.25 (Linden 1979, McEwan 1980, Oakey 1982). Equation 62 states that mixing or the diffusion coefficient increases with increasing energy input and decreases with increasing density gradient.

The computation of the local dissipation rate needs to consider the TKE inputs from the wind, inflows, and outflows separately, since the inputs from the inflows and outflows are not spread uniformly over the entire lake as the wind is but are restricted to the zone of inflow or outflow (Imberger and Patterson 1981). This finding was also verified in simulations of DeGray Lake.

The total TKE input rate from the wind is given by Equation 53. The rate of energy dissipation for wind per unit mass is

$$\bar{\epsilon}_w \propto \frac{\rho_w w_*^3 A_s}{\rho_w V} \propto \frac{w_*^3}{D_m} \quad (63)$$

where

$V$  = volume,  $m^3$

$D_m$  = mean depth,  $m$

This relationship is similar to the rate of dissipation in an unstratified uniform stress layer where shear-generated turbulence cascades to dissipation scales (e.g., Turner 1973). This is

$$\epsilon = \frac{\overline{u_x u_z}}{\partial z} \approx \frac{w_*^3}{kz} \quad (64)$$

where

$\overline{u_x u_z}$  = Reynolds stress,  $m^2/sec^2$

$\frac{\partial U}{\partial z}$  = velocity gradient,  $(m/sec)/m$

$k$  = von Karman's constant ( $\sim 0.4$ )

This relationship has been found to be valid in the surface layer of a reservoir (Dillon et al. 1981) and in the mixed layer off the Nova Scotia continental shelf (Oakey and Elliott 1980, 1982).

The TKE input from the inflow and outflow is given by Equation 50. The dissipation rate is therefore

$$\bar{\epsilon}_a = \frac{TKE_a}{\rho_w V_i} = \frac{1}{2} \left( \frac{Q_i U_i^2}{V_i} \right) \quad (65)$$

where  $V_i$  = volume of layer  $i$ ,  $m^3$ .

With the substitution of Equations 63 and 65 into Equation 62, the diffusion coefficient becomes

$$K_z = \frac{c_w \bar{\epsilon}_w + c_a \bar{\epsilon}_a}{N^2} \quad (66)$$

where

$c_w$  = calibration coefficient for wind mixing, dimensionless  
 $c_a$  = calibration coefficient for advective mixing, dimensionless

There are two problems with Equation 66. First, the diffusion coefficient becomes infinitely large when the density gradient (i.e.,  $N^2$ ) goes to zero (i.e., a well-mixed condition). Second, the diffusion coefficient is dependent on the density gradient to the -1 power, but field data indicate this power varies between -1/2 and -2 (Section 4.3.2). These deficiencies were corrected by defining the dimensionless stability factor

$$S_f = \frac{H}{\Delta\rho} \frac{\partial\rho}{\partial z} \quad (67)$$

where

$H$  = depth of lake, m  
 $\Delta\rho$  = density differential between bottom and surface waters,  $\text{kg/m}^3$

For well-mixed conditions,  $S_f = 1$ . Incorporation of  $S_f$  into Equation 66 requires the addition of a time constant to keep Equation 66 dimensionally correct. This time constant was assumed to be the computation interval. The formulation for the diffusion coefficient is therefore

$$K_z = \frac{(c_w \bar{\epsilon}_w + c_a \bar{\epsilon}_a) \Delta t^2}{(S_f)^n} \quad (68)$$

where  $n$  = calibration coefficient .

This formulation for the diffusion coefficient has several desirable features:

- a. Mixing increases with energy input.
- b. Mixing resulting from the wind and flow can be calibrated separately.
- c. The formulation is density dependent.
- d. The density dependency can be varied.

### 5.5 Applications and Verification

During the period 1976 to 1983, the recommended algorithm and its predecessors were used to simulate the thermal structures of over 15 reservoirs and lakes and numerous proposed reservoirs (i.e., over 40 data sets). A partial listing is given in Table 3. The reservoirs and lakes are from seven states and one province in Canada and represent all types of hydrometeorological conditions. The lakes vary in size from F. E. Walter Reservoir, Pennsylvania, which has a volume of  $2.47 \times 10^6 \text{ m}^3$  and mean annual hydraulic residence time of 1.7 days (Ford, Thornton, and Norton 1983), to Williston Reservoir which has a volume of  $5.7 \times 10^{10} \text{ m}^3$  and a mean annual hydraulic residence time of several years (Schultz International, Ltd. 1984).

The applications clearly illustrate that the recommended one-dimensional algorithm is:

- a. Sufficiently general to simulate the thermal structures of all types and sizes of CE reservoirs.
- b. Capable of simulating differences in a lake's thermal structure resulting from hydrometeorological conditions.
- c. Capable of simulating differences in a lake's thermal structure resulting from changes in operation (i.e., different withdrawal depth, different rule curve).
- d. Capable of simulating the thermal structure of a proposed reservoir after being calibrated on a morphometrically similar, existing reservoir.

To illustrate the last point, the model was calibrated on 1979 data from DeGray Lake using bottom withdrawal and then applied to Lakes Greeson, Ouachita, Hamilton, and Catherine. These four lakes are located within

Table 3  
Summary of Model Applications

Reservoir	Simulation Year(s)	Purpose
Beltzville Lake, Pennsylvania	1972	Verification of 1981 F. E. Walter calibration
	1981	Verification of 1981 F. E. Walter calibration
Lake Catherine, Arkansas	1982	Verification using 1979 DeGray calibration
Lake Calhoun, Minnesota	1974	Calibration
	1975	Verification
C. J. Brown Reservoir, Ohio	1974	Simulation of filling
	1975	Calibration
Lake Coralville, Iowa	1966-67	Calibration
	1969	Calibration
DeGray Lake, Arkansas	1974-78	Verification, surface withdrawal
	1979	Calibration, bottom withdrawal
	1980	Verification, bottom withdrawal
	1982	Verification, bottom withdrawal
F. E. Walter Reservoir, Pennsylvania	1977	Verification of 1981 on shallow pool, 16.8 m deep
	1979	Verification of 1981 on shallow pool, 16.8 m deep
	1981	Calibration on high pool, 44.8 m deep
Lake Greeson, Arkansas	1972-76	Verification of 1979 DeGray calibration
	1982	Verification of 1979 DeGray calibration
Lake Hamilton, Arkansas	1982	Verification of 1979 DeGray calibration

(Continued)

Table 3 (Concluded)

Reservoir	Simulation Year(s)	Purpose
McCarrons Lake, Minnesota	1974	Verification of 1974 Calhoun calibration
	1975	Verification of 1974 Calhoun calibration
Lake Ouachita, Arkansas	1982	Verification of 1979 DeGray calibration
Sardis Lake, Mississippi	1966	Verification of 1968 calibration
	1967	Verification of 1968 calibration
	1968	Calibration
	1969	Verification of 1968 calibration
	1970	Verification of 1968 calibration
Lake Shelbyville, Illinois	1973	Calibration
	1975	Verification of 1973-77 calibration
	1977	Calibration
Williston Lake, British Columbia	1976-77	Verification of 1981-82 calibration
	1981-82	Calibration

50 km of DeGray Lake in southwestern Arkansas. Their major morphometric characteristics are compared in Table 4. Johnson and Ford (1983) discuss the applications to several years of data for Lake Greeson while FTN (1983) presents the results for Lakes Ouachita, Hamilton, and Catherine.

Table 4  
Comparison of Major Morphometric Characteristics

Characteristic	Lake	Lake	Lake	Lake	Lake
	DeGray	Greeson	Ouachita	Hamilton	Catherine
Total drainage area, km <sup>2</sup>	1,173	614	2,700	3,779	4,011
Normal pool elevation, m NGVD	124.5	167.0	176.3	122.0	93.0
Volume, 10 <sup>6</sup> m <sup>3</sup>	791	345	2,653	233.7	43.5
Surface area, km <sup>2</sup>	53.4	29.1	162.3	29.1	7.9
Maximum depth, m	57	51	45.7	29.7	18.3
Mean depth, m	14.8	11.8	16.3	8.0	5.5
Hydraulic residence time, days	504	369	680	55	8.2
(years)	(1.38)	(1.01)	(1.86)	(0.15)	(0.02)

## SECTION 6. SUMMARY AND CONCLUSIONS

### 6.1 Literature Review Findings

The review of reservoir mixing processes indicated the observed thermal structure in a reservoir results from the cumulative effects of a number of complex, nonlinear, interdependent mixing processes. Although the sources of TKE for mixing are limited to solar and atmospheric heating, wind, inflows, and outflows (including outlet location), quantitative knowledge of specific mixing mechanisms such as wind mixing, penetrative convection, turbulent diffusion, and Kelvin-Helmholtz instabilities is limited. The TKE budgets for the entire lake do, however, clearly identify the physical causes of observed motion and thermal stratification. They also indicate which source of energy is controlling mixing at a particular time. It is common for wind to dominate at one time and inflows to dominate at another time.

The review of the influence of mixing on reservoir water quality indicated that mixing significantly impacts and sometimes controls the observed water quality by controlling horizontal and vertical constituent distributions and thereby influencing the physical, chemical, and biological regimes. The review also indicated that in order for a one-dimensional model to accurately simulate the effects of project operation on reservoir water quality, the mixing algorithm should be capable of accurately simulating the:

- a. Onset of stratification.
- b. Daily variations in mixed-layer depths and dynamics of short-term mixing events.
- c. Metalimnetic gradient.
- d. Variable mixing in the hypolimnion.
- e. Fall overturn.
- f. Inverse stratification during winter months.
- g. Effects of project operation.

The review of one-dimensional predictive techniques indicated that the recommended mixing algorithm should include formulations for both diffusion and mixed-layer dynamics (i.e., TKE models). Inclusion of only one type of formulation severely limits the applicability of the model for CE reservoirs.

## 6.2 Recommended Algorithm

Since the recommended mixing algorithm is intended to be used in a generalized one-dimensional water quality model (CE-QUAL-R1) to predict changes in reservoir water quality resulting from changes in hydrometeorological conditions and project operation, several requirements were considered during algorithm development:

- a. The algorithm had to be generalized with respect to CE reservoirs and therefore not be constrained by extensive morphometric and hydrometeorological data requirements nor limited in the mixing processes considered.
- b. The algorithm is to be used in a one-dimensional water quality model that does not compute the internal current structure.
- c. The algorithm must include all major mixing processes in order to predict changes in the mixing regime resulting from changes in hydrometeorological conditions and project operation.

Based on the review of reservoir mixing processes, an investigation of the physical basis for a number of algorithms, and applications to reservoirs representing different regions of the country, different hydrometeorological conditions, and different operating conditions, the recommended one-dimensional algorithm includes:

- a. Variable layer formulation (Section 5.4.1) to reduce numerical dispersion and to allow direct calibration of mixing resulting from inflows and outflows.
- b. Mixed-layer dynamics using the TKE available for possible entrainment from wind shear (Equation 53), TKE produced by convective currents during periods of cooling (Equation 57), and the efficiency function of Bloss and Harleman (1980) (Equation 59).

- c. Variable diffusion coefficient that depends on the energy inputs from the wind, inflows, and outflows and on the density gradient (Equation 68).

The recommended algorithm was used to simulate the thermal structures of over 15 reservoirs and lakes of varying geographical location, size, hydrometeorological regime, and operation configurations.

## REFERENCES

- Abbott, M. R., et al. 1984. "Mixing and Dynamics of the Deep Chlorophyll Maximum in Lake Tahoe," Limnology and Oceanography, Vol 29, pp 862-878.
- Akiyama, J., and Stefan, H. G. 1981. "Theory of Plunging Flow into a Reservoir," St. Anthony Falls Hydraulic Laboratory Internal Memorandum I-97, Minneapolis, Minn.
- Armstrong, F. A., and LaFond, E. C. 1966. "Chemical Nutrient Concentrations and Their Relationship to Internal Waves and Turbidity off Southern California," Limnology and Oceanography, Vol 11, pp 538-547.
- Bengtsson, L. 1978. "Wind Induced Circulation in Lakes," Nordic Hydrology, Vol 9, pp 75-94.
- Birge, E. A. 1910. "An Unregarded Factor in Lake Temperatures," Transactions of the Wisconsin Academy of Science and Arts Letters, No. 16, pp 989-1005.
- Blanton, J. O. 1973. "Vertical Entrainment into the Epilimnion of Stratified Lakes," Limnology and Oceanography, Vol 18, No. 5, pp 697-704.
- Bloss, S., and Harleman, D. R. F. 1980. "Effects of Wind Induced Mixing on the Seasonal Thermocline in Lakes and Reservoirs," Second International Symposium on Stratified Flow, Vol I, T. Carstens and T. McClimans eds., Trondheim, Norway, Tapir.
- Bohan, J. P., and Grace, J. L. 1973. "Selective Withdrawal from Man-Made Lakes," Technical Report H-73-4, US Army Engineer Waterways Experiment Station, Vicksburg, Miss.
- Bolz, R., and Tuve, G., eds. 1976. CRC Handbook of Tables for Applied Engineering Science, 2d ed., CRC Press, Cleveland, Ohio.
- Bouvard, M., and Dumas, H. 1967. "Application de la Methode du fil Chaud a la Mesure de la Turbulence dans L'eau," Houille Blanche, Vol 22, pp 257-278, 723-733.
- Boyce, F. M. 1974. "Some Aspects of Great Lakes Physics of Importance to Biological and Chemical Processes," Journal of the Fisheries Research Board of Canada, Vol 31, No. 5, pp 689-730.
- Brush, L. M., Jr. 1970. "Artificial Mixing of a Stratified Fluid Formed by Salt and Heat in a Laboratory Reservoir," New Jersey Water Research Institute.
- Coulter, G. W. 1968. "Hydrological Processes and Primary Production in Lake Tangayika," Proceedings of the 11th Conference on Great Lakes Research, International Association for Great Lakes Research, pp 609-626.

- Crapper, P. F. 1973. "An Experimental Study of Mixing Across Density Interfaces," Ph. D. Thesis, University of Cambridge.
- Crapper, P. F., and Linden, P. F. 1974. "The Structure of Turbulent Density Interfaces," Journal of Fluid Mechanics, Vol 65, pp 45-63.
- Cromwell, T. 1960. "Pycnoclines Created by Mixing in an Aquarium Tank," Journal of Marine Research, Vol 18, pp 73-82.
- Csanady, G. T. 1975. "Hydrodynamics of Large Lakes," Annual Review of Fluid Mechanics, Vol 7, pp 357-386.
- Davis, J. E., Holland, J. P., and Wilhelms, S. C. 1985. "SELECT: A Numerical One-Dimensional Model of Selective Withdrawal," Instruction Report in preparation, US Army Engineer Waterways Experiment Station, Vicksburg, Miss.
- Davison, W., Woof, C., and Rigg, E. 1982. "The Dynamics of Iron and Manganese in a Seasonally Anoxic Lake; Direct Measurement of Fluxes Using Sediment Traps," Limnology and Oceanography, Vol 27, pp 987-1003.
- Deardorff, J. W. 1970. Convective Velocity and Temperature Scales for the Unstable Planetary Boundary Layer and for Raleigh Convection," Journal of Atmospheric Science, Vol 27, pp 1121-1213.
- \_\_\_\_\_. 1979. "Prediction of Convective Mixed-Layer Entrainment for Realistic Capping Inversion Structure," Journal of Atmospheric Science, Vol 36, pp 424-436.
- Denman, K. L. 1976. "Covariability of Chlorophyll and Temperature in the Sea," Deep-Sea Research, Vol 23, pp 539-550.
- \_\_\_\_\_. 1977. "Short Term Variability in Vertical Chlorophyll Structure," Limnology and Oceanography, Vol 22, No. 3, pp 434-441.
- Denman, K. L., and Gargett, A. E. 1983. Time and Space Scales of Vertical Mixing and Advection of Phytoplankton in the Upper Ocean," Limnology and Oceanography, Vol 28, pp 801-815.
- Denman, K. L., and Platt, T. 1975. "Coherences in the Horizontal Distributions of Phytoplankton and Temperature in the Upper Ocean," Mem-oires Societe Royale des Sciences de Liege, Vol 6, No. 7, pp 19-30.
- Denton, R. A. 1978. "Entrainment by Penetrative Convection at Low Peclet Number," Ph. D. Thesis, University of Canterbury, Christchurch, New Zealand.
- De Pinto, J. V., Young, T. C., and Martin, S. C. 1982. "Aquatic Sediments," Journal of the Water Pollution Control Federation, Vol 54, pp 855-862.
- Dillon, T. M., et al. 1981. "Near-Surface Turbulence Measurements in a Lake," Nature, Vol 290, pp 390-392.
- Dortch, M. S. 1981. "Investigation of Release Temperatures for Kinzua Dam, Allegheny River, Pennsylvania," Technical Report HL-81-9, US Army Engineer Waterways Experiment Station, Vicksburg, Miss.

- Dunst, R. C. 1974. "In-Lake Nutrient Retention During Artificial Circulation and Bottom Water Discharge," presentation at American Society of Limnologists and Oceanographers meeting, Seattle, Wash.
- Edinger, J. E., Brady, D. K., and Geyer, J. C. 1974. Heat Exchange and Transport in the Environment," Cooling Water Discharge Project (RP-49), EPRI Report No. 14, Electric Power Research Institute, Palo Alto, Calif.
- Environmental Laboratory. 1982. "CE-QUAL-RI: A Numerical One-Dimensional Model of Reservoir Water Quality; User's Manual," Instruction Report E-82-1, US Army Engineer Waterways Experiment Station, Vicksburg, Miss.
- Farmer, D. M., and Carmack, E. 1982. "Wind-Mixing and Restratification in a Lake near the Temperature of Maximum Density," Journal of Physical Oceanography, Vol II, pp 1516-1533.
- Fasham, M. J. R., and Pugh, P. R. 1976. "Observations on the Horizontal Coherences of Chlorophyll a and Temperature," Deep-Sea Research, Vol 23, pp 527-538.
- Fee, E. J. 1976. "The Vertical and Seasonal Distribution of Chlorophyll in Lakes of the Experimental Lakes Area, Northwestern Ontario: Implications for Primary Production Estimates," Limnology and Oceanography, Vol 21, No. 6, pp 767-783.
- Fischer, H. B., et al. 1979. Mixing in Inland and Coastal Waters, Academic Press, New York.
- Fogg, G. E. 1975. Algal Cultures and Phytoplankton Ecology, The University of Wisconsin Press, Madison, Wis.
- Ford, D. E. 1976. "Water Temperature Dynamics of Dimictic Lakes: Analysis and Predictions Using Integral Energy Concepts," Ph. D. Thesis, University of Minnesota, Minneapolis.
- \_\_\_\_\_. 1978. "Temperature and Dissolved Oxygen Data Interpretation," Proceedings of a Seminar on Water Quality Data Interpretation, US Army Corps of Engineers Committee on Water Quality.
- Ford, D. E., and Johnson, M. C. 1983. "An Assessment of Reservoir Density Currents and Inflow Processes," Technical Report E-83-7, US Army Engineer Waterways Experiment Station, Vicksburg, Miss.
- Ford, D. E., Johnson, M. C., and Monismith, S. G. 1980. "Density Inflows to DeGray Lake, Arkansas," Second International Symposium on Stratified Flow, Vol II, T. Carstens and T. McClimans, eds., Trondheim, Norway, Tapir.
- Ford, D. E., and Stefan, H. G. 1980a. "Stratification Variability in Three Morphometrically Different Lakes Under Identical Meteorological Forcing," Water Resources Bulletin, Vol 16, No. 2, pp 243-247.
- \_\_\_\_\_. 1980b. "Thermal Predictions Using Integral Energy Model," Journal of the Hydraulics Division, Proceedings of the American Society of Civil Engineers, Vol 106, No. HY1, pp 39-55.

Ford, D. E., and Thornton, K. W. 1979. "Time and Length Scales for the One-Dimensional Assumption and Its Relation to Ecological Models," Water Resources Research, Vol 15, No. 1, pp 113-120.

Ford, D. E., Thornton, K. W., and Norton, J. L. 1983. "Thermal Analysis of the Proposed Francis E. Walter Reservoir Modification: Guidance on Selective Withdrawal," prepared by Ford, Thornton, Norton and Associates for US Army Engineer District, Philadelphia, Philadelphia Pa.

Ford, D. E., et al. 1981. "A Water Quality Management Model for Reservoirs," Proceedings of the Symposium on Surface Water Impoundments, H. G. Stefan, ed., American Society of Civil Engineers, New York, Vol 1, pp 624-633.

Frink, C. R. 1969. "Chemical and Mineralogical Characteristics of Eutrophic Lake Sediments," Soil Science Society of America Proceedings, Vol 33, pp 369-372.

FTN. 1983. "Arkansas Lakes Interim Study: Thermal Modeling of Lakes Ouachita, Hamilton, and Catherine," prepared by Ford, Thornton, Norton and Associates for Ouachita Baptist University, Arkadelphia, Ark., under contract to US Army Engineer District, Vicksburg, Vicksburg, Miss.

Garnich, N. G., and Kitaigorodskii, S. A. 1977. "On the Rate of Deepening of the Oceanic Mixed Layer," Isv. Akad. Nauk USSR, Atmos. and Ocean. Phys., Vol 13, pp 1287-1296.

\_\_\_\_\_. 1978. "On the Theory of the Deepening of the Upper Quasi-Homogeneous Ocean Layer Owing to the Processes of Purely Wind-Induced Mixing," Isv. Akad. Nauk USSR, Atmos. and Ocean. Phys., Vol 14, pp 748-755.

Garrett, C., and Munk, W. 1979. "Internal Waves in the Ocean," Annual Review of Fluid Mechanics, Vol 11, pp 339-370.

Gregg, M. C., and Briscoe, M. G. 1979. "Internal Waves, Finestructure, Microstructure and Mixing in the Ocean," Review of Geophysics and Space Physics, Vol 17(T), pp 1524-1548.

Hannan, H. H., and Cole, T. M. 1984. "Dissolved Oxygen Dynamics In (On-Stream) Reservoirs," Perspectives in Reservoir Limnology in preparation, K. W. Thornton, ed., John Wiley and Sons, New York.

Harleman, D. R. F. 1982. "Hydrothermal Analysis of Lakes and Reservoirs," Journal of the Hydraulics Division, Proceedings of the American Society of Civil Engineers, Vol 108, No. HY3, pp 302-325.

Harris, G. P. 1980. "Temporal and Spatial Scales in Phytoplankton Ecology; Mechanisms, Methods, Models, and Management," Canadian Journal of Fish and Aquatic Science, Vol 37, pp 877-900.

Haugen, K. A., ed. 1973. Workshop in Micrometeorology, American Meteorology Society, Boston, Mass.

Henderson-Sellers, B. 1976. "Role of Eddy Diffusivity in Thermocline Formation," Journal of the Environmental Engineering Division, Proceedings of the American Society of Civil Engineers, Vol 102, No. EE3, pp 517-531.

Hirshburg, R. I., Goodling, J. S., and Maples, G. 1976. "The Effects of Diurnal Mixing on Thermal Stratification of State Impoundments," Water Resources Bulletin, Vol 12, No. 6, pp 1151-1159.

Hopfinger, E. J., and Toly, J. A. 1976. "Spatially Decaying Turbulence and Its Relation to Mixing Across Density Interfaces," Journal of Fluid Mechanics, Vol 78, pp 155-177.

Huber, W. C., and Harleman, D. R. F. 1968. "Laboratory and Analytical Studies of the Thermal Stratification of Reservoirs," Technical Report No. 112, Ralph M. Parsons Laboratory, Massachusetts Institute of Technology, Cambridge, Mass.

Hurley-Octavio, K. A., Jirka, G. H., and Harleman, D. R. F. 1977. "Vertical Heat Transport Mechanisms in Lakes and Reservoirs," Technical Report No. 227, Ralph M. Parsons Laboratory, Massachusetts Institute of Technology, Cambridge, Mass.

Hutchinson, G. E. 1941. "Limnological Studies in Connecticut; IV. The Mechanism of Intermediary Metabolism in Stratified Lakes," Ecological Monographs, Vol 11, pp 21-69.

\_\_\_\_\_. 1957. A Treatise on Limnology, John Wiley and Sons, New York.

Hydrologic Engineering Center. 1974. "Water Quality for River-Reservoir Systems; User's Manual (Draft)," US Army Engineer Hydrologic Engineering Center, Davis, Calif.

Imberger, J. 1980. "Selective Withdrawal: A Review," Second International Symposium on Stratified Flow, Vol I, T. Carstens and T. McClimans, eds., Trondheim, Norway, Tapir.

Imberger, J., and Hamblin, P. F. 1982. "Dynamics of Lakes, Reservoirs, and Cooling Ponds," Annual Review of Fluid Mechanics, Vol 14, pp 153-187.

Imberger, J., and Patterson, J. C. 1981. "A Dynamic Reservoir Simulation Model-DYRESM; 5. Transport Models for Inland and Coastal Waters," H. B. Fischer, ed., Academic Press, New York.

Imberger, J., et al. 1978. "Dynamics of a Reservoir of Medium Size," Journal of the Hydraulics Division, Proceedings of the American Society of Civil Engineers, Vol 104, No. HY5, pp 725-743.

Imboden, D. M., and Emerson, S. 1978. "Natural Radon and Phosphorus as Limnologic Tracers: Horizontal and Vertical Eddy Diffusion in Greifensee," Limnology and Oceanography, Vol 23, No. 1, pp 77-90.

Imboden, D. M., et al. 1977. "Lake Tahoe Geochemical Study; 1. Lake Chemistry and Tritium Mixing Study," Limnology and Oceanography, Vol 22, No. 6, pp 1039-1051.

Jassby, A., and Powell, T. 1975. Vertical Patterns of Eddy Diffusion During Stratification in Castle Lake, California," Limnology and Oceanography, Vol 20, No. 4, pp 530-542.

Jirka, G. H., and Harleman, D. R. F. 1979. "Cooling Impoundments: Classification and Analyses," Journal of the Energy Division, Proceedings of the American Society of Civil Engineers, Vol 105, No. EY20, pp 291-309.

Jirka, G. H., and Watanabe, M. 1980. "Thermal Structure of Cooling Ponds. Journal of the Hydraulics Division, Proceedings of the American Society of Civil Engineers, Vol 106, No. HY5, pp 701-715.

Johnson, L. S., and Ford, D. E. 1981. "Verification of a One-Dimensional Reservoir Thermal Model," presented at 1981 American Society of Civil Engineers Convention and Exposition, St. Louis, Mo.

\_\_\_\_\_. 1983. "Thermal Modeling of DeGray Lake," Symposium on DeGray Lake, J. Nix and R. H. Kennedy, eds., Technical Report in preparation, US Army Engineer Waterways Experiment Station, Vicksburg, Miss.

Kaeff, J., and Knoechel, R. 1978. "Phytoplankton and Their Dynamics in Oligotrophic and Eutrophic Lakes," Annual Review of Ecological Systems, Vol 9, pp 475-495.

Kantha, L. H., Phillips, O. M., and Azad, R. S. 1977. "On Turbulent Entrainment at a Density Interface," Journal of Fluid Mechanics, Vol 79, pp 753-768.

Kato, H., and Phillips, O. M. 1969. "On the Penetration of a Turbulent Layer into a Stratified Fluid," Journal of Fluid Mechanics, Vol 37, pp 643-655.

Kennedy, R. H., Gunkel, R. C., and Carlile, J. M. 1983. "Riverine Influence on the Water Quality Characteristics of West Point Lake," Technical Report in preparation, US Army Engineer Waterways Experiment Station, Vicksburg, Miss.

Kimmel, B. L., Lind, O. T., and Paulson, L. J. 1984. "Reservoir Primary Production," Perspectives in Reservoir Limnology in preparation, K. W. Thornton, ed., John Wiley and Sons, New York.

Knapp, R. T. 1942. "Density Currents: Their Mixing Characteristics and Their Effect on the Turbulence Structure of the Associated Flow," Proceedings of the Second Hydraulic Conference, University of Iowa, Iowa City, pp 289-306.

Koberg, G. E. 1962. "Methods to Compute Long Wave Radiation from the Atmosphere and Reflected Solar Radiation from a Water Surface," Geological Survey Professional Paper, US Geological Survey, Washington, DC.

- Kraus, E. B. 1977. Modeling and Prediction of the Upper Layers of the Ocean, Pergamon, Oxford.
- Kraus, E. B., and Turner, J. S. 1967. "A One-Dimensional Model of the Seasonal Thermocline; Part 2: The General Theory and Its Consequences," Tellus, Vol 19, pp 98-106.
- Kullenburg, G., Murthy, C. R., and Westerberg, H. 1973. "An Experimental Study of Diffusion Characteristics in the Thermocline and Hypolimnion Regions of Lake Ontario," Proceedings of the Sixteenth Conference on Great Lakes Research.
- LaFond, E. C. 1962. "Internal Waves: Part 1," The Sea, Vol 1, M. N. Hill, ed., Wiley Interscience, New York, pp 731-751.
- Langmuir, I. 1938. "Surface Motion of Water Induced by Wind," Science, Vol 87, pp 119-123.
- Larson, D. W. 1979. "Turbidity-Induced Meromixis in an Oregon Reservoir: Hypothesis," Water Resources Research, Vol 15, No. 6, pp 1560-1566.
- Leibovich, S. 1983. "The Form and Dynamics of Langmuir Circulations," Annual Review of Fluid Mechanics, Vol 15, pp 391-427.
- Lerman, A. 1971. "Time to Chemical Steady-States in Lakes and Oceans," Advances in Chemistry Series, Vol 106.
- Linden, P. F. 1973. "The Interaction of a Vortex Ring with a Sharp Density Interface: A Model for Turbulent Entrainment," Journal of Fluid Mechanics, Vol 75, No. 2, pp 305-320.
- \_\_\_\_\_. 1975. "The Deepening of a Mixed Layer in a Stratified Fluid," Journal of Fluid Mechanics, Vol 71, pp 385-405.
- \_\_\_\_\_. 1979. "Mixing in Stratified Fluids," Geophysical and Astrophysical Fluid Dynamics, Vol 13, pp 3-23.
- Lund, J. W. G. 1950. Studies on *Asterionella formosa* Hass; Vol II: Nutrient Depletion and the Spring Maximum," Journal of Ecology, Vol 38, pp 1-35.
- \_\_\_\_\_. 1954. "The Seasonal Cycle of the Plankton Diatom, *Melosira italica* (Ehr.) Kuitz., Subsp. Subarctica O. Mull.," Journal of Ecology, Vol 42, pp 151-179.
- Lund, J. W. G., Mackereth, F. J. H., and Mortimer, C. H. 1963. Changes in Depth and Time of Certain Chemical and Physical Conditions and of the Standing Crop of *Asterionella formosa* Hass. in the North Basin of Windermere in 1947," Phil. Trans. Roy. Soc., Vol B246, pp 255-290.
- Mahrt, L. 1979. "Penetrative Convection at the Top of a Growing Boundary Layer," Quarterly Journal of the Royal Meteorological Society, Vol 105, pp 469-485.
- McEwan, A. D. 1980. "Mass and Momentum Diffusion in Internal Breaking Events," Second International Symposium on Stratified Flow, Vol I, T. Carstens and T. McClimans, eds., Trondheim, Norway, Tapir.

- Mellor, G. L., and Yamada, T. 1974. "A Hierarchy of Turbulence Closure Models for Planetary Boundary Layers," Journal of Atmospheric Science, Vol 31, pp 1791-1806.
- Monismith, S. G. 1983. "Dynamic Response of Stratified Reservoirs to Surface Shear Stress," Ph. D. Thesis, University of California, Berkeley, Calif.
- Moore, M. J., and Long, R. R. 1971. "An Experimental Investigation of Turbulent Stratified Shearing Flow," Journal of Fluid Mechanics, Vol 49, pp 635-656.
- Mortimer, C. H. 1974. "Lake Hydrodynamics," International Association of Applied Limnology Mitteilungen, Vol 20, pp 124-197.
- Munk, W., and Anderson, E. R. 1948. "Notes on a Theory of the Thermocline," Journal of Marine Research, Vol 7, pp 276-295.
- Neal, V. T., Neshyba, S. J., and Denner, W. T. 1971. "Temperature Microstructure in Crater Lake, Oregon," Limnology and Oceanography, Vol 16, pp 695-700.
- Niiler, P. P. 1975. "Deepening of the Wind-Mixed Layer," Journal of Marine Research, Vol 33, pp 405-422.
- Niiler, P. P., and Kraus, E. B. 1977. "One Dimensional Models of the Upper Ocean," Modeling and Prediction of the Upper Layer of the Ocean, E. B. Kraus, ed., Pergamon Press, Oxford, England.
- Nix, J. 1981. "Contribution of Hypolimnetic Water on Metalimnetic Dissolved Oxygen Minima in a Reservoir," Water Resources Research, Vol 17, pp 329-332.
- \_\_\_\_\_. 1984. "Transport of Iron and Manganese in a Deep Storage Reservoir," Symposium on DeGray Lake, J. Nix and R. H. Kennedy, eds., Technical Report in preparation, US Army Engineer Waterways Experiment Station, Vicksburg, Miss.
- Norton, W. R., Roesner, L. A., and Orlob, G. T. 1968. "Mathematical Models for Prediction of Thermal Energy Changes in Impoundments," EPA Water Pollution Control Research Series, US Environmental Protection Agency.
- Oakey, N. S. 1982. "Determination of the Rate of Dissipation of Turbulent Energy from Simultaneous Temperature and Velocity Shear Microstructure Measurements," Journal of Physical Oceanography, Vol 12, pp 256-271.
- Oakey, N. S., and Elliott, J. A. 1980. "Dissipation in the Mixed Layer near Emerald Basin," Marine Turbulence, J. C. Nihoul, ed., pp 123-133.
- \_\_\_\_\_. 1982. "Dissipation Within the Surface Mixed Layer," Journal of Physical Oceanography, Vol 12, pp 171-185.
- Ottesen Hansen, N-E. 1978. "Mixing Processes in Lakes," Nordic Hydrology, Vol 9, pp 57-74.

- Ozmidov, R. V. 1965. "On the Turbulent Exchange in a Stably Stratified Ocean," Atmospheric and Oceanic Physics Series, Vol 1, pp 853-860.
- Pedersen, F. B. 1980. "A Monograph of Turbulent Entrainment and Friction in Two-Layer Stratified Flow," Series Paper No. 25, Institute of Hydrodynamics and Hydraulic Engineering, Technical University of Denmark.
- Phillips, O. M. 1977. The Dynamics of the Upper Ocean, Cambridge University Press, London and New York.
- Pita, F. W., and Hyne, N. J. 1974. "The Depositional Environment of Zinc, Lead, and Cadmium in Reservoir Sediments," Water Research, Vol 9, pp 701-706.
- Pharo, C. H., and Carmack, E. C. 1979. "Sedimentation Processes in a Short Residence-Time Intermontane Lake Kamloops, B. C.," Sedimentology, Vol 24, pp 523-542.
- Platt, T. 1972. "Local Phytoplankton Abundance and Turbulence," Deep-Sea Research, Vol 19, pp 183-187.
- Platt, T., and Denman, K. L. 1975a. "Spectral Analysis in Ecology," American Review of Ecology and Systematics, Vol 6, pp 189-210.
- \_\_\_\_\_. 1975b. "A General Equation for the Mesoscale Distribution of Phytoplankton in the Sea," Memoires Societe Royale des Sciences de Liege, Vol 6, No. 7, pp 31-42.
- Pollard, R. T. 1977. "Observations and Theories of Langmuir Circulations and Their Role in Near Surface Mixing," A Voyage to Discovery, Martin Angel, ed., Supplement to Deep-Sea Research, Pergamon Press, Oxford, England, pp 235-251.
- Pollard, R. T., Rhines, P. B., and Thompson, R. O. R. Y. 1973. "The Deepening of the Wind-Mixed Layer," Geophysical Fluid Dynamics, Vol 3, pp 381-404.
- Powell, T. M., et al. 1975. "Spatial Scales of Current Speed and Phytoplankton Biomass Fluctuations in Lake Tahoe," Science, Vol 189, pp 1088-1090.
- Quay, P. D., et al. 1980. "Vertical Diffusion Rates Determined by Tritium Tracer Experiments in the Thermocline and Hypolimnion of Two Lakes," Limnology and Oceanography, Vol 25, No. 2, pp 201-218.
- Rao, D. V. S. 1977. "Effect of Physical Processes on the Production of Organic Matter in the Sea," Symposium on Modeling of Transport Mechanisms in Oceans and Lakes, Manuscript Report Series, Vol 43, pp 161-169, Marine Sciences Directorate, Department of Fisheries and the Environment, Ottawa.
- Reid, J. L. 1956. "Observations of Internal Tides in October 1950," Transactions of the American Geophysical Union, Vol 37, pp 278-286.

- Reynolds, C. S., and Rogers, D. A. 1976. "Seasonal Variations in the Vertical Distribution and Buoyancy of *Microcystis aeruginosa* Kuitz. Emend. Elenkin in Rostherne Mere, England," Hydrobiologia, Vol 48, No. 1, pp 17-23.
- Roberts, P. J. W. 1981. "Jet Entrainment in Pumped-Storage Reservoirs," Technical Report E-81-3, US Army Engineer Waterways Experiment Station, Vicksburg, Miss.
- Roberts, P. J. W., and Dortch, M. S. 1985. "Entrainment Descriptions for Mathematical Modeling of Pumped-Storage Inflows in Reservoirs," Technical Report E-85-12, US Army Engineer Waterways Experiment Station, Vicksburg, Miss.
- Rouse, H., and Dodu, J. 1955. "Turbulent Diffusion Across a Density Discontinuity," La Houille Blanche, Vol 10, pp 530-532.
- Ruttner, F. 1963. Fundamentals of Limnology, University of Toronto Press.
- Safaie, B. 1978. "Mixing of Horizontal Buoyant Surface Jet Over Sloping Bottom," Report HEL-27-4, Hydraulic Engineering Laboratory, University of California, Berkeley, Calif.
- Schultz International, Ltd. 1984. "Development of a Reservoir Water Quality Model for Reservoirs in British Columbia," Technical Report prepared for British Columbia Hydro Power Authority, Vancouver, B. C.
- Sharpley, A. N., and Segers, J. K. 1979. "Phosphorus Inputs into a Stream Draining an Agricultural Watershed; Vol II: Amounts Contributed and Relative Significance of Runoff Types," Water, Air, and Soil Pollution, Vol 11, pp 417-428.
- Sherman, F. S., Imberger, J., and Corcos, G. M. 1978. "Turbulence and Mixing in Stably Stratified Waters," Annual Review of Fluid Mechanics, Vol 10, pp 267-288.
- Simpson, J. H., and Woods, J. D. 1970. "Temperature Microstructure in a Fresh Water Thermocline," Nature, Vol 226, pp 832-834.
- Smith, F. B. 1975. "Turbulence in the Atmosphere Boundary Layer," Scientific Programs of Oxford, Vol 62, pp 127-151.
- Smith, I. R. 1979. "Hydraulic Conditions in Isothermal Lakes," Freshwater Biology, Vol 9, pp 119-145.
- Stafford, J. P., III. 1978. "Thermal Analysis of Lake Greeson, Arkansas and Sardis Lake, Mississippi," M.S. Thesis, Mississippi State University, Starkville, Miss.
- Stauffer, R. E., and Lee, G. F. 1974. "The Role of Thermocline Migration in Regulating Algal Blooms," Modeling the Eutrophication Process, E. J. Middlebrooks, D. H. Falkenberg, and T. E. Maloney, eds., Ann Arbor Science Publishers, Inc., Ann Arbor, Mich., pp 73-82.

- Stefan, H., and Ford, D. E. 1975a. "Mixed Layer Depth and Temperature Dynamics in Temperate Lakes," Verh. Internat. Verin. Limnol., Vol 19, pp 149-157.
- \_\_\_\_\_. 1975b. "Temperature Dynamics in Dimictic Lakes," Journal of the Hydraulics Division, Proceedings of the American Society of Civil Engineers, Vol 101, No. HY1, pp 97-114.
- Steward, R. W. 1959. "The Natural Occurrence of Turbulence," Journal of Geophysical Research, Vol 64, No. 12, pp 2112-2115.
- Stull, R. B. 1976a. "The Energetics of Entrainment Across a Density Interface," Journal of Atmospheric Science, Vol 33, pp 1260-1267.
- \_\_\_\_\_. 1976b. "Mixed-Layer Depth Model Based on Turbulent Energetics," Journal of Atmospheric Science, Vol 33, pp 1268-1278.
- Sundaram, T. R. 1973. "A Theoretical Model for the Seasonal Thermocline Cycle of Deep Temperate Lakes," Proceedings of the Sixteenth Conference on Great Lakes Research, pp 1009-1025.
- Sundaram, T. R., and Rehm, R. G. 1971. "Formation and Maintenance of Thermoclines in Temperate Lakes," American Institute of Aeronautics and Astronautics Journal, Vol 9, No. 7, pp 1322-1329.
- \_\_\_\_\_. 1973. "The Seasonal Thermal Structure of Deep Temperate Lakes," Tellus, Vol 25, No. 2, pp 157-167.
- Tennekes, H. 1973. "A Model for the Dynamics of the Inversion Above a Convection Boundary Layer," Journal of Atmospheric Science, Vol 30, pp 558-567.
- Tennekes, H., and Driedonks, A. G. M. 1980. "Basic Entrainment Equations for the Atmospheric Boundary Layer," Second International Symposium on Stratified Flow, Vol I, T. Carstens and T. McClimans, eds., Trondheim, Norway, Tapir.
- Tennekes, H., and Lumley, J. L. 1972. A First Course in Turbulence, The MIT Press, Cambridge, Mass.
- Tennessee Valley Authority. 1972. "Heat and Mass Transfer Between a Water Surface and the Atmosphere," Water Resources Research Laboratory Report 14, Norris, Tenn.
- Thompson, S. M., and Turner, J. S. 1975. "Mixing Across an Interface Due to Turbulence Generated by an Oscillating Grid," Journal of Fluid Mechanics, Vol 67, No. 2, pp 349-368.
- Thornton, K. W., Nix, J. F., and Bragg, J. D. 1980. "Coliforms and Water Quality: Use of Data in Project Design and Operation," Water Resources Bulletin, Vol 16, pp 86-92.
- Thornton, K. W., et al. 1979. "Improving Ecological Simulation Through Sensitivity Analysis," Simulation, Vol 32, No. 5, pp 155-166.
- Turner, J. S. 1968. "The Influence of Molecular Diffusivity on Turbulent Entrainment Across a Density Interface," Journal of Fluid Mechanics, Vol 33, pp 639-656.

- Turner, J. S. 1973. Buoyancy Effects in Fluids, Cambridge University Press, London and New York.
- Turner, J. S., and Kraus, E. B. 1967. "A One-Dimensional Model of the Seasonal Thermocline; Part 1: A Laboratory Experiment and Its Interpretation," Tellus, Vol 19, pp 88-97.
- US Army Engineer District, Baltimore. 1974. Thermal Simulation of Lakes, User's Manual," Program Numbers 722-F5-E1010 and 722-F5-E1011, Baltimore, Md.
- Van Mieghem, J. 1973. Atmospheric Energenics, Clarendon Press, Oxford, England.
- Walters, R. A., Carey, G. F., and Winter, D. F. 1978. "Temperature Computation for Temperate Lakes," Applied Mathematical Modeling, Vol 2, No. 3, pp 41-48.
- Ward, P. R. B. 1977. "Diffusion in Lake Hypolimnia," Proceedings of the Congress of the International Association of Hydraulic Research, 17th Baden-Baden, Vol 2, pp 103-110.
- Weinstock, J. 1978. "Vertical Diffusion in a Stably Stratified Fluid," Journal of Atmospheric Science, Vol 35, pp 1022-1027.
- Welander, P. 1968. "Theoretical Forms for the Vertical Exchange Coefficients in a Stratified Fluid with Application to Lakes and Seas," Acta. R. Soc. Sci. Litt., Gothoburgensis, Geophysics, Vol 1, pp 1-16.
- Wetzel, R. G. 1983. Limnology, 2d ed., Saunders College Publishing, Philadelphia, Pa.
- Whitney, L. V. 1938. "Microstratification of Inland Lakes," Transactions of the Wisconsin Academy of Science and Arts Letters, Vol 31, pp 155-173.
- Williams, D. T., et al. 1981. "Determination of Light Extinction Coefficients in Lakes and Reservoirs," Proceedings of the Symposium Surface Water Impoundments, H. G. Stefan, ed., American Society of Civil Engineers, New York, Vol 2, pp 1329-1335.
- Wolanski, E. J. 1972. "Turbulent Entrainment Across Stable Density-Stratified Liquids and Suspensions," Ph. D. Thesis, The Johns Hopkins University, Baltimore, Md.
- Wolanski, E. J., and Brush, L. M. 1975. "Turbulent Entrainment Across Stable Density Step Structures," Tellus, Vol 27, No. 3, pp 259-268.
- Wu, J. 1973. "Wind Induced Entrainment Across a Stable Density Interface," Journal of Fluid Mechanics, Vol 61, pp 275-287.
- \_\_\_\_\_. 1980. Wind Stress Coefficients over Sea Surface near Neutral Conditions - A Revisit," Journal of Physical Oceanography, Vol 10, pp 727-740.
- Zeman, O. 1981. "Progress in the Modeling of Planetary Boundary Layers," Annual Review of Fluid Mechanics, Vol 13, pp 253-272.

Zeman, O., and Tennekes, H. 1977. "Parameterization of the Turbulent Energy Budget at the Top of the Daytime Atmospheric Boundary Layer," Journal of Atmospheric Science, Vol 34, pp 111-123.

Zilitinkevich, S. S. 1975. "Comments on 'A Model for the Dynamics of the Inversion Above a Convective Boundary Layer,'" Journal of Atmospheric Science, Vol 32, pp 991-992.

## APPENDIX A: STRATIFICATION COMPUTATIONS

### A.1 Introduction

Most lakes and reservoirs stratify, albeit weakly and intermittently, at one time or another. The major factors that limit stratification are the lake depth, flowthrough rate, and the wind. These factors have been used by several investigators to develop criteria for stratification potential (i.e., the likelihood that a particular body of water will stratify). In general, lakes with depths greater than 10 m and mean annual residence times greater than 20 days stratify. These numbers differ slightly from Harleman (1982), who states that lakes with depths greater than 5 m stratify except if the residence time is less than 36 days. In addition to these general rules, several computations can be made to evaluate the stratification potential of a reservoir. Note, however, that these calculations are merely indicators and, as shown in the examples, all methods do not always yield the same conclusion.

### A.2 Densimetric Froude Number

#### A.2.1 Description

Norton, Roesner, and Orlob (1968) proposed a more scientifically based stratification criterion in the form of the densimetric Froude number

$$F_d = \sqrt{\frac{1}{ge} \frac{L\bar{Q}}{D_m V}} \quad (A1)$$

where

- $F_d$  = densimetric Froude number, dimensionless
- $g$  = acceleration of gravity,  $m/sec^2$
- $e$  = dimensionless density gradient,  $10^{-6}/m$
- $L$  = reservoir length, m

$\bar{Q}$  = average reservoir discharge,  $m^3/sec$

$D_m$  = reservoir mean depth, m

$V$  = reservoir volume,  $m^3$

An  $F_d \gg 1/\pi$  indicates a well-mixed system;  $F_d \ll 1/\pi$  indicates a strongly stratified system; while  $F_d \sim 1/\pi$  indicates a weakly or intermittently stratified system.

This criterion compares the destratifying force of the flowthrough with the stratifying potential of the assumed density gradient. It can be simplified and rewritten in terms of the residence time  $t_r$  ( $t_r$  = volume/flow rate)

$$F_d = \frac{319}{t_r} \frac{L}{D_m} \quad (A2)$$

For the critical  $F_d$  of  $1/\pi$  and a residence time of 20 days,  $L/D_m = 1,724$  or the bottom slope is on the order of  $5.8 \times 10^{-4}$ . Since this slope is characteristic of many CE reservoirs, the critical residence time of 20 days is consistent with the Norton, Roesner, and Orlob (1968) criterion.

#### A.2.2 Examples

DeGray Lake is a CE impoundment located on the Caddo River in south-central Arkansas. It has the following characteristics:

$$L = 32,000 \text{ m}$$

$$D_m = 14.8 \text{ m}$$

$$V = 7.91 \times 10^8 \text{ m}^3$$

$$\bar{Q} = 18.2 \text{ m}^3/\text{sec}$$

The densimetric Froude number is, therefore,

$$F_d = \sqrt{\frac{1}{g} \frac{L\bar{Q}}{D_m V}} = \sqrt{\frac{1}{(9.8)(10^{-6})} \frac{(32,000)(18.2)}{(14.8)(7.91 \times 10^8)}} = 0.02$$

Since  $F_d = 0.02 \ll 1/\pi$ , DeGray Lake should be a strongly stratified system, which it is (see Figure 6). Its maximum depth of 57 m and mean annual residence time of 1.38 years also confirm this conclusion.

F. E. Walter Reservoir is a small CE project located on the Lehigh River in the Pocono Mountains of northeastern Pennsylvania. It has the following characteristics:

$$L = 2,700 \text{ m}$$

$$D_m = 6.8 \text{ m}$$

$$V = 2.47 \times 10^6 \text{ m}^3$$

$$\bar{Q} = 17.6 \text{ m}^3/\text{sec}$$

The densimetric Froude number is, therefore,

$$F_d = \sqrt{\frac{1}{g\epsilon} \frac{L\bar{Q}}{D_m V}} = \sqrt{\frac{1}{(9.8)(10^{-6})} \frac{(2,700)(17.6)}{(6.8)(2.47 \times 10^6)}} = 0.9$$

indicating a weakly or intermittently stratified system. In contrast, its maximum depth of 16.8 m would indicate a stratified system and its mean annual residence time of 1.7 days would indicate a well-mixed system. Since F. E. Walter Reservoir intermittently stratifies, the densimetric Froude number computation gives the proper result while the conflicting maximum depth and residence time criteria compensate one another.

### A.3 Wind Mixing Depth

#### A.3.1 Description

The depth of the lake is important when evaluating stratification potential since the effects of wind mixing and the penetration of solar radiation are depth limited. If solar radiation does not penetrate to the bottom of the lake, wind mixing is required to prevent stratification

from forming. Since the average Secchi disc depth of CE reservoirs is 1.1 m (Thornton, Nix, and Bragg 1980), wind mixing is required in most CE reservoirs to mix the heat to depths greater than 2.2 m. The importance of wind mixing can be evaluated using the length or depth scale (Sundaram 1973):

$$D_t = \frac{w_*^3}{\beta \alpha g \frac{H_n}{\rho_w c_p}} \quad (A3)$$

where

- $w_*$  = shear velocity of wind in water, m/sec
- $\beta$  = empirical coefficient, dimensionless
- $\alpha$  = volumetric coefficient of thermal expansion,  $1.8 \times 10^{-4}/^\circ\text{C}$
- $H_n$  = net surface heat flux,  $\text{W}/\text{m}^2$
- $\rho_w$  = density of water,  $\text{kg}/\text{m}^3$
- $c_p$  = specific heat of water,  $4,186 \text{ J}/(\text{kg}\text{-}^\circ\text{C})$

The value for empirical coefficient  $\beta$  can be taken as 0.4 (i.e., von Karman's constant) although Sundaram (Mortimer 1974) recommends 0.2 to 0.4. The surface heat flux can be estimated from

$$H_n = K(T_e - T_s) \quad (A4)$$

where

- $K$  = heat exchange coefficient,  $\text{W}/(\text{m}^2 \text{-}^\circ\text{C})$
- $T_e$  = equilibrium temperature,  $^\circ\text{C}$
- $T_s$  = surface temperature,  $^\circ\text{C}$

Procedures for computing  $K$  and  $T_e$  can be found in Edinger, Brady, and Geyer (1974).

The physical significance of  $D_t$  is that it is a measure of the depth the wind can distribute a given surface heat input. Lakes with depths greater than  $D_t$  and not dominated by advection (flowthrough) will probably stratify.

### A.3.2 Examples

Since the wind mixing depth scale (Equation A3) is dependent only on meteorological conditions, computations will be made for southern Minnesota (Minneapolis) and central Louisiana (Monroe) to illustrate geographic variations in  $D_t$ . Equation A3 reduces to

$$D_t = \frac{5.9 \times 10^9 w_*^3}{H_n} \quad (A5)$$

with substitution for the various coefficients and constants. Assuming a drag coefficient  $C_d$  of  $1.3 \times 10^{-3}$  (see Equations 54 and 55), the shear velocity  $w_*$  can be obtained directly from the wind speed  $W$  using

$$w_* = 1.27 \times 10^{-3} W \quad (A6)$$

where  $W$  = wind speed, m/sec.

The surface heat is obtained from Equation A4 using Figure A1 to obtain  $K$  and approximating  $T_e$  by

$$T_e = T_d + \frac{H_s}{K} \quad (A7)$$

where

$T_d$  = dew point temperature, °C

$H_s$  = gross rate of solar radiation,  $W/m^2$

Computation of  $D_t$  therefore requires values for the wind speed, dew point temperature, water surface temperature, and solar radiation for the period of interest. Assuming the period of interest for Minnesota was May through September and for Louisiana was April through November, the following meteorological parameters were obtained from historical records and used as input.

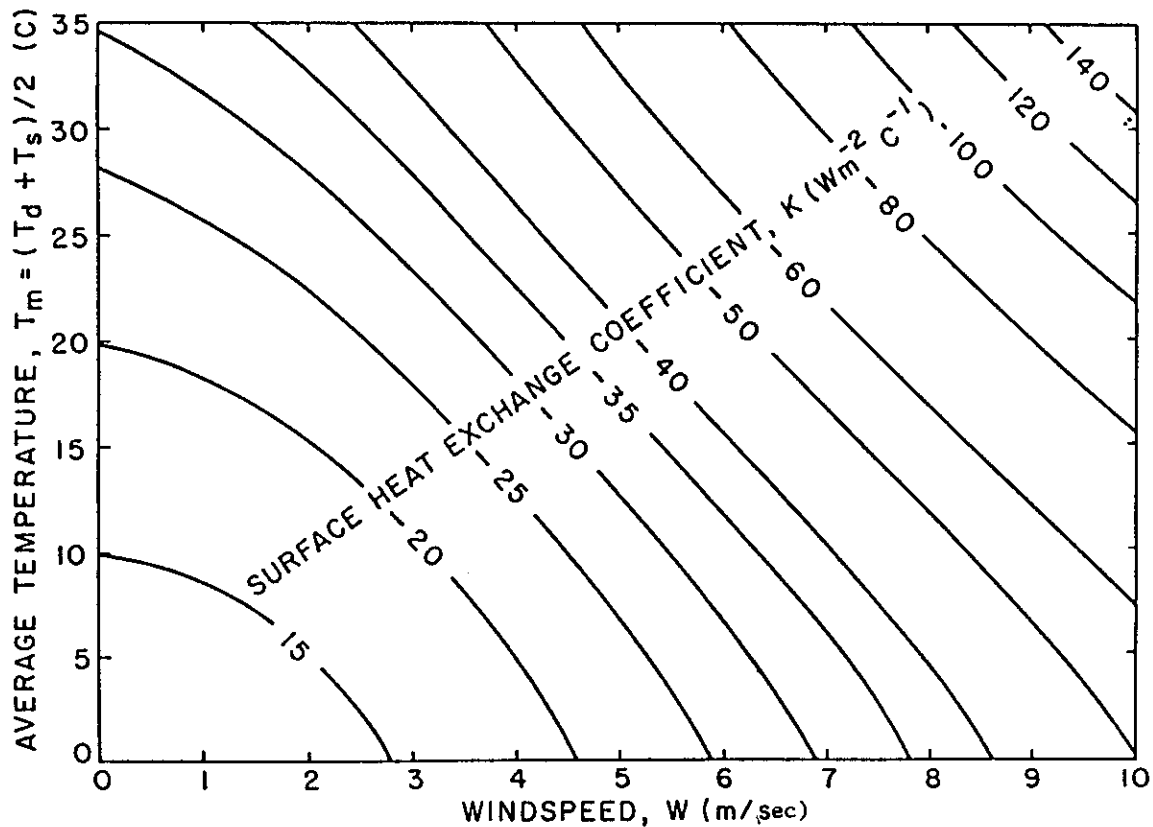


Figure A1. Design curve for surface heat exchange coefficient K (after Edinger, Brady, and Geyer 1974)

	<u>Minnesota</u>	<u>Louisiana</u>
Wind speed, m/sec	4.3	2.6
Dew point temperature, °C	11.3	16.7
Solar radiation, W/m <sup>2</sup>	230	223
Water surface temperature, °C	15.2	23.0

The computed quantities are:

	<u>Minnesota</u>	<u>Louisiana</u>
K from Figure A1	29	29
T <sub>e</sub> from Equation A7	19.2	24.8
H <sub>n</sub> from Equation A4	117	49.8
w* from Equation A6	0.0055	0.0033
D <sub>t</sub> from Equation A5	8.4	4.3

Since these  $D_t$  values are less than the general rule of 10 m, they indicate the importance of other mixing processes in determining the stratification potential.

#### A.4 Pond Number

##### A.4.1 Description

For reregulation pools or multiple reservoirs in series, a more sophisticated stratification criterion has been proposed by Jirka and Harleman (1979) and Jirka and Watanabe (1980). Although this criterion was originally developed for cooling ponds, it can be used on any system characterized by large unsteady inflows of different density (temperature) water. Jirka and Harleman (1979) proposed the Pond number,  $P_o$ , which is defined by:

$$P_o = \left[ \frac{f_i}{4} \frac{Q^2}{\alpha \Delta T g D_m^3 B_c^2} D_v^3 \frac{L}{D_m} \right]^{1/4} \quad (A8)$$

where

- $f_i$  = interfacial friction coefficient (~0.01), dimensionless
- $\alpha$  = coefficient of thermal expansion, per °C
- $\Delta T$  = temperature differential between inflow water and ambient reservoir water, °C
- $D_v$  = dilution ratio for entrance mixing (~1.0), dimensionless

The Pond number includes four separate factors:

- a. The parameter  $f_i/4$  describes the magnitude of the internal turbulent shear.
- b. The densimetric Froude number  $Q^2 (\alpha \Delta T g D_m^3 B_c^2)^{-1}$  compares the destabilizing kinetic energy of inflow with the stabilizing buoyant energy.
- c. The factor  $D_v^3$  considers the destabilizing entrance mixing.
- d. The parameter  $L/D_m$  is an aspect ratio comparing length to depth dimensions.

The larger the values of  $Po$ , the weaker the stratification. If  $Po < 0.3$ , the pool is well stratified. If  $0.3 \leq Po \leq 1.0$ , the pool is weakly stratified with a vertical temperature difference of  $\Delta T_v = 0.45T_o(1-Po)$ , where  $T_o$  = epilimnetic temperature, °C. If  $Po > 1.0$ , the pool is vertically well mixed.

#### A.4.2 Examples

Lakes Catherine and Hamilton are two small hydropower projects located downstream of Lake Ouachita, a large CE reservoir, on the Ouachita River in south-central Arkansas. All of these projects have bottom releases and are operated in series such that the cold, hypolimnetic releases from Lake Ouachita pass through Lake Hamilton as an underflow and then through Lake Catherine as an underflow. The Pond number criterion is used to evaluate the stratification potential of Lakes Catherine and Hamilton because there is a large unnatural temperature difference between the inflowing release waters from the upstream reservoir and natural reservoir surface temperatures.

In this example, the following coefficients were used

$$\begin{aligned}
 f_i &= 0.01 \\
 \alpha &= 1.8 \times 10^{-4}/^{\circ}\text{C} \\
 g &= 9.8 \text{ m/sec}^2 \\
 D_v &= 1.0
 \end{aligned}$$

reducing Equation A8 to

$$Po = 1.09 \left[ \frac{Q^2 L}{\Delta T D_m^3 B^2 D_m} \right]^{1/4} \tag{A9}$$

The lakes have the following morphometric characteristics:

<u>Characteristic, m</u>	<u>Catherine</u>	<u>Hamilton</u>
$D_m$	5.5	8.0
B	400	970
L	19,500	29,900

and mean monthly values were used for the flows  $Q$  and the temperature differentials. The temperature differentials were obtained from sine curves fitted to field measurements (see Figure A2). The following values were used

	<u>Catherine</u>	<u>Hamilton</u>
May - $Q, m^3/sec$	42.5	42.0
$\Delta T, ^\circ C$	9.0	9.8
July - $Q, m^3/sec$	28.3	25.0
$\Delta T, ^\circ C$	10.5	10.3
October - $Q, m^3/sec$	34.0	27.0
$\Delta T, ^\circ C$	2.3	2.5

which, when substituted into Equation A9, resulted in the following Pond numbers:

	<u>Catherine</u>	<u>Hamilton</u>
May	0.44	0.21
July	0.34	0.19
October	0.55	0.25

These results indicate Lake Hamilton should be well stratified since  $Po < 0.3$  and Lake Catherine should be weakly stratified since  $0.3 \leq Po \leq 1.0$ . Field measurements verify these results with midsummer temperatures in Lake Hamilton varying from  $14^\circ C$  in the hypolimnion to  $30^\circ C$  in the epilimnion and in Lake Catherine varying from  $18^\circ C$  in the hypolimnion to  $28^\circ C$  in the epilimnion. In Lake Catherine, the vertical temperature differential can be estimated from

$$\Delta T = 0.45T_o (1 - Po)$$

If  $Po = 0.34$  and  $T_o = 28^\circ C$ , then  $\Delta T = 8.3^\circ C$ , which is similar to the measured  $10^\circ C$ .

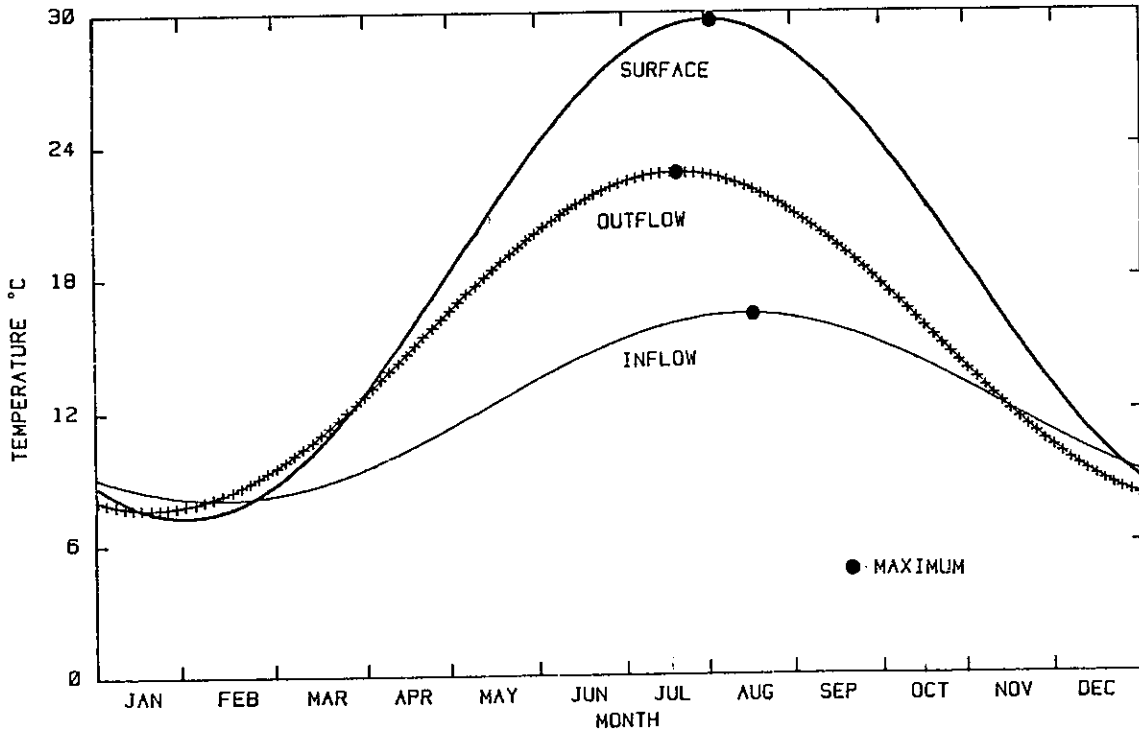


Figure A2. Sine curves fit to surface, outflow, and inflow temperatures for Lake Hamilton

#### A.5 Summary

The methods presented to evaluate the stratification potential of a reservoir range from a general rule to simple computations. Used independently, these methods can provide an indication of the stratification potential. However, because of the many factors involved in the development and maintenance of stratification, the use of more than one of the methods is suggested to provide a broader basis for the evaluation of the stratification potential of a given reservoir (see Section A.2.2).

## NOTATION

$A_j$	Cross-sectional area of inflow, $m^2$
$A_s$	Water surface area, $m^2$
$A(z)$	Horizontal area of reservoir at elevation $z$ , $m^2$
$a$	Dimensionless coefficient
$B_c$	Width of zone of conveyance, $m$
$B(z)$	Reservoir width at elevation $z$ , $m$
$C$	Concentration, $g/m^3$
$C_d$	Drag coefficient, dimensionless
$c$	Empirical coefficient or proportionality constant, $m$
$c_l$	Dimensionless calibration coefficient
$c_a$	Calibration coefficient for advective mixing
$c_c$	Empirical calibration coefficient
$c_p$	Heat capacity of water, $J/(kg-^{\circ}C)$
$c_t, c_f, c_d$	Constants determined from experimental data
$c_w$	Calibration coefficient for wind mixing
$c_*$	$c/a^b$ , $m$
$D$	Water depth, $m$
$D_i$	Thickness of top layer, $m$
$D_m$	Reservoir mean depth, $m$
$D_t$	Wind mixing depth scale, $m$
$D_v$	Dilution ratio for entrance mixing ( $\sim 1.0$ ), dimensionless
$\frac{dz}{dx}$	Slope of water surface, $m/m$
$e$	Dimensionless density gradient = $10^{-6}/m$
$F_d$	Densimetric Froude number, dimensionless
$f$	Coriolis parameter ( $f = 2\omega \sin \theta$ )
$f_i$	Interfacial friction coefficient ( $\sim 0.01$ ), dimensionless
GSWH	WQRRS stability criterion
$g$	Acceleration due to gravity, $m/sec^2$
$H$	Thickness, depth, or height, $m$
$H_n$	Net heat flux across the air/water interface, $W/m^2$
$H_s$	Surface heat flux, $W/m^2$

$H_w$	Wave height, m
$H_z$	Heat flux at elevation z, $W/m^2$
$h$	Depth (thickness) of upper turbulent layer or mixed layer, m
$h_g$	Depth of center of mass of the mixed layer, m
$h_p$	Hydraulic plunge depth, m
$K$	Heat exchange coefficient, $W/(m^2-^{\circ}C)$
KE	Kinetic energy, J
$K_d$	Dispersion coefficient, $m^2/sec$
$K_m$	Molecular diffusivity or diffusion coefficient, $m^2/sec$
$K_t$	Turbulent diffusion coefficient, $m^2/sec$
$K_z$	Global vertical diffusion coefficient, $m^2/sec$
$K_{zo}$	Eddy diffusion coefficient at neutral stability, $m^2/sec$
$k$	von Karman's constant ( $\sim 0.4$ )
L	Length scale or reservoir length, m
M	Mass, kg
$m$	Total mass of the reservoir, kg
$N^2$	$\frac{g}{\rho} \frac{\partial \rho}{\partial z} =$ buoyancy frequency, $sec^{-2}$
$n$	Coefficient, dimensionless
Po	Pond number, dimensionless
Pr	Prandtl number = 1 for water, dimensionless
PE	Potential energy, J
$p'$	Turbulent fluctuations of pressure, Pa
$\bar{Q}$	Average reservoir discharge, $m^3/sec$
$Q_i$	Flow rate in layer i, $m^3/sec$
$Q_j$	Inflow rate, $m^3/sec$
$Q_v$	Vertical flow rate, $m^3/sec$
$q^2$	TKE per unit mass = $(u_x^2 + u_y^2 + u_z^2)/2$
$q_d$	Flux due to dispersion, $kg/(m^2-sec)$
$q_m$	Flux due to molecular diffusion, $kg/(m^2-sec)$
$q_t$	Flux due to turbulent diffusion, $kg/m^2-sec)$
Ri	Richardson number, dimensionless
RPE	Relative potential energy, J

r	Radius of an inertial circle, m
S	Water surface slope, m/m
$S_f$	Stability factor, dimensionless
$S_i$	Interface slope, m/m
T	Water temperature, °C
$TKE_a$	Turbulent kinetic energy from advection, $(\text{kg}\cdot\text{m}^2)/\text{sec}^2$
$TKE_c$	Turbulent kinetic energy from convection, $(\text{kg}\cdot\text{m}^2)/\text{sec}^2$
$TKE_w$	Wind shear turbulent kinetic energy, $(\text{kg}\cdot\text{m}^2)/\text{sec}^2$
$T_d$	Dew point temperature, °C
$T_e$	Equilibrium temperature, °C
$T_j$	Inflow temperature, °C
$T_s$	Surface temperature, °C
t	Time, sec
$t_r$	Hydraulic residence time, sec
$t_s$	Seiche period, sec
U	Velocity in direction of flow, m/sec
$\bar{U}$	Mean horizontal component, m/sec
$U_i$	Flow velocity in layer i, m/sec
$U_j$	Inflow velocity, m/sec
$U_x, U_y, U_z$	Instantaneous velocity components, m/sec
$\bar{U}_x, \bar{U}_y, \bar{U}_z$	Mean velocity components, m/sec
$u_j(z)$	Inflow velocity distribution, m/sec
$u_o(z)$	Outflow velocity distribution, m/sec
$u_s$	Surface drift velocity, m/sec
$u'w'$	Reynolds stress, $\text{m}^2/\text{sec}^2$
$u_x, u_y, u_z$	Turbulent fluctuations of the horizontal (x,y) and vertical (z) velocity components, m/sec
$\overline{u_x u_z}$	Reynolds stress, $\text{m}^2/\text{sec}^2$
$u^2$	$\overline{u_x^2 + u_y^2 + u_z^2}$
V	Volume, $\text{m}^3$
$V_i$	Volume of layer i, $\text{m}^3$
W	Wind speed, m/sec

$W_e$	Wedderburn number
$W_L$	Entrainment work, $(\text{kg}\cdot\text{m}^2)/\text{sec}^2$
$w_e$	$\frac{dh}{dt}$ = entrainment velocity, m/sec
$w_*$	Shear or friction velocity, m/sec
$Z_j$	Difference in depth between center of mass of inflow and center of mass of inflow placement, m
$Z_m$	Maximum elevation or depth, m
$z$	Vertical coordinate, m
$z_s$	Elevation of water surface, m
< >	Ensemble mean (i.e., mean over many trials)
$\langle u^2 \rangle^{1/2}$	Root mean square velocity, m/sec
$\alpha$	Coefficient of thermal expansion of water, per $^\circ\text{C}$
$\beta$	Coefficient, dimensionless
$\Delta D$	Setup of water surface, m
$\Delta T$	Temperature differential between inflow water and ambient reservoir water, $^\circ\text{C}$
$\Delta V$	Incremental volume to be entrained, $\text{m}^3$
$\Delta t$	Time step, sec
$\Delta \rho$	Density difference, $\text{kg}/\text{m}^3$
$\Delta \rho_j$	Density difference between inflow and reservoir surface waters, $\text{kg}/\text{m}^3$
$\bar{\epsilon}$	Rate of dissipation of TKE, $\text{m}^2/\text{sec}^3$
$\epsilon$	Local dissipation rate of TKE, $\text{m}^2/\text{sec}^3$
$\lambda$	Wavelength, m
$\rho$	Density, $\text{kg}/\text{m}^3$
$\rho'$	Turbulent fluctuations of density, $\text{kg}/\text{m}^3$
$\rho_a$	Density of air, $1.177 \text{ kg}/\text{m}^3$
$\rho_j$	Inflow density, $\text{kg}/\text{m}^3$
$\rho_m$	Maximum water density, $\text{kg}/\text{m}^3$
$\rho_o$	Mean density, $\text{kg}/\text{m}^3$
$\rho_w$	Water density, $\text{kg}/\text{m}^3$
$\rho(z,t)$	Reservoir density at elevation $z$ and time $t$ , $\text{kg}/\text{m}^3$
$\sigma$	Velocity scale, m/sec

$\tau$	Shear stress, $\text{kg}/(\text{m}\text{-sec}^2)$
$\tau_s$	Shear stress at air/water interface, $\text{kg}/(\text{m}\text{-sec}^2)$
$\phi$	Latitude
$\frac{\partial C}{\partial x}$	Concentration gradient, $\text{mg}/\ell/\text{m}$
$\frac{\partial U}{\partial z}$	Velocity gradient, $(\text{m}/\text{sec})/\text{m}$
$\frac{\partial \rho}{\partial z}$	Local density gradient
$\omega$	Angular velocity of the earth's rotation, $7.29 \times 10^{-5}$ rad/sec